

**Development of a novel vaccine against
Cryptosporidium parvum using an attenuated
Salmonella Typhimurium vector**

Iris Yu Heng Du

Department of Microbiology and Immunology, Faculty of Medicine

McGill University, Montreal

August 2021

A thesis submitted to the Faculty of Graduate Studies and Research in partial fulfillment of the requirements for the degree of Master of Science

©Iris Du, 2021

Table of Contents

Abstract	4
Résumé	5
Acknowledgements	7
Literature Review	8
A History of Cryptosporidiosis	8
Transmission and Epidemiology	8
<i>Cryptosporidium parvum</i> Life Cycle	9
Human Cryptosporidiosis	10
The Immune Response against <i>Cryptosporidium</i>	11
Innate Immune Response	11
Adaptive Immune Response: CD4+ T-Cells	14
Adaptive Immune Response: CD8+ T-Cells	15
Adaptive Immune Response: Humoral immunity	16
Diagnostics	17
Microscopy and Histology	17
Immunoassays	18
PCR.....	18
Vaccine Development against <i>Cryptosporidium</i> spp.	19
Attenuated Vaccines	19
Cryptosporidium Antigens and their Potential as Vaccine Candidates.....	19
Recombinant Protein Vaccines.....	20
DNA-Based Vaccines.....	20
The Use of Bacterial Vectors	21
The Prime-Pull Vaccine Approach.....	23
The Role of Adjuvants.....	23
<i>Salmonella enterica</i> Typhimurium YS1646	24
Treatments	25
Conclusions and Future Directions	26
Rationale and Research Objectives	27
Methods	28
Plasmid Construct Preparation	28
For Protein Expression by YS1646	28
Codon Optimization of Cp15-23	28
pQE30 Plasmid Construction for Cp15, Cp23, and Cp15-23 Protein Expression by YS1646	29
PCR Amplification of Cp15, Cp23, and Cp15-23 Sequences.....	29
Digestion of Amplified Cp15, Cp23, and Cp15-23.....	29
Ligation of Cp15, Cp23, and Cp15-23 into pQE30 constructs	29
Transformation of Ligated pQE30 constructs into DH5a <i>E. coli</i>	30
Sequencing of Constructs	30
Oral Gavage Vaccine Preparation: Transformation of YS1646	30

pET-28b Plasmid Construction for Cp15, Cp23, and Cp15-23 Recombinant Protein Expression by <i>E. coli</i>	31
Intramuscular Vaccine Preparation: Purification of 6xHis-tagged Cp15, Cp23, and Cp15-23 Recombinant Protein	31
Transformation of BLR(DE3) Competent <i>E. coli</i>	31
Protein Expression.....	32
Protein Purification.....	32
Western Blot.....	32
Protein Dialysis	33
Protein Quantification	33
Concentrating Protein Sample.....	33
Cp15, Cp23, and Cp15-23 Immunogenicity Studies: Protocol and Timeline	33
Cp15-23 Immunogenicity Study	33
Cp15 and Cp23 Immunogenicity Study	35
Humoral Response Analysis: Enzyme-Linked Immunosorbent Assay	37
Cell-Mediated Response Analysis: Flow Cytometry	37
Serum Antibody Adoptive Transfer Protection Study against <i>C. parvum</i> Challenge	38
Intestinal Processing and Oocyst Count.....	39
Results	41
<i>C. parvum</i> antigen sequences inserted into pQE30 and pET28 vectors.....	41
Recombinant Cp15, Cp23, and Cp15-23 Protein Expression	41
Immunogenicity of Cp15-23 in C57BL/6 mice.....	42
Immunogenicity of Cp15 and Cp23 in C57BL/6 mice	42
Serum Antibody Adoptive Transfer Protection Study against <i>C. parvum</i> Challenge	44
Figures	45
Discussion	57
Future Directions	68
References	70

Abstract

Cryptosporidium parvum is ubiquitous protozoan parasite recognized as a frequent cause of diarrheal disease in humans. While *Cryptosporidium* infections are typically self-limiting in immunocompetent hosts, immunocompromised individuals may develop a chronic and life-threatening illness. Currently, neither curative therapeutics nor prophylactic vaccines exist for *Cryptosporidium* infections. In this study, *C. parvum* surface proteins Cp15 and Cp23 as well as a fusion protein of the two (Cp15-23) were chosen as the target vaccine antigens. All of the candidate proteins were previously shown to induce partial protection in murine hosts. Using a plasmid-based system, an attenuated strain of *Salmonella enterica* serovar Typhimurium, YS1646, was designed to express Cp15, Cp23, and Cp15-23 during invasion of the intestinal epithelium. Two YS1646 strains exploiting different promoter-secretory signal pairings (e.g., PsspH2-SspH2 and pNirB_SspH1, referred to as pSspH2_X and pNirB_X respectively) were generated to express each protein. Female C57BL/6 mice (6-8-week-old) were vaccinated using a multi-modality schedule comprised of a single intramuscular (IM) dose of recombinant Cp15, Cp23, or Cp15-23 on day 1 (D1) and three oral (PO) doses of Cp15-, Cp23-, or Cp15-23-expressing YS1646 candidates over 5 days (D1, D3, D5). Control groups received either IM or PO schedules alone. Two Cp23 vaccination groups (rCp23 IM only, pNirB_Cp23 PO and rCp23 IM), two Cp15-23 vaccination groups (rCp15-23 IM only, pSspH2_Cp15-23), and one multi-modality group (pSspH2_Cp15 + pSspH2_Cp23 PO with rCp15 and rCp23) were found to induce significant increases in serum IgG titers compared to the PBS control. Only the pNirB_Cp23 PO and rCp23 IM vaccination group induced significant intestinal IgA titers compared to the PBS control. Significant increases in CD8⁺ CD44⁺ T cells in the non-stimulated pSspH2_Cp15/23 + rCp15/23 vaccinated group, CD4⁺ IFN- γ ⁺ T cells in the Cp23-stimulated pSspH2_Cp15/23 + rCp15/23 vaccinated group, CD4⁺ TNF- α ⁺ T cells in the Cp23-stimulated pSspH2_Cp23 + rCp23 vaccinated group, and CD8⁺ TNF- α ⁺ T cells in the non-stimulated pSspH2_Cp23 + rCp23 vaccinated group were observed. No difference in oocyst burden was observed following adoptive transfer of vaccine-induced serum antibodies. Overall, while select vaccine candidates were immunogenic, an evaluation of the protective efficacy of an induced cellular response to cryptosporidial infection through adoptive transfer of splenocytes (CD4⁺ and CD8⁺ T cells) from vaccinated animals is planned.

Résumé

Cryptosporidium parvum est un parasite protozoaire ubiquitaire reconnu comme étant une cause fréquente de maladie diarrhéique chez les humains. Alors que les infections de *Cryptosporidium* sont généralement résolues chez les hôtes immunocompétents, les personnes immunodéprimées peuvent développer une maladie chronique et mortelle. Actuellement, il n'existe ni traitement curatif ni vaccin prophylactique pour les infections de *Cryptosporidium*. Dans cette étude, les protéines de surface de *C. parvum* Cp15 et Cp23 ainsi qu'une protéine de fusion (Cp15-23) ont été ciblées comme antigènes de vaccin. Il a déjà été démontré que toutes ces protéines candidates induisaient une protection partielle dans des modèles murins. À l'aide d'un système à base de plasmide, une souche atténuée de *Salmonella enterica* sérovar Typhimurium, YS1646, a été conçue pour exprimer Cp15, Cp23 et Cp15-23 lors de l'invasion de l'épithélium intestinal. Deux souches YS1646 exploitant différentes combinaisons de promoteur et signal de sécrétion (par exemple, pSspH2-SspH2 et pNirB_SspH1, appelés respectivement pSspH2_X et pNirB_X) ont été construits pour exprimer chaque protéine. Des souris femelles C57BL/6 (âgées de 6 à 8 semaines) ont été vaccinées selon une stratégie multimodale comprenant une dose unique intramusculaire (IM) de Cp15, Cp23 ou Cp15-23 recombinant le jour 1 (J1) et trois doses orales (PO) des candidats YS1646 exprimant Cp15-, Cp23- ou Cp15-23 sur 5 jours (J1, J3, J5). Les groupes de contrôle ont reçu soit IM ou PO seuls. Deux groupes de vaccination Cp23 (rCp23 IM uniquement ainsi que pNirB_Cp23 PO et rCp23 IM), deux groupes de vaccination Cp15-23 (rCp15-23 IM uniquement, pSspH2_Cp15-23) et un groupe multimodalité (pSspH2_Cp15 + pSspH2_Cp23 PO avec rCp15 et rCp23) ont induit des augmentations significatives des titres d'IgG dans le sang par rapport au groupe PBS. Seul le groupe de vaccination pNirB_Cp23 PO et rCp23 IM a induit des titres d'IgA significatifs dans l'intestin par rapport au groupe PBS. L'augmentation significative des niveaux de lymphocytes T CD8+ CD44+ dans le groupe vacciné pSspH2_Cp15/23 + rCp15/23 non stimulé, lymphocytes T CD4+ IFN- γ + dans le groupe vacciné pSspH2_Cp15/23 + rCp15/23 stimulé par Cp23, CD4+ TNF- α + T des cellules dans le groupe vacciné pSspH2_Cp23 + rCp23 stimulé par Cp23 et des cellules T CD8+ TNF- α + dans le groupe vacciné pSspH2_Cp23 + rCp23 non stimulé ont été observées. Aucune différence dans la charge d'oocystes n'a été observée après le transfert adoptif d'anticorps sériques induits par le vaccin. Dans l'ensemble, alors que certains candidats vaccins étaient immunogènes, l'efficacité protectrice

induite par la réponse cellulaire à l'infection cryptosporidienne par des expériences de transfert adoptif de splénocytes (cellules T CD4+ et CD8+) d'animaux vaccinés est prévu.

Acknowledgements

I would like to thank my supervisors Dr. Brian Ward and Dr. Momar Ndao for their endless support throughout both my Honors and my Masters. To Brian, thank you always for your wisdom and words of encouragement, for answering my e-mails at the dead of night, and of course, for the countless wild stories that you share with us. From you I've learned that life is a journey with many paths and many endings. I can only hope that one day I'll have as many adventures and stories (as exciting as yours!) to share with you. To Momar, thank you for your mentorship and your expertise in the field of parasitology. You taught me of the importance of always being curious, whether it be for science or otherwise, and to never stop learning in life. Thank you both for all the time you've invested in helping me grow, not just as a scientist, but as a person.

I'd like to thank Kaitlin for showing me the ropes when I first arrived in the Ward-Ndao lab. I've asked you just about a million questions in the time that I've been here and thank you for always taking the time to answer every last one. Thank you, Selena for being my emotional support human. You were definitely one of the reasons I made it through the year. I'm forever grateful for our camaraderie and I'm excited to see all the amazing things you will accomplish in the future. To Adam, Fatima, and Pavitra too, thank you for all of your friendships, both inside and out of lab. I'll miss laughing it up with you guys as we wait on incubations and I hope that we'll be friends for many, many years to come.

To Drs. Thibault, Hanh, and Elizabeth, thank you all for helping me overcome the dread that was cloning. To Tania, Gio and Kevin, thank you for making late nights and long weekends that much more bearable at the lab. To Annie and Karine, thank you for your technical expertise and knowledge in mice and *Cryptosporidium*. And lastly, thank you to the rest of the Ward-Ndao lab. I've had a wonderful time being a part of this big family, and I'm endlessly grateful to each and every one of you all.

1. Literature Review

1.1 A History of Cryptosporidiosis

Cryptosporidiosis is a diarrheal disease caused by species of the protozoan parasite *Cryptosporidium*. *Cryptosporidium* was first identified and characterized in the gastric glands of mice by Ernest Edward Tyzzer in 1907¹. The veterinary importance of *Cryptosporidium* spp. was highlighted in 1950s with the association of *C. meleagridis* with morbidity and mortality in turkeys², and again in the 1970s with the association of *C. parvum* and bovine diarrhea³. The first cases of human cryptosporidiosis were reported in 1976^{4, 5}, with *C. hominis* and *C. parvum* accounting for over 90% of cases^{6, 7}. While *C. hominis* is primarily limited to infecting human hosts, *C. parvum* is capable of infecting a wide array of hosts, including major domestic livestock species^{6, 8}. The public health significance of human cryptosporidiosis rose to prominence in the 1980s, when co-infection with *Cryptosporidium* spp. was found to result in debilitating disease and high mortality in immunocompromised AIDS patients⁹. Further medical interest was generated when infection with *Cryptosporidium* was recognized to cause acute diarrhea in immunocompetent individuals⁹.

This project will focus on the species *C. parvum*.

1.2 Transmission and Epidemiology

Diarrheal diseases are a global issue that affect all regions and populations. In 2016, diarrhea was the eighth leading cause of mortality, claiming over 1.6 million lives, with 26.93% of those deaths occurring among children younger than 5 years of age¹⁰. While cryptosporidiosis is prevalent worldwide, the burden of disease is significantly higher in low-and-middle income countries that lack access to safe drinking water, sanitation, and urgent medical care¹¹. *C. hominis* and *C. parvum* are the second most common cause of moderate-to-severe diarrhea in 0-11-month-old infants, and the third most common cause in 12-23-month-old children in sub-Saharan Africa and south Asia¹².

While there exist over 30 named species of *Cryptosporidium*, only 14 have been demonstrated to infect humans¹³, with *C. hominis* and *C. parvum* accounting for the majority of human cryptosporidiosis cases. The former is exclusively anthroponotic but the latter is both

zoonotic and anthroponotic¹⁴. Transmission of *Cryptosporidium* spp. occurs primarily via the fecal-oral route, mainly through food and water contamination¹⁵. Food-borne outbreaks result from consumption of fruits or vegetables irrigated or washed with water contaminated with *Cryptosporidium*¹⁶. Waterborne outbreaks are a result of oocyst contamination of drinking water (due to lack of untreated water, water-testing limitations, or water-treatment limitations) or recreational water (i.e. swimming pools)¹⁷. Interestingly, one of the largest outbreaks of cryptosporidiosis occurred in 1993, in Milwaukee, USA, due to the limited filtration standards of the city's water treatment facility. 58 cryptosporidiosis-associated deaths were attributed to the outbreak, with AIDS being the underlying cause of 85% of deaths¹⁸. It was estimated, however, that over 403,000 people were affected and presented symptoms of severe watery diarrhea over a very short period of time^{18,19}.

It is important to also note the veterinary importance of *Cryptosporidium* spp., which infect a wide range of animals, including calves, horses, sheep, goats, dogs, cats, rabbits, rodents, and birds^{14,20}. Luckily, transmission of infection from sheep, horses, goats, and rodents to humans has only rarely been reported²⁰. Infection with *C. canis* and *C. felis*, the dog- and cat-adapted species respectively, have not been reported to cause symptomatic disease in people^{20,21}. On the other hand, *C. parvum* is a major problem in the dairy industry. Longitudinal studies have demonstrated that 100% of dairy calves will become infected with *C. parvum* during early life^{22,23,24}. Not only can bovine cryptosporidiosis cause life-threatening disease in dairy calves²⁵, each calf can produce up to 10⁷ oocysts per gram of feces²⁶, resulting in the possibility of billions of oocysts being excreted into the environment during the one-to-two-week period of infection. As it only takes approximately 10-30 *C. parvum* oocysts to cause a symptomatic human infection²⁷, it is important to effectively monitor and control the spread of *C. parvum* in calves through the use of good management and proper husbandry. This includes maintaining a closed herd, supplying clean and dry bedding, isolation of sick animals, adequate general hygiene, and ensuring calves receive adequate transfer of passive immunity through colostrum²⁸.

1.3 Cryptosporidium parvum Life Cycle

C. parvum infection begins with the ingestion of as few as 10 thick-walled oocysts²⁹. As the oocysts progress through the digestive tract, the reducing conditions and presence of pancreatic enzymes and bile salts in the small intestinal lumen trigger excystation⁷. Four sporozoites exit from

each oocyst as the infectious form of the parasite and invade surrounding intestinal epithelial cells (IECs). The invading sporozoites develop into trophozoites which can undergo asexual division to form merozoites in type 1 meronts³⁰. Following release from type 1 meronts, invasive merozoites can enter into adjacent IECs to form additional type 1 meronts, or they can develop into type 2 meronts. Merozoites released from type 2 meronts may enter host cells to form microgamonts and macrogamonts, the sexual stages of *C. parvum*. Fertilization of the microgamont by the macrogametes (released by the macrogamont) result in a zygote. The zygote may then evolve into either a thick or a thin wall oocyst containing four sporozoites. 80% of all oocysts produced are thick wall oocysts, which are released into the lumen of the intestine and excreted into the feces to infection other hosts. The remaining 20% are thin wall oocysts which excyst upon separation from the epithelium to perpetuate autoinfection in the current host⁷ (Fig 1).

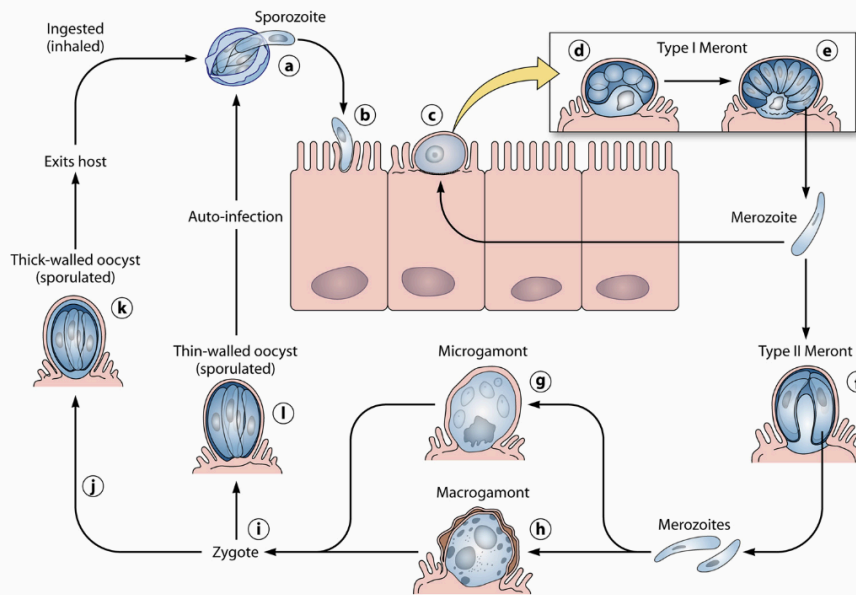


Figure 1: *Cryptosporidium* spp. life cycle⁷. Oocysts excyst from the lumen of the intestine (a). Sporozoites (b) enter the host cell and develop into trophozoites (c). Trophozoites undergo asexual division (merogony) (d and e) and form merozoites. Merozoites released from type 1 meronts enter adjacent host cells to form type I meronts or type II meronts (f). Type II meronts form the sexual stages, microgamonts (g) and macrogamonts (h) of *C. parvum*. Zygotes formed from the fertilization of the microgamont by microgametes, released from the macrogamont, develop into thick-walled oocysts (j) that are released into the lumen of the intestine to be excreted into the feces. A smaller percentage of zygotes form thin-walled oocysts that excyst to perpetuate auto-infection in the current host.

1.4 Human Cryptosporidiosis

Symptomatic infection by *C. parvum* is called cryptosporidiosis. The most characteristic symptom of cryptosporidiosis is profuse and prolonged watery diarrhea⁹. Other clinical features

include abdominal pain, nausea, vomiting, and low-grade fever. In addition, non-specific symptoms such as myalgia, weakness, malaise, headache, and anorexia may also occur on occasion⁹. The severity of human cryptosporidiosis is dependent on several host factors, mainly the hosts' immune status and the frequency of their exposure to *Cryptosporidium*.

In immunocompetent patients, cryptosporidiosis is often a transient and self-limiting disease, lasting up to 2-3 weeks. However, in immunocompromised patients, cryptosporidiosis can be extremely debilitating, resulting in progressive weight loss, dehydration, and wasting due to voluminous, persistent and life-threatening diarrhea (up to 17 L/day of stool)^{31, 32}. In addition, *Cryptosporidium* infection in immunocompromised individuals can also result in atypical manifestations, for example, biliary tract disease, respiratory tract disease, and pancreatitis³³.

1.5 The Immune Response against *Cryptosporidium*

1.5.1 Innate Immune Response

Intestinal epithelial cells (IECs) serve as the first mechanical barrier, as well as the initial target cell, of infectious sporozoites upon their release into the small intestine. IECs are capable of secreting anti-microbial peptides (AMPs), small polypeptides of less than 100 amino acids, with anti-microbial and immunomodulatory properties. AMPs produced by human IECs during a *C. parvum* infection include α - and β -defensins, as well as cathelicidins³⁴. IECs, in addition to expressing major histocompatibility complex (MHC) class I and class II molecules for antigen presentation³⁵, can constitutively express different pathogen pattern recognition receptors (PRRs), for example, toll-like receptors (TLRs) and nod-like receptors (NLRs)³⁶.

The TLR signaling pathway involves the recruitment of MyD88 and nuclear translocation of NF- κ B for subsequent chemokine and proinflammatory cytokine expression³⁵. *In vitro* studies using human biliary epithelial cells indicate that TLRs are integral in the initial of the inflammatory responses during *C. parvum* infection; TLR2 and TLR4, specifically, were recruited to the site of infection. Knockdown of MyD88, TLR2, or TLR4 expression in biliary epithelial cells resulted in the exacerbation of the *C. parvum* infection in cells due to the inhibition of downstream signaling pathways^{37, 38}. To date, no studies have investigated the role of TLR-mediated pathways in IECs or other immune cells with which the parasite is known to interact.

Chemokines produced by infected IECs promote the migration of a variety of innate leukocytes and phagocytic cells. At times, recruitment of such cells (e.g., example inflammatory

monocytes to the subepithelial space) can contribute to a loss of intestinal barrier function³⁹. Chemokines such as CCL2, CCL7, and CCL20 can also be beneficial, promoting dendritic cells migration into the ileum to allow for subsequent activation of naïve lymphocytes⁴⁰.

Cytokines also play an essential role in the anti-parasite response against *Cryptosporidium*. In particular, IL-18 is known to play a key role in limiting *C. parvum* infection. Upregulated IL-18 gene expression has also been found as a response to a *C. parvum* infection in many different contexts^{41, 42}. In addition, depletion of IL-18 in SCID (T- and B-cell deficient) mice significantly worsens disease outcomes; an effect that is reversed upon treatment with recombinant IL-18⁴³. IL-15 is also hypothesized to play an important role in *C. parvum* clearance. IL-15 is known to activate natural killer (NK) cells, $\gamma\delta$ -T cells, and other cell types to facilitate clearance of *C. parvum* from infected IECs⁴⁴. In seronegative individuals that do not produce IFN- γ in response to *C. parvum* infection, those with higher levels of IL-15 in their jejunal mucosa shed fewer oocysts than individuals that did not express IL-15⁴⁵.

Similarly, IFN- γ has also been found to play an integral role in the early clearance of *C. parvum* infection. Resistance to *C. parvum* infection was shown to be dependent on IFN- γ production in both nude mice (CD4+ T-cell depleted)⁴⁶, and in SCID mice^{47, 48}. Initial IFN- γ secretion by IECs inhibits the invasion and replication of *Cryptosporidium* spp. in host cells via an intracellular Fe²⁺ deprivation mechanism⁴⁹.

Macrophages and NK cells are also known secretors of IFN- γ ^{47, 50}. Macrophages, in addition to secreting IFN- γ , are also stimulated by IFN- γ . In both humans and in mice, activated macrophages can produce IL-12 to activate NK cells⁵¹; they may also produce nitric oxide (NO) from inducible nitric oxide synthase (iNOS) via the NF- κ B pathway to activate stress signaling cascades that ultimately results in apoptosis of infected cells⁵². Disruption to the iNOS pathway during a *C. parvum* infection can result in increased epithelial infection as well as oocyst shedding^{53, 54}.

NK-cells are regarded as a major source of IFN- γ early in the innate immune response. They are activated by various cytokines, for example IL-12, IFN- α/β , IL-15, TNF- α , and IL-18, produced by other innate immune cells present at the site of infection (i.e., DCs, macrophages, and IECs)⁵¹. Upon activation, NK cells have been shown to alleviate disease burden *in vitro* by lysing *Cryptosporidium*-infected epithelial cells via the release of cytotoxic granules⁴⁴. Mouse models lacking NK cells were found to be more susceptible to *C. parvum* infection. Compared to

Rag2^{-/-} mice deficient in T and B cells, Rag2^{-/-} γ_c^{-/-} mice that lack T cells, B cells, and NK cells, on average had higher oocyst excretion, as well as higher morbidity and mortality rates; the protective role of NK cells during a *C. parvum* infection was found to be primarily IFN-γ-dependent⁵⁵.

Unlike the previously mentioned cell types, the role of dendritic cells (DCs) in response to *C. parvum* infection is less well-understood. During infection, migration of DCs towards the site of *C. parvum* infection was found to be IFN-γ dependent⁴⁰. *In vitro*, DCs challenged with *C. parvum* sporozoites or antigens were found to release a plethora of cytokines, including type 1 IFNs, TNF-α, IL-6, IL-1b, IL-12, and IL-18^{56, 57}. In mice, DCs were observed to transport *Cryptosporidium* parasites and antigens to mesenteric lymph nodes, presumably to promote activation of adaptive immunity⁵⁸. Depletion of DCs in adult mice result in worsened intestinal pathology as well as a significant increase in the number of oocysts shed. Interestingly, when DC counts were increased by adoptive transfer, parasite burden was reduced once more⁵⁹. While there is a consensus that DCs contributes to the host immune response against *C. parvum*, further research is required to understand the role of DCs in the activation of the adaptive immune response.

Many innate immune knockout models are commonly used for the study of *Cryptosporidium* spp. infection. IFN-γR^{-/-} mice were initially developed as an alternative method for the large-scale production of *C. parvum* oocysts⁶⁰. Since then, the IFN-γR^{-/-} model, for which a *C. parvum* infection is lethal, compared to immunocompetent mice, has been used to evaluate a wide range of anti-*Cryptosporidium* agents^{60, 61}. Similarly, IFN-γ^{-/-} mice have also been engineered with a disruption to the IFN-γ gene and are extremely susceptible to *C. parvum* infection⁶². However, unlike the corresponding receptor knock out model, IFN-γ^{-/-} mice, despite their immunodeficiency, recover from *C. parvum* infection within a 3- to 4-week period⁶³. IL-12p40^{-/-} mice (deficient in both IL-12 and IL-23) are also commonly used as a model to investigate host resistance to *C. parvum* infection^{64, 65, 66}.

In conclusion, the innate immune responses have a significant protective role and are essential to control the intensity of *C. parvum* infection^{36, 51}. Even without any significant capacity to mount an adaptive immune response (e.g., SCID or Rag2^{-/-} mouse models), resistance to *C. parvum* infection can still be achieved.

1.5.2 Adaptive Immune Response: CD4+ T-Cells

The essential role of cell-mediated immune responses in a *C. parvum* infection has been well-established. Heine et al. were the first group to demonstrate the importance of T-cells; nude mice deficient in CD4+ T cells and infected with *Cryptosporidium* oocysts developed a persistent infection that was characterized by severe pathology, diarrhea, and death, whereas the wild type (WT) mice resolved *Cryptosporidium* infection between days 21 to 30⁶⁷. Adoptive transfer of WT thymocytes, spleen, and bone marrow cells into infected SCID mice showed functional immunological reconstitution, followed by the complete clearance of *C. parvum*⁶⁸.

Further research in SCID mice demonstrated that CD4+ T cells were the predominant cell type necessary to fight against *C. parvum*. Mice specifically deficient in major histocompatibility complex (MHC) class II, important for antigen presentation to CD4+ T cells, were significantly more susceptible to *C. parvum* infection compared to mice deficient in MHC class I which is important for antigen presentation to CD8+ T cells⁶⁹. Furthermore, administration of anti-CD4 monoclonal antibodies (mAb) reduced or completely eliminated the ability of SCID mice to resolve *C. parvum* infection, following adoptive transfer of splenocytes from immunocompetent donors⁷⁰. The same effect was not observed following treatment with either anti-CD8 mAbs or anti-asialo-GMI (to deplete NK cells) mAbs. Similarly, human studies have consistently shown that fulminant cryptosporidiosis predominantly occurs in immunocompromised individuals with CD4+ T cell counts of less than 50 cells/mm³. Individuals with CD4+ T cell counts greater than 180-200 cells/mm³ typically only experience a transient and self-limited form of the disease⁷¹.

To date, the role of T_h17 cells, derived from naïve CD4+ cells, in the context of a *C. parvum* infection remains unclear. During a *C. parvum* infection in immune-suppressed mice, IL-17, IL-6, TNF- α , TGF- β , and IL-23 levels, among other T_h17-produced cytokines, were significantly increased in gut-associated lymphoid tissue and the spleen, suggesting that T_h17 cells harbour a role in the host-*C. parvum* interaction⁷². However, no studies have investigated the direct involvement of T_h17 cells during infection.

In contrast, the contribution of T_h1 cells has also been thoroughly explored. IFN- γ , an integral cytokine in the innate immune response against *Cryptosporidium*, is produced by macrophages, NK cells, dendritic cells, and later by CD4+ T cells. Together with IL-12, this broad-based production of IFN- γ strongly promotes a T_h1-biased environment. These T_h1-type CD4+ cells will subsequently further secrete IFN- γ . induce IgG2 production⁷³, and promote the

differentiation of cytotoxic T cells from CD8+ precursors while simultaneously inhibiting T_h2 differentiation^{74, 75}. Together, the positive feedback of IFN- γ production and the stimulation of phagocytosis, neutrophil degranulation, and release of reactive oxygen species by T_h1 cells contributes to the elimination of intracellular pathogens, such as *C. parvum*^{76, 77}. Overall, it appears that a T_h1 response is necessary for the immunological control of a *Cryptosporidium* spp. infection.

Unlike the T_h1 response, the contribution of the T_h2 response during *Cryptosporidium* spp. infection is less clear⁷⁸. IL-4 promotes the differentiation of T_h2-type CD4+ T cells which then subsequently produce IgG1, IL-4, IL-5, and IL-10, as well as activate eosinophils⁷⁵. Enriquez and Sterling found that mice treated with mAbs that targeted IL-5 alone or both IL-4 and IL-5 experienced significant increases in their parasite burden and oocyst excretion⁷³. Similar results were obtained using IL-4 deficient mice: *C. parvum* infection was prolonged for 23 days compared to WT mice. Nevertheless, infection in IL-4^{-/-} mice was eventually resolved, with or without additional treatment⁷⁹. IL-4-producing CD4+ T cells in the mucosa were observed to increase during the latter stage of infection. This suggests that while T_h1 responses are important in controlling the severity early on, T_h2 responses may accelerate the termination of a *Cryptosporidium* infection.

In conclusion, the existing literature indicates that the predominant adaptive immune response required to control and resolve *C. parvum* infection is that of a T_h1-type CD4+ cell-mediated response. However, T_h2-type immune responses may play a supportive role later in infection, contributing to the rate at which the parasites are cleared.

1.5.3 Adaptive Immune Response: CD8+ T-Cells

Unlike CD4+ T cells, the role of CD8+ T cells in the context of a *C. parvum* infection remains less studied, and more speculative. An early study by Abrahamsen et al. revealed that CD8+ T cell counts increased by 60% following *C. parvum* infection in naïve calves. The CD8+ T cell counts within the intestinal villi of calves was increased after recovery from *C. parvum* challenge – an effect not observed with CD4+ T cells⁸⁰. *In vitro* studies of CD8+ T cells isolated from patients previously exposed to *Cryptosporidium* have showed that these cells are capable of lysing *C. parvum*-infected IECs, likely due to the release of cytotoxic granules⁸¹. However, to date, no study has shown the direct cytotoxic activity of CD8+ T cells on *Cryptosporidium* or

Cryptosporidium-infected cells. While CD8+ T cells also produce IFN- γ , in general, it is thought that CD8+ T cells primarily play a supportive role in cryptosporidiosis⁸¹.

1.5.4 Adaptive Immune Response: Humoral immunity

The role of humoral immune responses in *Cryptosporidium* spp. infection remains poorly understood. In general, antibodies produced against *Cryptosporidium* spp. play only a minor supportive role; they are insufficient by themselves to prevent infection^{82, 83} and are not needed for parasite clearance⁸⁴.

Cryptosporidium-specific serum IgG, IgM, and IgA, and fecal IgA have all been detected in humans following infection⁸⁵. In addition, higher IgG, IgM, and IgA responses are associated with cases of acute and asymptomatic disease compared to persistent cryptosporidiosis^{86, 87, 88}. Borad et al. found significantly increased serum IgG, IgM, and IgA responses to the *C. parvum* antigen P23 in *C. hominis*-infected children in Bangladesh compared to uninfected children. Similarly, Allison et al. observed increased IgG and IgA responses specific to the *C. parvum* antigen gp15 detected in the same Bangladeshi children⁸⁸. However, neither of these studies demonstrated that the increased antibody titers protected against infection.

In immunocompromised mouse models, mAbs against specific *C. parvum* antigens were found to partially reduce oocysts shedding and parasite burden. For example, oral gavage of anti-*C. parvum*-antigen-1 IgM mAbs was found to significantly reduce both intestinal infectivity scores and oocyst shedding in SCID mice⁸⁹. Riggs et al. also discovered that administering anti-CSL IgM mAbs provided a 39% reduction in intestinal infection in SCID mice depleted of IFN- γ , a highly significant reduction compared to the untreated control⁹⁰. In a separate study, Enriquez and Riggs demonstrated that IgA mAbs specific for the P23 *C. parvum* surface protein reduced intestinal parasite burden by up to 72%⁹¹. While these data indicate that anti-*C. parvum* mAbs are can modulate persistent infection by *Cryptosporidium*, they appear incapable of fully eliminating parasite burden by themselves.

In humans, the use of hyperimmune bovine colostrum (HBC) has demonstrated positive therapeutic effects. HBC is obtained from cows hyperimmunized with oocyst-sporozoite mixtures, with approximately 10% of the total antibodies being parasite-specific⁹². In two separate case studies, use of HBC to treat cryptosporidiosis in immunocompromised hosts led to temporary resolution of disease (cessation of diarrhea and oocyst presence in the stool), indicating partial

protection, but eventually, cryptosporidiosis did recur in each case^{93, 94}. Nord et al. also demonstrated reductions, albeit non-significant, in diarrhea and excreted oocysts in two of three patients treated patients⁹⁵. Treatment with bovine colostrum immunoglobulins (BCIg) alone has more clearly exhibited reductions in clinical pathology. Plettenberg et al. discovered treatment with 10 g of BCiG led to either a complete or partial remission of chronic diarrhea in five of seven AIDS patients with cryptosporidiosis⁹⁶. Similar, Rump et al. observed that five of seven immunocompromised patients afflicted with cryptosporidiosis cleared the parasite following 10 days treatment with 10% BCiG in their drinking water⁹⁷. Unfortunately, due to the variety of different colostrum administered between different studies as well as the conflicting information presented in the literature, it remains difficult to ascertain the exact therapeutic effects of bovine colostrum in the treatment of cryptosporidiosis.

In conclusion, the importance of humoral immunity during a *C. parvum* infection remains an open question. As *Cryptosporidium* spp. are intracellular pathogens, the antibody response raised during infection is speculated to target extracellular invasive stages. The binding of antibodies to such surface antigens of the parasite could disrupt attachment or entry into host enterocytes⁹². However, as previously noted, the humoral response to *C. parvum* infection appears to play only a supportive role in protection and parasite clearance. It is unclear whether or not antibody responses represent a redundant and non-essential mechanism, or perhaps are markers of other underlying immune responses⁸⁵.

1.6 Diagnostics

1.6.1 *Microscopy and Histology*

Detection of oocysts in stool samples by microscopic examination remains one of the most common ways for the clinical diagnosis of cryptosporidiosis. However, this technique is limited in its detection sensitivity due to both the small size of oocysts, (detection limit of $\sim 10^4$ oocysts/gram of feces), as well as the differing consistencies of the stool sample. While oocysts can be detected by light microscopy or phase-contrast microscopy, the smooth, colourless, and small size of oocysts (ranging from 3-8 μm) make them extremely difficult to identify for non-expert microscopists⁹⁸. As such, oocyst samples are often concentrated in a sugar solution and stained to allow for a 100-fold increase in sensitivity, resulting in a 100-fold improvement in sensitivity (i.e., a detection limit of 10^6 oocysts/g of feces⁹⁹). Staining is performed with tinctorial

stain, such as acid fast, or, to achieve higher sensitivity, with fluorescent or immunofluorescent labelled antibodies for against oocyst wall proteins¹⁰⁰.

Observation of *Cryptosporidium* in intestinal mucosal biopsies was also an early method of cryptosporidiosis diagnosis. Various stages of the parasite could be observed in the brush border of the intestinal mucosa without special staining of the tissue sections. The parasites may appear as small, basophilic spherical structures ranging from 3-5 µm, arranged in rows or clusters¹⁰¹. Presently, histological analysis is rarely used as a diagnostic method due to the invasive procedure to obtain samples, random sampling (as not all regions of the intestine are infected during cryptosporidiosis), and the expertise required to carefully process the sample. Additionally, the procedure is both expensive and time-consuming, making it inefficient as a routine diagnostic method.

1.6.2 Immunoassays

Immunological methods of diagnosis rely on either antigen or antibody detection. While antigen assays vary in their sensitivity (66.3-100%), they are often a preferential diagnostic method as they do not require skills in microscopic identification, and have very high specificities (93%-100%)¹⁰². These tests offer the advantage of fast and efficient processing of multiple samples.

Antibodies specific against *C. parvum* oocyst wall antigens are commercially available for diagnostic purposes. However, as different species and genotypes of *Cryptosporidium* vary to some degree in their expression of individual epitopes on the oocyst surface, fluorescence levels can vary widely in intensity and negative samples should be confirmed with another technique (e.g. PCR)¹⁰¹. Enzyme reporter-labelled antibodies are also available commercially, in enzyme immunoassay (EIA), enzyme-linked immunosorbent assays (ELISAs), and immunochromatographic (IC) formats, for diagnostic purposes. Copro-antigen detection with ELISA tests are reported to have variable detection limits, ranging from 3 x 10⁵ to 10⁶ oocysts/g of feces, similar to that of microscopy¹⁰³.

1.6.3 PCR

PCR-based methods are reported to be higher in sensitivity than conventional and immunological assays for the detection of *Cryptosporidium* oocysts¹⁰⁴. However, the cost of PCR, as well as the time and the expertise required for this technique are all high compared to other

diagnostic approaches. Furthermore, PCR detection from tissue or stool samples are dependent on effective DNA extraction¹⁰⁵, and the natural robustness of oocysts often require additional rigorous steps, such as chemical treatment, freeze-thaw cycles, or boiling, to access sporozoite DNA⁷. The 18s ss rRNA gene¹⁰⁶, the *Cryptosporidium* oocyst wall protein¹⁰⁷, a 70kDA heat shock protein¹⁰⁸, and a 60kDA glycoprotein¹⁰⁵ serve as the most common targets for PCR-based diagnoses. When included in multiplex gastrointestinal parasite panels, PCR assays are typically only able to identify the *Cryptosporidium* genus. However, PCR-restriction fragment length polymorphism, PCR sequencing, or real-time PCR assays are frequently used for specific species identification⁷.

1.7 Vaccine Development against *Cryptosporidium* spp.

1.7.1 Attenuated Vaccines

The use of attenuated *Cryptosporidium* spp. as a prophylaxis vaccine has been limited in the field. While previous research has shown live-attenuated vaccines to be the most effective at generating a long-lasting memory immune response¹⁰⁹, not only may attenuated vaccines cause disease in immunocompromised hosts, the impossibility of continuously propagating *C. parvum* *in vitro* makes this approach completely impractical at the current time⁵⁰. One study, however, demonstrated the use of γ -irradiation as a means to attenuated oocysts. In this work, *C. parvum* oocysts exposed to 400 Gy were incapable of replicating in the host and provided partial protection in calves, but only when challenged three weeks post-vaccination¹¹⁰.

1.7.2 *Cryptosporidium* Antigens and their Potential as Vaccine Candidates

Development of subunit-based vaccines against *C. parvum* depends on the selection of either one, or multiple, immunogenic antigens. Specifically, in the case of *Cryptosporidium*, proteins involved in locomotion, attachment, and invasion of host cells are of the most interest, for example, P23, CSL, Cp15/17, Cp23/27, Cp40/45, gp900, Muc4, and Muc5^{7,50,84}.

The surface proteins Cp15 and Cp23 in particular are attractive targets. Cp15 is surface protein present on both sporozoite and merozoite stages of *C. parvum*. It is a proteolytic product of the precursor glycoprotein Cp60 and remains non-covalently associated to Cp40 following cleavage¹¹¹, attached to the parasite membrane surface via a glycosylphosphatidylinositol linkage¹¹². Similarly, Cp23 is a surface protein present on both the sporozoite and merozoite stages of *C. parvum*. Both Cp15 and Cp23 antigens were recognized by serum antibodies in infected

mice, rabbits, calves, lambs, pigs, as well as 10 AIDS patients, suggesting their immunogenicity across different species¹¹³.

1.7.3 Recombinant Protein Vaccines

Recombinant protein vaccines involve manipulation of bacterial, yeast, mammalian, or insect cells to induce the expression of engineered antigenic sequences, and subsequent purification of the resulting protein.

Recombinant Cp23 has been previously demonstrated to induce cellular proliferative responses from splenocytes *in vitro*⁶². Furthermore, subcutaneous administration of recombinant Cp15-23, a fusion product of Cp15 and Cp23, in BALB/c mice demonstrated significant increases in not only serum IgG titers, but also antigen-specific CD4+ and CD8+ cell recruitment¹¹⁴. Subcutaneous vaccination of the same recombinant Cp15-23 fusion protein resulted in a reduction in oocyst shedding in BALB/c mice challenged with *C. parvum*¹¹⁵. Perryman et al. showed that treatment of calves with immune colostrum, generated by hyper immunization of cows with recombinant Cp23, prevented diarrhea and decreased oocyst excretion following *C. parvum* challenge¹¹⁶. The use of recombinant protein vaccines, however, is often insufficient to elicit a protective and long-lasting immune response¹¹⁷.

1.7.4 DNA-Based Vaccines

DNA-based vaccines were developed in the mid-twentieth century and proved to be more effective in stimulating both humoral and cellular responses *in vivo*, in addition to being safer and more cost efficient, compared to more traditional methods of vaccination¹¹⁸. DNA vaccines allow for the delivery of one or more genes, leading to the direct expression of the encoded antigen(s) by host cell machinery.

Numerous DNA vaccines encoding *C. parvum* antigens have been tested for their immunogenicity and efficacy in animal models. Nasal immunization with Cp15-DNA cloned onto a plasmid in BALB/c mice developed specific and long-lasting intestinal IgA and serum IgG antibodies that lasted up to one year following initial vaccination¹¹⁹. DNA vectors encoding a combination of *C. parvum* surface proteins Cp12 and Cp21 were delivered intranasally to BALB/c mice, resulting in the increase of serum IgG and significant increases in *Cryptosporidium*-specific CD4+ and CD8+ counts in the spleen, which likely explains the observed decrease in oocyst

shedding by up to 77.5% following challenge¹²⁰. In IL-12p40 knock-out (KO) mice, subcutaneous injection of Cp23 cloned into a DNA vector induced significant anti-Cp23 IgG responses, as well as antigen-specific *in vitro* splenocyte proliferation, both of which likely contributed to a 50-60% reduction in oocyst shedding following challenge⁶⁶. A second research group, also using IL-12p40 KO mice, showed intramuscular (IM) vaccination with a recombinant plasmid containing both Cp15 and Cp23 encoding genes gave both a strong lymphoproliferation response, as well as a significant increase in serum IgG, which led to a decrease in the oocyst burden and a shortening of the infection period upon subsequent challenge⁶⁵. Together, the data from these papers indicate that in both wild type and immunocompromised mouse models, administration of DNA vaccines encoding *C. parvum* antigenic proteins can be both immunogenic, and at times protective, against *C. parvum* infection.

1.7.5 The Use of Bacterial Vectors

Parasite and bacterial vectors expressing *Cryptosporidium* spp. antigens have been explored extensively in *C. parvum* vaccine research. In addition to their ease of administration and the low production costs, bacterial vectors can also offer the advantages of a localized antigen delivery and a directed immune response^{121, 122}. The use of *Salmonella enterica*, in particular, has been favoured as a delivery vector for *C. parvum* antigens in the past decade. Orally-delivered *Salmonella* not only has the ability to survive the physiological stresses encountered in the gastrointestinal tract, *S. enterica* invasion of IECs occurs at the same location as *C. parvum*, resulting in a strong mucosal immune response.¹²² Furthermore, the type 3 secretion system (T3SS) of *Salmonella* spp. can be exploited to translocate recombinant antigens into the host cell cytoplasm at specific stages of invasion.

Several attenuated *S. enterica* serovars were previously investigated as possible vectors for the delivery of *C. parvum* antigens. An attenuated *S. enterica* serovar Typhimurium strain SL3261 was engineered as the delivery system for the *C. parvum* antigens Cp23 and Cp40 fused to fragment C of the tetanus toxin. When IL-18 KO mice were vaccinated orally with 5 x 10⁹ colony forming units (CFU)/mouse of *S. Typhimurium* expressing either Cp23 or Cp40, serum IgG specific for both Cp23 and Cp40 were detected 35 days after immunization. Serum and mucosal IgA were also detected in 30% of the mice immunized with the Cp23-expressing vector. In addition, when evaluating a prime-boost immunization with an initial subcutaneous immunization

using DNA vectors encoding either Cp23 or Cp40, followed by oral immunization with the transformed *Salmonella* live vector expressing each respective antigen, antibody responses were significantly higher¹²³. Two additional studies have evaluated a different serovar, *S. enterica* serovar Typhi CVD 908-*htrA*, as a live delivery vector. In C57BL/6 mice, Manque et al. delivered an intranasal inoculation of 1×10^9 CFU/mouse of *Salmonella* Typhi containing either Cp15, profilin, or a *Cryptosporidium* apyrase (CApy) fused to cytolysin A (ClyA). A secondary immune “boost” was delivered intraperitoneally 14 days following initial vaccination with each respective recombinant protein. All antigens appeared to elicit a strong antibody response in mice consisting of predominantly of IgG1 antibodies, indicating induction of a T_h1 skewed immune response. In addition, cytokines profiling of restimulated splenocytes revealed that all three antigens induced the production of IFN- γ and IL-6, characteristic of a T_h1 response¹²⁴. In a later study, Roche et al. then explored the effects of the same Cp15 antigen fused to ClyA expressed by *Salmonella* Typhi in a malnourished mouse model. Nourished and malnourished mice were inoculated intranasally (IN) twice with 1×10^9 CFU/mouse of attenuated *Salmonella* Typhi expressing Cp15-Cly A. Mice then received intraperitoneal injections of recombinant Cp15 10 days following initial inoculation, and again ten days after each of the IN doses. Despite increased production of IL-6, IFN- γ , and Cp15-specific IgG in both nourished and malnourished mice after vaccination, the prime-boost regimen was not sufficient to prevent weight loss and only resulted in the transient reduction of oocyst shedding in stool¹²⁵. While data in this field remain limited, these studies demonstrate that recombinant *Salmonella* can serve as a feasible vaccine delivery system for *C. parvum* vaccines.

Parasite vectors have also been previously investigated as a delivery method for *Cryptosporidium* spp. antigens. Use of apicomplexan parasites similar to *Cryptosporidium*, for example *Toxoplasma gondii*, to express *C. parvum* antigens offers the added advantage of post-translational modifications to produce antigens more similar to native *C. parvum* proteins¹²⁶. Gp40, a third immunodominant *C. parvum* surface antigen, Cp15, and Cp23 have all been successfully expressed in *T. gondii*, and the resulting antigen products were found to have similar glycosylation patterns, molecular weights, and antigenic properties to that of their native protein equivalents¹²⁷.¹²⁸. In addition, a study by Shirafuji et al. showed that mice immunized intraperitoneally with lysed *T. gondii* expressing Cp23 produced high levels of serum IgG1, indicative of a T_h1 response¹²⁸. However, despite the promise of generating recombinant antigens similar to native proteins, the

use of live *T. gondii* as a delivery vector poses a significant disease risk in humans. Future uses of *T. gondii* as a parasite vector would require its attenuation to some degree at the very least. Alternatively, immunization with solely the purified recombinant protein expressed by *T. gondii* is also an option¹²⁹.

1.7.6 *The Prime-Pull Vaccine Approach*

As previously described, the prime-pull strategy involves an initial “priming” step using conventional vaccination to elicit systemic T-cell responses, followed by a secondary localized application of a stimulus to “pull” immune cells to a target tissue to establish long-term local immunity¹³⁰. The prime and pull approach is one method of increasing and establishing persistent mucosal responses, presumably an important characteristic for any candidate *C. parvum* vaccine. Current studies featuring prime-pull strategies have varied greatly in the components administered as the “prime” and the “pull”. Overall, however, prime-pull methods in general have been found to outcompete other vaccination strategies in eliciting strong local immune responses^{123, 124, 125}.

1.7.7 *The Role of Adjuvants*

Adjuvants, in the context of vaccine studies, are additional components administered along with a vaccine to both direct the pattern of the immune response, as well as build a more protective and long-lasting response. Adjuvants can also act to broaden the immune response that would not otherwise be elicited. For example, recombinant protein vaccines often lack the inherent immunostimulatory property of the native antigen, and thus limit the host to a modest antibody response with minimal T cell activation. Introduction of an adjuvant that stimulates specifically a cell-mediated immune response can then better establish that initial immune response. In the case of *C. parvum*, as cell-mediated immune responses, in particular CD4+ T cell responses, are crucial for overcoming infection, adjuvants that enhance a TH1 response, such as dsRNA analogues, lipid A analogues, imidazoquinolines, and CpG oligodeoxynucleotide (ODN), would be a much added benefit to any vaccine candidate¹³¹. All four of the aforementioned adjuvants are immunomodulatory molecules that can serve as ligands for toll-like receptors (TLRs) to activate downstream transcription factors, for example, nuclear factor-kB (NF-kB).

In the development of different *C. parvum* candidate vaccines, Freund’s Complete Adjuvant (CFA) has been a very popular choice as an adjuvant^{114, 115, 124, 125}. CFA is composed of a

mixture of light mineral oil, mannide monooleate, and heat-killed mycobacterial cells. While effective in stimulating both a significant humoral and cellular-mediated immune response, CFA is toxic and induces not only inflammation, but also tissue necrosis and ulceration¹³². Thus, consideration of not only the effectiveness of adjuvants, but their safety, is essential in the vaccine development process.

1.8 *Salmonella enterica* Typhimurium YS1646

Salmonella enterica are gram-negative, facultative anaerobic bacilli. They are motile by their peritrichous flagella, and range in size from 2-5 microns long to 0.5-1.5 microns wide. In total, amongst the two species of Salmonellae, *S. enterica* and *S. bongori*, there are six documented subspecies that include over 2,500 serovars¹³³.

In the United States, *Salmonella* is the number one foodborne pathogen with the greatest mortality and highest cost burden¹³⁴. In humans, *S. enterica* invades IECs where it causes salmonellosis that typically manifests as gastroenteritis, but can more rarely cause sepsis or enteric fever¹³³. As previously mentioned, *S. enterica* serovars use a T3SS during defined stages of invasion that inject *Salmonella* effector proteins directly into the host cell cytoplasm to allow for manipulation of host cell functions¹³⁵. In the case of *Salmonella*, these effector proteins produced promote the internalization of the bacterium into a *Salmonella*-containing vacuole (SCV) in the non-phagocytic host cell¹³⁶. Programmed cell death of the infected cell by pyroptosis of the infected cell may then contribute to an inflammatory host response as *Salmonella* continues to replicate rapidly in the cytoplasm for re-entry into other epithelial cells¹³⁷.

Despite the pathogenic potential of *S. enterica* serotypes, many researchers have worked on attenuating and adapting *S. enterica* for numerous other uses^{138, 139, 140}. In particular, live attenuated *S. enterica* strains have been explored extensively for use as vaccine vectors, not only because they can induce long-lasting mucosal, humoral, and cellular immunity, but also because they are inexpensive¹⁴¹. Among the candidate *S. enterica* vectors, *S. enterica* Typhimurium YS1646 (previously known as VNP20009) may have particular promise. With deletions of the *purI* (purine biosynthesis pathway) and *msbB* (lipopolysaccharide production) genes¹⁴², the potential pathogenicity of the YS1646 strain has been greatly reduced. In addition, because of these mutations, the YS1646 strain does not induce TNF- α production, thus reducing the risks of septic shock in the host¹⁴³. In the late 1980s and early 1990s, *Salmonella* YS1646 was tested

extensively in animal models as a possible cancer therapeutic and was safely in humans during a phase 1 clinical trial in subjects with advanced cancer at doses up to 3×10^8 CFU delivered intravenously¹⁴⁴. In the Ward/Ndao laboratories, YS1646-based vaccine candidates for *Clostridium difficile* and *Schistosoma mansoni*, have also been created, both of which show considerable promise in murine vaccination-challenge models^{145, 146}.

1.9 Treatments

Treatment for cryptosporidiosis is very limited. Currently, nitazoxanide (Alinia®, Romark Laboratories, Tampa, FL), a broad-spectrum anti-parasitic/anti-viral drug, is the only FDA approved treatment available for individuals one year of age and older. While nitazoxanide has been shown to be 93% effective in facilitating parasite clearance in immunocompetent patients¹⁴⁷, it is ineffective in immunocompromised patients, for example, in AIDS patients¹⁴⁸ and in organ transplant recipients¹⁴⁹. Azithromycin can provide some symptomatic relief for cryptosporidiosis in AIDS patients, but it is not effective in parasite clearance from the host¹⁵⁰. Although paromomycin can reduce/stop oocyst shedding when used as a treatment in BALB/c mice¹⁵¹ and prevent infection when used prophylactically in goat kids¹⁵², it was not helpful in treating cryptosporidiosis in AIDS patients¹⁵³. In otherwise healthy Egyptian children, however, treatment with 25 mg/kg/day of paromomycin for a period of two weeks resulted in complete clearance of oocysts and cessation of clinical symptoms in 68.8% of individuals¹⁵⁴. Rifamycins have also been studied for their anti-*Cryptosporidium* activity. Rifabutin, when tested *in vitro* on toe cell monolayers, revealed a 25% decrease in *C. parvum* infection by itself, and a 75% decrease when combined with nitazoxanide¹⁵⁵. In HIV-infected patients, rifabutin was shown to have a prophylactic effect of 85% compared to the negative treatment group¹⁵⁶. Rifaximin, a non-absorbed derivative of rifamycin, effectively treated diarrheal symptoms in a small group study of five HIV patients diagnosed with symptomatic cryptosporidial diarrhea¹⁵⁷. The use of hyperimmune bovine colostrum (HBC) has also, in isolated cases, been proven to be effective in eliminating *Cryptosporidium*-caused diarrhea, as well as reducing, or even eliminating, oocyst counts in the stool^{94, 95}.

In more recent years, drug development against cryptosporidiosis has focused on identifying specific targets of *Cryptosporidium* with no human homologue. Current research has identified several *Cryptosporidium* enzymes as potential targets. Inhibitors of *Cryptosporidium*

CDPK1, a unique calcium-dependent protein kinase essential for cell invasion, have been found to exhibit anti-*Cryptosporidium* activity, decreasing and, at times, eradicating, the parasite in both an *in vitro* HCT-8 cell model, as well as in SCID-beige mice¹⁵⁸. K11777, an inhibitor of Clan CA cysteine, a protease also essential for cell invasion, has also been shown to rescue immunocompromised IFN γ -receptor KO mice from an otherwise lethal infection in the Ndao laboratory⁶¹. While numerous inhibitor drugs are currently being evaluated, the limitations of the current experimental models for cryptosporidiosis have slowed the discovery and progression of novel drugs for this parasite. Animal models are often suboptimal representations of human infections¹⁵⁹. The use of human cell lines is also limited as many parasites – including *Cryptosporidium* species – are unable to propagate even in primary human cells as they would *in vivo*¹⁶⁰. Thus, the research presented above highlights the need for new approaches to *C. parvum* infection including prophylactic vaccines, especially strategies with the potential to be effective in immunocompromised individuals.

1.10 Conclusions and Future Directions

The current understanding of the elicited immune responses following *C. parvum* infection remains incomplete, acting as a barrier to the development of an effective, prophylactic vaccine. The innate immune system functions to help control the intensity of a *C. parvum* infection primarily through the production of proinflammatory cytokines (i.e. IL-18 and IFN- γ) and the recruitment and activation of macrophages and NK cells. The subsequent adaptive immune response acts to clear *C. parvum* infection and prevent later reinfection predominantly via the action of a TH1-type cell-mediated response including the expansion of CD4+ T cells that produce IFN- γ which mediates the killing of infected IECs. Humoral responses play a secondary, supportive role in resolving cryptosporidiosis. However, even without an adaptive immune response, as is the case in SCID or Rag2^{-/-} mouse models, resistance to *C. parvum* infection can still be achieved.

Thus, a vaccine against *Cryptosporidium* spp. should prioritize the establishment of a strong TH1 cell-mediated immune response with a supporting TH2 humoral immune response. A significant mucosal response would also be beneficial in the case of a prophylactic *C. parvum* vaccine as the parasite infects the host at the intestinal epithelia and typically lives out its entire life cycle in this peripheral position. In addition, incorporation of vaccine strategies such as the

prime-pull approach may enhance the effectiveness of a vaccine, providing a more targeted and localized immune response to fight *C. parvum* infection.

1.11 Rationale and Research Objectives

Classified by the US Centers for Disease Control as a Bioterrorism Category B agent and present in over 95 countries, *Cryptosporidium parvum* is a human pathogen of significant concern^{161, 162}. Currently, treatment of cryptosporidiosis with nitazoxanide is only marginally effective in immunocompetent hosts, hence no treatment strategies are available to the most at-risk immunocompromised populations. This thesis explores the development of a novel vaccine against *C. parvum* using an attenuated *Salmonella* strain as a delivery vector. *C. parvum* surface proteins Cp15 and Cp23, both individually and as a combined fusion protein Cp15-23, were selected as the target vaccine antigens. As the selected proteins are present during multiple stages of the life cycle of *Cryptosporidium*, we reasoned that this would increase the probability of vaccine-induced protection against *Cryptosporidium* infection. Both proteins were also previously shown to be immunogenic in multiple animal models as well as in 10 AIDS patients¹¹³, and have previously been expressed using an attenuated *S. enterica* vector^{123, 124, 125}. In addition, vaccination with a recombinant Cp15-23 protein has previously been shown to increase antigen-specific humoral and cellular-mediated responses in BALB/C mice, as well as reduce oocyst shedding upon *C. parvum* challenge^{114, 115}. Through delivering these three antigens using an attenuated *Salmonella* vector to IECs, coincidentally also the site of a natural *C. parvum* infection, we hope to establish a lasting cellular and mucosal immune response that is protective against a secondary infection. To date, no studies have investigated the immunological effects of these three antigens, delivered via an attenuated *Salmonella* vector, in the context of a *C. parvum* infection model.

The first and principal objective of this thesis was to generate a candidate YS1646-based oral vaccine to deliver the Cp15-23 fusion protein in a prime-boost, multi-modality vaccination strategy in C57BL/6 mice (i.e., combined intramuscular and oral vaccination). The second objective was to evaluate the immunogenicity of the Cp15 and Cp23 antigens, both individually and in combination, again using a prime-boost, multi-modality vaccination strategy in C57BL/6 mice. The last objective was to evaluate the protection against *C. parvum* challenge afforded by prime-boost vaccination of intact animals and adoptive transfer of serum IFN- γ receptor knock out mice.

2. Methods

2.1 Plasmid Construct Preparation

2.1.1 For Protein Expression by YSI646

The Ward lab has previously designed plasmid constructs for the purpose of antigen expression by *S. Typhimurium*. *Salmonella* spp. encode two different effector transport systems (i.e., type III secretion systems) within *Salmonella* pathogenicity islands (SPI) 1 and 2. Two promoter-secretion signal combinations were engineered. The first contained the NirB promoter (pNirB) and SspH1 secretion signal that guide proteins into either SPI1 or SPI2 type III secretion system and allows for translocation of the protein across the plasma membrane or the vacuolar membrane, respectively¹⁶³. The SspH1 secretion signal was found under Genbank CP001363.1 locus STM14_1483. The second contained the SspH2 promoter (pSspH2) and SspH2 secretion signal, which allows for translocation through only the vacuolar membrane via SPI2¹⁶⁴. The SspH2 secretion signal was found under Genbank CP001363.1 locus STM14_2769. Primers were designed to flank each promoter-secretion signal sequence with the Xho1 and Not1 restriction sites at the 5' and 3' end, respectively. The two promoter-secretory signal combinations were then inserted into a pQE-30 backbone containing an ampicillin resistance gene (Qiagen; Hilden, Germany). The empty pQE30 backbone was designated as pQE_Null.

2.2 Codon Optimization of Cp15-23

The Iowa strain of *Cryptosporidium parvum* Cp15 and Cp23 nucleotide sequences (GenBank Accession Numbers XM_628602 and U34390, respectively), joined via a four amino acid (GSSG) linker sequence, were used to construct the Cp15-23 fusion protein sequence¹¹⁴. The full sequence was optimized for *Salmonella* protein expression using the Java Codon Adaptation Tool (JCat)¹⁶⁵. The end of the recombinant sequence included an additional proline linker, 6X histidine tag, and a final TAA stop codon. The optimized cDNA was synthesized by GenScript in a pcDNA3 vector.

2.3 pQE30 Plasmid Construction for Cp15, Cp23, and Cp15-23 Protein Expression by YS1646

2.3.1 *PCR Amplification of Cp15, Cp23, and Cp15-23 Sequences*

Four primers were designed for the amplification of the individual Cp15 and Cp23 sequences, to exclude any linker sequences, as well as the whole Cp15-23 fusion sequence. The following primers were used: Cp15 Fwd, 5'-AAG GAA AAA AGC GGC CGC ATG GGC AAC CTG AAA T-3'; Cp15 Rvs, 5'-GGC GCG CCT TAA TGA TGA TGA TGA TGA TGC GGG TTG AAG TTC GGT TTG AAT-3'; Cp23 Fwd, 5'-AAG GAA AAA AGC GGC CGC GGC TGC TCT TCT TCT AAA C-3'; Cp23 Rvs, 5'-GGC GCG CCT TAA TGA TGA TGA TGA TGA TG-3'. Both forward primers carry the Not1 restriction enzyme site, and both reverse primers carry the Asc1 restriction enzyme site for subsequent integration into expression plasmids. PCR using Q5 ultrahigh fidelity DNA polymerase (New England Biolabs; Ipswich, USA) was used to amplify the full Cp15, Cp23, and Cp15-23 sequences, independent of the pcDNA3 plasmid.

2.3.2 *Digestion of Amplified Cp15, Cp23, and Cp15-23*

1 µg of Cp15, Cp23, or Cp15-23 was digested with 1 µL of Not1 and 1 µL of Asc1 restriction enzymes (New England Biolabs; Ipswich, USA) in 5 µL of 10X NEBuffer. The total reaction volume brought to 50 µL total using sterile demineralized distilled water (ddH₂O). The mixture was incubated at 37°C for 2 hours. pSspH2 and pNirB pQE30 constructs were digested in the same manner. Following incubation, 5 µL of 6X loading dye was added into each digestion and the samples were separated via gel electrophoresis on a 1.0% agarose Tris-acetate-EDTA gel. The digested fragments and vectors were visualized on a UV table and excised from the gel using a scalpel blade. DNA fragments were purified from the agarose gel using the Monarch Gel Extraction Minikit (New England Biolabs, Ipswich, USA).

2.3.3 *Ligation of Cp15, Cp23, and Cp15-23 into pQE30 constructs*

5 µL of a selected digested vector, 5 µL of a selected purified digested insert, 7 µL of nuclease-free water, 2 µL of the 10X T4 DNA ligase buffer, and 1 µL of T4 DNA ligase (ThermoFisher Scientific; Waltham, USA) were mixed together in a 1.5 mL Eppendorf tube. The ligation mixture was incubated at room temperature overnight. pSspH2 or pNirB were used as vectors, and Cp15, Cp23, or Cp15-23 used as inserts.

2.3.4 Transformation of Ligated pQE30 constructs into DH5α *E. coli*

Eppendorf tubes of 25 µL of DH5α competent *E. coli* cells (ThermoFisher Scientific, Eugene, USA) were thawed on ice for 10 minutes. 2 µL of the selected ligation mixture was added to the cells and mixed gently by flicking. Mixtures were kept on ice for 30 minutes. The tubes were then heat shocked at 42°C for 45 seconds and then immediately placed back on ice for 5 minutes. 100 µL of Luria-Bertani (LB) broth was added to the mixture and the tubes were kept on a shaking incubator at 37°C and 250 RPM for one hour. The liquid cultures were then plated on LB-agar plates containing 50 µg/mL ampicillin and incubated overnight at 37°C. Individual colonies were then selected and evaluated for sequence insert integration by colony PCR. Colonies that had successfully been transformed with ligated pQE30 constructs were selected for DNA extraction. Selected colonies were used to inoculate 5 mL of LB broth with 50 µg/mL ampicillin. Liquid cultures were grown overnight at 37°C and 250 RPM. Plasmid extractions were performed the following day, as per the manufacturer's protocol, using the QIAprep Spin Miniprep Kit (Qiagen; Germantown, USA). Purified plasmids were stored at -20°C.

2.3.5 Sequencing of Constructs

Six constructs were successfully created for the expression of either Cp15, Cp23, or Cp15-23 by *S. Typhimurium* YS1646: pSspH2_Cp15, pSspH2_Cp23, pSspH2_Cp15-23, pNirB_Cp15, pNirB_Cp23, and pNirB_Cp15-23. To verify proper insertion of the *C. parvum* antigenic sequences, the purified constructs were sent to Genome Quebec for Sanger Sequencing. The previously designed amplification primers were used for sequencing.

2.4 Oral Gavage Vaccine Preparation: Transformation of YS1646

pSspH2_Cp15, pSspH2_Cp23, pSspH2_Cp15-23, pNirB_Cp15, pNirB_Cp23, pNirB_Cp15-23, and pQE_Null were transfected into *S. Typhimurium* YS1646 via electroporation. Electrocompetent YS1646 cells were thawed on ice. 40 µL of *Salmonella* and 20 µL of the selected plasmid miniprep were added to a pre-chilled electroporation cuvette and loaded into the Gene Pulser Xcell (BioRad; Hercules, USA). The cell mixture was pulsed at 3.0kV, 200W and 25µF. 1 mL of cold LB broth was then immediately added to the cuvette and the mixture transferred to a 15 mL polypropylene tube. The tube was incubated on a shaker at 37°C and 250 RPM for 2 hours. The mixture was then plated on 50 µg/mL ampicillin LB-agar plates and left to

incubate overnight at 37°C. The following day, any observed colonies were picked and grown again overnight in 50 mL LB broth with 50 µg/mL ampicillin. The cultures were spun down and resuspended in LB with 15% glycerol and stored at -80°C.

2.5 pET-28b Plasmid Construction for Cp15, Cp23, and Cp15-23 Recombinant Protein Expression by *E. coli*

The pET-28b plasmid (Novagen; Burlington, USA) was used as the backbone for the purposes of recombinant protein expression by competent BLR DE3 *E. coli* (Millipore-Sigma; Burlington, USA). In addition to a kanamycin resistance gene, the pET-28b plasmid contains an isopropyl-β-D-1-thiogalactopyranoside (IPTG)-inducible promoter. Identical to the cloning protocol to create the pQE30 constructs, the pET-28b plasmid was first subjected to restriction enzyme digestion with Not1 and Asc1, before undergoing ligation with either the Cp15, Cp23, or Cp15-23 sequence insert. Completed ligations were then used to transform DH5α competent *E. coli*, and successful colonies observed on the 50 µg/mL kanamycin-containing LB-agar plates were selected and grown for plasmid extraction. Three constructs, pET28_Cp15, pET28_Cp23, and pET28_Cp15-23, were sent for Sanger Sequencing to verify proper insertion of the targeted *C. parvum* protein sequences.

2.6 Intramuscular Vaccine Preparation: Purification of 6xHis-tagged Cp15, Cp23, and Cp15-23 Recombinant Protein

2.6.1 Transformation of BLR(DE3) Competent *E. coli*

Sequenced pET28_Cp15, pET28_Cp23, and pET28_Cp15-23 constructs were transformed into BLR(DE3) competent *E. coli* cells (Novagen; Burlington, USA). BLR(DE3) competent *E. coli* cells were thawed on ice. 2 µL of each plasmid were added to the cells and mixed gently by flicking. Mixtures were kept on ice for 30 minutes. The tubes were then heat shocked at 42°C for 45 seconds and immediately placed back on ice for 5 minutes. 100 µL of LB broth was added to the mixture and the tubes were kept on a shaking incubator at 37°C and 250 RPM for one hour. Stocks were frozen in 15% glycerol in LB at -80°C.

2.6.2 Protein Expression

30 mL of LB kanamycin (30 µg/mL) were inoculated with either pET28_Cp15, pET28_Cp23, or pET28_Cp15-23 clone. The culture was grown overnight on a shaking incubator at 37°C and 250 RPM. The following day, the culture was added to 1L of LB kanamycin (50 µg/mL). Cultures were incubated at 37°C and 250 RPM for one to two hours until the optical density at 600 nm (OD₆₀₀) reached 0.4-1, with the optimal OD at 0.5-0.6. IPTG was added to a final concentration of 1 mM, and the culture was left to incubate at 37°C and 250 RPM overnight. Cultures were transferred to 50 mL conical tubes and centrifuged at 3000xg for 30 minutes at 4°C. The supernatants were discarded in bleach. The pellets collected from each culture were resuspended in an 8M Urea solution (pH = 8.0) and lysed.

2.6.3 Protein Purification

Nickle-NTA (Ni-NTA) affinity chromatography was employed to purify lysates. In an Econo-Pac Chromotography column, 1 mL of Ni-NTA Superflow (Qiagen; Hilden, Germany) was added for every 10 mL of lysate and the mixture rotated for one hour at 4°C. The supernatant was drained from the column by gravity flow, and the beads were washed with 12 mL of five different wash buffer, each decreasing in urea molarity from 7M to 3M (pH = 6.3). Urea is a chaotropic compound and is capable of eliminating unwanted secondary protein structures through disrupting hydrogen bonds and hydrophobic interactions and solubilizing proteins^{166, 167}. His-tagged protein were then eluted with elution buffers of decreasing pH. Three aliquots were collected of each of the four elution buffers, labelled elutions D to G of pH= 5.4, 5.0, 4.7, to 4.3, respectively.

2.6.4 Western Blot

NuPAGE Lithium Dodecyl Sulfate (LDS) sample buffer was added to each of the four protein elutions, for all three *C. parvum* antigens. Protein samples were run on a 12% Bis-Tris Protein Gel for 45 minutes at 200V, and then transferred to a nitrocellulose membrane using the Trans-Blot Turbo RTA Mini Nitrocellulose Transfer Kit (Bio-Rad, Hercules, CA). The membrane was blocked with phosphate-buffered saline (PBS; (pH = 7.4; 0.01 M phosphate buffer, 0.14 M NaCl) containing 0.05% Tween 20 (Sigma-Aldrich; Oakville, Canada) (PBST) and 5% bovine serum albumin (BSA) (Sigma-Aldrich; Oakville, Canada) for 1 hour at room temperature with gentle agitation. Membranes were incubated overnight at 4°C with a murine, monoclonal anti-

polyhistidine primary antibody (1:20,000 dilution; Sigma-Aldrich, St. Louis, USA). The following day, membranes were washed three times with PBST. Membranes were then incubated for one hour at room temperature with a goat, anti-mouse secondary antibody conjugated to horseradish peroxidase (1:20,000 dilution; Sigma-Aldrich). Membranes were washed five more times with PBST and incubated with SuperSignal West Pico chemiluminescent substrate (ThermoFisher Scientific, Eugene, USA) for 5 minutes. Immunoreactive protein bands were visualized using an auto radiography cassette (Sigma-Aldrich), film (Denville Scientific; Holliston, USA) and the Kodak X-OMAT 2000 system (Kodak; Rochester, USA).

2.6.5 Protein Dialysis

The elution conditions presenting the most distinct bands were selected to undergo dialysis to exchange the elution buffer for 1X PBS. Protein samples were injected into a Slide-A-Lyzer 10,000 MCWO Dialysis Cassette (ThermoFisher; Waltham, USA). Each sample was dialyzed in 1X PBS buffer. Purified protein samples were removed and stored at -20°C until quantification.

2.6.6 Protein Quantification

Purified Cp15, Cp23, and Cp15-23 protein samples were quantified using a BCA Protein Assay Kit (ThermoFisher; Waltham, USA),

2.6.7 Concentrating Protein Sample

Protein samples were concentrated using an AMiconUltra-15 10,000 MCWO centrifugal filter device (Millipore-Sigma; Burlington, USA) if the calculated protein concentration was under 100 µg/mL. Samples were pooled and then centrifuged at 2440 *xg* for 12 minutes. The new protein concentration was then determined using the BCA protein assay kit.

2.7 Cp15, Cp23, and Cp15-23 Immunogenicity Studies

2.7.1 Cp15-23 Immunogenicity Study

Six-week-old female C57BL/6 mice (Charles River Laboratories; Montreal, Canada) were purchased and kept under pathogen-free conditions for a week in the Animal Resource Division at

Group	Number of mice	IM vaccination	YS1646 PO vaccination (10 ⁹ CFU/mouse)
1	5	0 µg	PBS
2	5	0 µg	pQE30_Null
3	5	0 µg	pSspH2_Cp15_23
4	5	0 µg	pNirB_Cp15-23
5	5	10 µg rCp15-23 + 10 µg CpG	PBS
6	5	10 µg rCp15-23 + 10 µg CpG	pSspH2_Cp15_23
7	6	10 µg rCp15-23 + 10 µg CpG	pNirB_Cp15-23

the Research Institute of McGill University Health Center (RI-MUHC). All experimental conditions and controls consisted of 5-6 mice/group.

Table 1: Cp15-23 multi-modality vaccination conditions.

A multimodality vaccination schedule was employed with a single IM dose of the selected recombinant protein on day 1, and three PO doses of the corresponding *C. parvum* antigen expressing YS1646 strain on days 1, 3, and 5 (Fig 2). For IM immunization, 10 µg of selected recombinant protein, with 10 µg of CpG adjuvant in 50 µL of PBS, was administered into the gastrocnemius muscle using a 28-gauge needle. For combination IM doses, 5 µg of each recombinant protein, with 10 µg of CpG adjuvant, in 50 µL of PBS, was administered. For PO immunization, transformed YS1646 were given at a concentration of 1x10⁹ CFU/mouse in 0.2 mL of PBS. Mice were weighed every day during the first week of immunization (D0-D7).

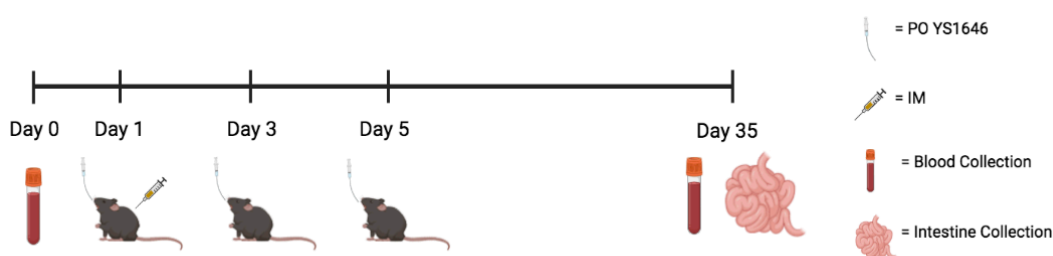


Figure 2: Cp15-23 multi-modality vaccination timeline. A single IM dose of rCp15-23 was administered on day 1. Three PO immunization doses of one or more of the *C. parvum* antigen expressing YS16464 was administered on days 1, 3, and 5. Blood was collected on day 0 and 35. Intestines were collected on day 35.

Blood samples were collected from the saphenous vein on day 0, prior to immunization. All mice were euthanized on day 35 using isoflurane-CO₂. Blood (via cardiac puncture), and the top 10 cm of the small intestine, beginning at the stomach, were collected from all mice.

Serum separation was conducted using microtainer serum separator tubes (Sarstedt, Nümbrecht, Germany) and centrifuged at 8000 *xg* at room temperature for 10 minutes. Aliquots were stored at -20°C until analysis.

Intestinal contents were removed, and the intestines were weighed prior to processing. A Protease Inhibitor (PI) Cocktail (Sigma-Aldrich) was added to the tissue samples at a 1:5 dilution (weight/volume). Samples were homogenized (Homogenizer 150; Fisher Scientific; Ottawa, Canada) and centrifuged at 2500 *xg* at 4°C for 30 minutes, and the supernatants collected for storage at -80°C until analysis.

2.7.2 Cp15 and Cp23 Immunogenicity Study

Six-week-old female C57BL/6 mice (Charles River Laboratories; Montreal, Canada) were

Group	Number of mice	IM vaccination	YS1646 PO vaccination (10 ⁹ CFU/mouse)
1	5	0 µg	PBS
2	5	0 µg	pQE30_Null
3	5	0 µg	pSspH2_Cp15
4	5	0 µg	pNirB_Cp15
5	5	10 µg rCp15 + 10 µg CpG	PBS
6	5	10 µg rCp15 + 10 µg CpG	pSspH2_Cp15
7	5	10 µg rCp15 + 10 µg CpG	pNirB_Cp15
8	5	0 µg	pSspH2_Cp23
9	5	0 µg	pNirB_Cp23
10	5	10 µg rCp23 + 10 µg CpG	PBS
11	5	10 µg rCp23 + 10 µg CpG	pSspH2_Cp23
12	5	10 µg rCp23 + 10 µg CpG	pNirB_Cp23
13	6	5 µg rCp15 + 5 µg rCp23 + 10 µg CpG	pSspH2_Cp15 + pSspH2_Cp23 (pSspH2_Cp15/23)
14	5	5 µg rCp15 + 5 µg rCp23 + 10 µg CpG	pNirB_Cp23 + pNirB_Cp23 (pNirB_Cp15/23)

purchased and kept under pathogen-free conditions for a week in the Animal Resource Division at the McGill University Health Center Research Institute (RI-MUHC). All experimental conditions and controls consisted of 5-6 mice/group (Table 2).

Table 2: Cp15 and Cp23 multi-modality vaccination conditions.

The same multi-modality vaccination schedule described above was used (Fig 3). For combination PO doses, 0.5×10^8 CFU/mouse of each YS1646 strain was administered. Mice were weighed every day during the first week of immunization (D0-D7).



Figure 3: Cp15 and Cp23 multi-modality vaccination timeline. A single IM dose of rCp15-23 was administered on day 1. Three PO immunization doses of a select *C. parvum* antigen expressing YS16464 was administered on days 1, 3, and 5. Blood was collected on day 0 and 35. Intestines and spleens were also collected on day 35.

Blood samples were collected from the saphenous vein on day 0 and from the heart on day 35, when isoflurane-CO₂ euthanasia was used on all mice. The top 10 cm of the small intestine, beginning at the stomach, were also collected from all mice. Spleens were collected from a total of 12 mice: three each from the PBS group, pSspH2_Cp15 + rCp15, pSspH2_Cp23 + rCp23, and pSspH2_Cp15/Cp23 + rCp15/23

Serum and intestines were processed in the same manner as the previous Cp15-23 vaccination experiment. Spleens were crushed with syringe through a 0.22-micron syringe filter (ThermoFisher; Waltham, USA) into 50 mL conical tubes. Filters were washed twice, each time with 5 mL of HBSS (with phenol red, with calcium, without magnesium; Wisent; St. Bruno, Canada). The samples were centrifuged at 400 *xg* for 10 minutes at 4°C. Supernatant were decanted and 3 mL of ammonium-chloride potassium lysing buffer was used to resuspend the pellet and lyse any remaining red blood cells. HBSS was added and samples were centrifuged again at 400 *xg* for 10 minutes at 4°C and supernatants were decanted one final time and the pellets resuspended in RPMI-1640 supplemented with 10% fetal bovine serum, 1 mM penicillin/streptomycin, 10 mM HEPES, 1X MEM non-essential amino acids, 1 mM sodium pyruvate, 1 mM L-glutamine (Wisent Bioproducts), and 0.05 mM 2-mercaptoethanol (Sigma Aldrich) ('fancy' RPMI or fRMPI). Cells were counted using a compound microscope, diluted to the desired concentration (10^7 cells/well) with fRMPI, and distributed into flat bottom 96-well plates.

2.8 Humoral Response Analysis: Enzyme-Linked Immunosorbent Assay

96-well round-bottom plates were coated (50 $\mu\text{L}/\text{well}$) of either 1 $\mu\text{g}/\text{mL}$ of rCp15/rCp23 or 4 $\mu\text{g}/\text{mL}$ of rCp15-23. Plates were incubated overnight at 4°C. The following day, plates were washed three times with PBST and then incubated with 150 $\mu\text{L}/\text{well}$ of blocking buffer (PBS, 5% bovine serum albumin (Sigma-Aldrich; Oakville, Canada), 0.1% Tween 20 (Sigma-Aldrich; Oakville, Canada)) at 37°C for one hour. Serum samples were heat inactivated at 56°C and then diluted 1:50 in blocking buffer. Intestinal samples were not heat inactivated and were added without dilution. Samples were plated in duplicates (50 $\mu\text{L}/\text{well}$) and incubated for one hour at 37°C. Plates were washed four times with PBST. 75 $\mu\text{L}/\text{well}$ of horseradish peroxidase (HRP)-conjugated anti-mouse IgG secondary antibodies (diluted 1:20,000 in blocking buffer; Sigma-Aldrich) or HRP-conjugated anti-mouse IgA secondary antibodies (diluted 1:10,000 in blocking buffer; Sigma-Aldrich) were then added and the plates incubated for 30 minutes at 37°C. Plates were washed six times with PBST. 100 $\mu\text{L}/\text{well}$ of 3,3',5,5'-tetramethylbenzidine (TMB) detection substrate (Millipore, Billerica, MA) was then added. After 15 minutes, 0.5 M H_2SO_4 (50 $\mu\text{L}/\text{well}$) was added to stop the reaction. The plates were read at 450 nm on an EL800 microplate reader (BioTek Instruments Inc., Winooski, USA).

Mouse weights and ELISA data were analyzed using GraphPad Prism 6 (LaJolla, USA). The means of each experimental condition were compared with the PBS negative control group using a one-way ANOVA with Dunnett's multiple comparison test. Antibody titers were graphed as a measure of optical density (O.D). P-values < 0.05 were considered significant.

2.9 Cell-Mediated Response Analysis: Flow Cytometry

Splenocytes plated previously in flat bottom 96-well plate were centrifuged at 400 xg for 7 minutes. The supernatants were removed, and cells were washed once with PBS (200 $\mu\text{L}/\text{well}$) centrifuged again. rCp15 and rCp23 (2 $\mu\text{g}/\text{mL}$) were used to stimulate cells for 6 hours. Cells were labelled with Fixable Viability Dye eFluor 780 (eBioscience; Waltham, USA) and incubated at 4°C. PBS was added to unstained controls and single stains used for compensation. Cells were washed again before 50 $\mu\text{L}/\text{well}$ of FC block (BD Bioscience; New Jersey, USA) was added to each well to prevent unspecific binding with the constant FC domain of antibodies. Extracellular staining with a cocktail of anti-CD3 FITC, anti-CD4 V500, anti-CD8 PerCP-CY5.5, and anti-CD44 BUV737 antibodies (BD Bioscience) were added to samples left to incubate at 4°C for 25

minutes. Excess, unbound antibody was removed PBS-1% BSA was added to unstained controls, intracellular single stains, and the viability control. Dyes were washed three times with PBS-1% BSA. Prior to acquisition, cells were fixed overnight with Fix/Perm solution (BD Biosciences). To detect the presence of intracellular cytokines, fixed cells were washed three times in 200 μ L of Perm/Wash buffer (BD Biosciences) before staining with anti-IFN- γ PE (BD Biosciences) and anti-TNF- α eFlour450 (eBioscience). Cells were washed three times in perm-wash buffer and then resuspended in PBS. Events were acquired for two minutes per sample using a BD LSRFortessa cell analyzer. Data were analyzed using FlowJo software.

Cell population data were analyzed using GraphPad Prism 6 (LaJolla, USA). The means of each experimental condition was compared with the respective non-stimulated or antigen stimulated condition of the PBS control group using a two-way ANOVA with Dunnett's multiple comparison test. Cell counts were graphed as a measure of the frequency of live cells, and P-values < 0.05 were considered significant.

2.10 Serum Antibody Adoptive Transfer Protection Study against *C. parvum* Challenge

Six-week-old female IFN- γ R KO mice were bred and kept under pathogen-free conditions in the Animal Resource Division at the McGill University Health Center Research Institute (RI-MUHC). All experimental conditions and controls consisted of 2-3 mice/group. Mice were saphenous bled prior to the adoptive transfer. On day one, 200 μ L of either PBS or serum was injected intravenously (IV) in the lateral tail vein of mice. Serum used in this experiment was obtained from C57BL/6 mice vaccinated in the previous Cp15 and Cp23 immunogenicity experiment (Table 3). Serum was pooled so that the final Cp23-specific antibody titers of the experimental conditions ranged from O.D 1.19 to 1.56.

Group	Condition	Number of Mice	Intravenous injection received	Average Antibody Titer Received (O.D)
1	Control	2	N/A	0
2	Control	3	PBS	0
2	Control	3	Antibodies from PBS vaccinated mice	0.01
3	Experimental	2	Antibodies from rCp15 vaccinated mice	1.32
4	Experimental	2	Antibodies from pNirB_Cp23 + rCp23 vaccinated mice	1.19

5	Experimental	3	Antibodies from pSspH2_Cp15/23 + rCp15/23 vaccinated mice	1.58
---	--------------	---	---	------

Table 3: Experimental conditions used in the adoptive transfer

Mice were challenged with 3000 oocysts, delivered via oral gavage, later on the same day. Weights were monitored daily. Ten days after the initial adoptive transfer and challenge, mice were subjected to isoflurane-CO₂ euthanasia. Blood (via cardiac puncture), stool, the small intestine, the cecum, and the colon were collected from all mice (Fig 4).

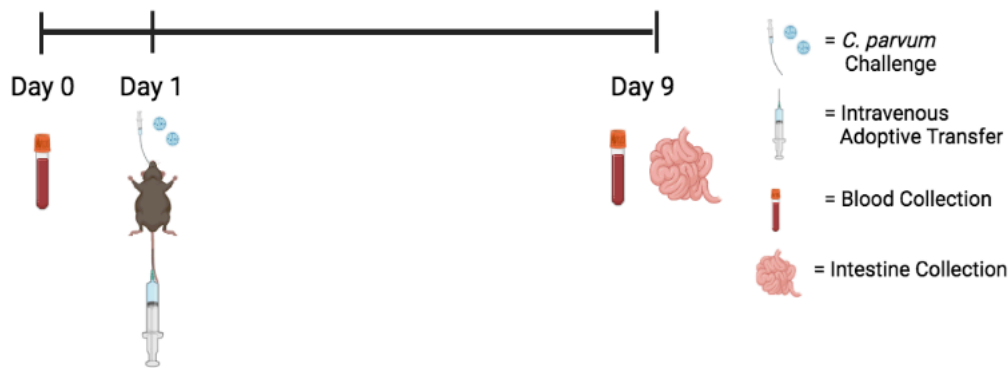


Figure 4: Serum antibody adoptive transfer *C. parvum* challenge study timeline. Blood was collected on day 0 and 9. Mice were administered 200 uL of either PBS or serum antibodies intravenously into the lateral tail vein via adoptive transfer, and then infected with 3000 *C. parvum* oocysts orally. On day 10, mice were euthanized, and intestines were collected to calculate oocyst burden.

2.10.1 Intestinal Processing and Oocyst Count

Nine days following the initial challenge with *C. parvum* oocysts, both the small and large intestines were collected in PBS containing 0.04% Tween (Sigma-Aldrich; Oakville, Canada) and weighed prior to processing. Sputasol (0.05 g), which is a dry mixture of 10% DTT, 76% NaCl, 2% KCl, 10% Na₂HPO₄ and 2% KH₂PO₄, was added to each sample prior to homogenization to free oocysts from the cells. The samples were then homogenized and left to shake at 4°C for 1.5 hours. Samples were then centrifuged at 2500 *xg* at 4°C for 10 minutes, and the supernatants removed. 8 mL of sterile water containing 0.04% Tween (Sigma-Aldrich; Oakville, Canada) was added and the sample vortexed. 4 mL diethyl ether was added, and the samples were centrifuged at 2500 *xg* at 4°C for 10 minutes. Supernatants were removed before 20 mL of sterile water was added and the samples were then centrifuged again at 2500 *xg* at 4°C for 10 minutes. The supernatants were removed and 20 mL of NaCl was used to resuspend the pellet. 5 mL of water was then very gently added to create a water:NaCl interface. The samples were then centrifuged

at 2500 g at 4°C for 10 minutes. 4 mL of liquid was extracted from the water:NaCl interface; oocysts are trapped in the water:NaCl interface as they float in NaCl but sink in water. The samples were centrifuged at 13,200 g at 4°C for 30 minutes and the final volume adjust to 1 mL.

100 uL of each oocysts sample was incubated with 1 μ L mouse anti-*Cryptosporidium* Alexa Fluor 488 monoclonal antibody (BEL 0126; AbD. Serotec; Raleigh, USA) for 30 minutes at room temperature. To quantify *C. parvum* oocysts, oocyst samples were incubated with 8% paraformaldehyde (Sigma-Aldrich; Oakville, Canada) overnight at 4°C. CountBright Absolute Counting beads (2x 10⁴ beads/20 μ L; ThermoFisher; Burlington, Canada) were added to each sample for a total volume of 200 μ L. Events were obtained using a BD LSRFortessa cell analyzer.

Total oocyst counts obtained from the gating strategy were blanked first with a non-infected sample (Fig 19a). Oocyst burden was calculated using the formula below and analyzed using GraphPad Prism 6 (LaJolla, USA). The mean of each experimental condition was compared with each of the three negative controls (i.e., no IV injection, PBS IV, and PBS serum IV) using a one-way ANOVA with Dunnett's multiple comparison test. Oocyst counts were graphed as a measure of oocysts per gram and P-values < 0.05 were considered significant.

$$Oocysts/sample = \frac{(oocyst\ counts) \times (number\ of\ beads\ in\ the\ sample)}{number\ of\ beads\ acquired} \times 50$$

3. Results

3.1 *C. parvum* antigen sequences inserted into pQE30 and pET28 vectors

Codon optimization of the original Cp15 and Cp23 GenBank sequences to *Salmonella enterica* raised the GC 42.2% to 54.4% (Fig 5). The antigenic sequences for Cp15, Cp23, and Cp15-23 was amplified by PCR. Bands at 444 bp, 354 bp, and 810 bp, respectively, were detected following gel electrophoresis (Fig 6). Following initial ligation attempts, troubleshooting PCR using one antigen sequence-binding primer with one plasmid-binding primer revealed unsuccessful ligation of Cp15 and Cp15-23 into pSspH1_pQE30 and pET28 vectors at the Not1 restriction site (data not shown). Additional overhang 5'-AAG GAA AAA A-3' nucleotides were added to both Cp15 and Cp23 forward primers to encourage successful ligation.

After repeated attempts, successful isolation of recombinant pQE30 and pET28 vectors containing either Cp15, Cp23, or Cp15-23 antigenic sequences from DH5a cells into both plasmid vectors was demonstrated by Sanger Sequencing (data not shown).

3.2 Recombinant Cp15, Cp23, and Cp15-23 Protein Expression

Following transformation of antigen-containing pET28 plasmids into BLR DE3 *E. coli*, Cp15, Cp23, and Cp15-23 recombinant proteins were detected by immunoblotting using the anti-His tag specific for the C-terminus 6x histidine tag of each protein.

Both recombinant Cp15 (rCp15) and recombinant Cp23 (rCp23), of sizes 17 kDA and 27 kDA respectively, were clearly detected in bacterial lysates following purification (Fig 7). Interestingly, in addition to the expression of rCp15, a second protein band of size <3.5 kDA was detected in the bacterial lysate (Fig 7a).

Expression of the recombinant Cp15-23 (rCp15-23) protein was also confirmed. As mentioned previously, three aliquots of four elution buffers were collected sequentially. A protein band of approximately 46 kDA was visible in both the native and the reducing conditions of aliquot 1 (E1) and aliquot 3 (E3) of elution group E (pH = 5.0). Several additional his-tagged proteins of approximate sizes 38, 45, 50, and 80 kDA and 30, 38, 45, 50 kDA were present in the E3 and E3 reducing conditions, respectively, which included dithiothreitol (DTT) (Fig 8a). The Coomassie Blue stain of the purified protein elution revealed proteins of various sizes with the darkest band suggesting of a protein of approximately 46 kDA. Densitometry analysis estimated the size of this

single band to be approximately 46.2 kDA and quantified its relative percentage composition to be 40% of the total protein detected (Fig 8b). Upon a second protein purification, only bands of approximate sizes 15, 20, 40, and 46 kDA were detected. This time, the 46 kDA band indicative of rCp15-23 was present mainly in elutions F and G (Fig 8c). The sample containing beads from the protein purification also had a prominent 46 kDA protein band (Fig 8c). Densitometry analysis was not conducted for the second protein purification.

3.3 Immunogenicity of Cp15-23 in C57BL/6 mice

Upon administration, both PO vaccination with the attenuated YS1646 and IM vaccination with rCp15-23 did not appear to induce signs of distress in mice nor significant weight loss during the first week (Fig 9). Mice vaccinated with rCp15-23 alone and mice vaccinated with both pSspH2_Cp15-23 YS1646 and rCp15-23 demonstrated significant increases in serum IgG compared to the PBS control group ($P < 0.01$, $P < 0.01$; Fig 10a). No significant increases in mucosal IgA were detected for any of the experimental conditions (Fig 10b).

3.4 Immunogenicity of Cp15 and Cp23 in C57BL/6 mice

The multi-modal vaccination group pNirB_Cp15 + rCp15 experienced a non-significant 7% weight loss on day two, following the first dose of YS1646 and IM administration of rCp15. This weight was recovered by day four and remained consistent for a period of one week thereafter (Fig 11a). Multi-modal vaccination with the Cp23 candidate did not cause significant weight loss during the first 11 days (Fig 11b). However, in the combination group pNirb_Cp15/23 YS1646 with both rCp15 and rCp23, the average weight of mice decreased by 14.5% from day one to day two. By day nine, mice in this group appeared thin and lethargic. All mice in this group were euthanized at day nine (Fig 11c). Because of this incident, daily weight monitoring of all mice resumed from day nine until day 11, when average weights stabilized once more.

Surprisingly, at week five, rCp23 only, pSspH2_Cp23 + rCp23, and pNirB_Cp23 + rCp23 vaccination groups had significant increases in Cp15-specific serum IgG titers compared to the PBS group ($P = 0.0001$, $P = 0.0001$, and $P < 0.05$ respectively; Fig 12a). Similarly, significant cross-reactivity was also observed in the rCp15 only vaccination group; mice vaccinated with rCp15 only had significantly increased Cp23-specific serum IgG titers compared to the PBS group ($P < 0.01$; Fig 12b). However, the pNirB_Cp23 + rCp23 and the mixed pSspH2_Cp15/23 +

rCp15/23 groups had greater increases in their Cp23-specific IgG titers ($P = 0.0002$ and $P = 0.0001$ respectively; Fig 12b). The rCp23 only vaccination group also had a significant increase in Cp23-specific IgG compared to the PBS group ($P < 0.05$; Fig 12b). No increase in Cp15-specific mucosal IgA titers was observed for any experimental group (Fig 13a). Cp23-specific mucosal IgA titers were significantly increased only in the multi-modal pNirB_Cp23 + rCp23 group ($P < 0.01$; Fig 13b).

Spleens were collected and processed for three mice from four vaccination conditions: PBS, pSspH2_Cp15 + rCp15, pSspH2_Cp23 + rCp23, and pSspH2_Cp15/23 + rCp15/23. The groups selected for flow cytometry analysis were selected prior to the ELISA analysis based on their anticipated immunogenic potential. A significant increase in splenocyte cell counts were detected in multi-modal vaccination groups pSspH2_Cp15 + rCp15 and pSspH2_Cp23 + rCp23 compared to the PBS control (Fig 14). CD4⁺ and CD8⁺ T cell populations were identified based on the gating strategies shown in Figure 15.

No significant differences in CD4⁺ T cell (Fig 16a) or in CD8⁺ T cell (Fig 16b) populations were observed between the PBS group and the vaccination groups. CD44⁺ upregulation was also analyzed as a marker of T cell activation, distinguishing the differentiation of naïve T cells into their memory and effector T cell counterparts (Fig 17a)¹⁶⁸. No difference was observed in CD4⁺ CD44⁺ T cell populations between vaccinated groups compared to the PBS group (Fig 17b). However, increases in CD8⁺ CD44⁺ T cell populations can be observed in all vaccinated groups, both in stimulated and non-stimulated conditions. In particular, a significant increase in CD8⁺ CD44⁺ T cells was seen in the non-stimulated pSspH2_Cp15/23 + rCp15/23 vaccinated group ($P < 0.05$; Fig 17c).

Increases in the means of CD4⁺ T cells producing IFN- γ were observed in both Cp15- and Cp-23 stimulated splenocytes of the pSspH2_Cp15 + rCp15, pSspH2_Cp23 + rCp23, and pSspH2_Cp15/23 + rCp15/23 vaccinated groups. A significant increase in CD4⁺ IFN- γ ⁺ T cells was detected for the Cp23-stimulated pSspH2_Cp15/23 + rCp15/23 vaccinated group ($P < 0.05$; Fig 18a). No significant increases were present in CD8⁺ IFN- γ ⁺ T cells compared to the PBS group (Fig 18b). Increases in the means of CD4⁺ T cells producing TNF- α were observed for both Cp15- and Cp-23 stimulated splenocytes of the pSspH2_Cp15 + rCp15, pSspH2_Cp23 + rCp23, and pSspH2_Cp15/23 + rCp15/23 vaccinated groups. A significant increase in CD4⁺ TNF- α ⁺ T cells was seen for the Cp23-stimulated pSspH2_Cp23 + rCp23 vaccinated group ($P < 0.05$; Fig

18c). Increases in the means of CD8+ T cells producing TNF- α were detected for the Cp15-stimulated pSspH2_Cp15 + rCp15 vaccinated condition, as well as the Cp23-stimulated pSspH2_Cp23 + rCp23 vaccinated condition. A significant increase in CD8+ TNF- α + T cells was observed for the non-stimulated pSspH2_Cp23 + rCp23 vaccinated group (P<0.05; Fig 18d).

3.5 Serum Antibody Adoptive Transfer Protection Study against *C. parvum* Challenge

Beads and oocyst populations were identified using the gating strategy shown in Figure 19a. No significant differences were observed from the oocyst burden of mice that received transferred serum from the previously vaccinated rCp15, pNirB_Cp23 + rCp23, or pSspH2_Cp15/23 + rCp15/23 groups (Fig 19b).

4. Figures

Figure 5: Original Cp15-23 Sequence and the Codon Optimized Sequence

	Score	Expect	Identities	Gaps	Strand
	542 bits(600)	4e-158	606/810(75%)	0/810(0%)	Plus/Plus
Original	1	ATGGGTAACCTGAAATCCTGTTGTTCTTTTGCCGATGAACACTCCCTAACCTCTACTCAA			
Optimized	1	ATGGGCAACCTGAAATCTTGCTGCTCTTTTCGCGGACGAACACTCTCTGACCTCTACCCAG			
Original	61	CTAGTAGTTGGAAATGGTTTCAGGAGCTTCAGAAACTGCTTCCAACCACCCCAAGAAGAA			
Optimized	61	CTGGTTGTTGGCAACGGCTCTGGCGCGTCTGAAACCGCGCTAACCACCCGCAGGAAGAA			
Original	121	GTTAATGATATCAATACTTTTAAATGTAAAGTTAATAATGCAAGATAGAAGTAAGCTTGAC			
Optimized	121	GTTAACGACATCAACACCTTCAACGTTAAACTGATCATGCAGGACCGTTCTAAACTGGAC			
Original	181	TGCGAGGTAGTATTTGATAGCACAAAGTATTTTCGCTTTCGGAGATGGAAAATGCAGAAAT			
Optimized	181	TGCGAAGTTGTTTTGACTCTACCTCTATCTCTGTCTGGCGACGGCAAATGCCGTAAC			
Original	241	ATTGCTTTGGATGAAATCCACCAATTATTATATTCAAAGGAAGAGCTTTCTAGAGTTGAA			
Optimized	241	ATCGCGCTGGACGAAATCCACCAGCTGCTGTACTCTAAAGAAGAACTGTCTCGTGTGAA			
Original	301	AGTAGTGC TGGAATCAGCGATTCCGACAATTGTGTTGCAATTCATCTCAAAGAATCAGGA			
Optimized	301	TCTTCTGCGGGCATCTCTGACTCTGACAACTGCGTTGCGATCCACCTGAAAGAATCTGGC			
Original	361	AACTGTATTCCCTTTTCTTTAATAATTCGCAAGACAAAGAAAAGATTTGTTGCAACAGCA			
Optimized	361	AACTGCATCCCGCTGTTCTTCAACAACCTCTCAGGACAAAGAACGTTTCGTTGCGACCGCG			
Original	421	AACAAATTCAAACCAAACCTTTAACGGTGGCTCTGGTGGTTGTTTCATCATCAAAGCCAGAA			
Optimized	421	AACAAATTCAAACCGAACTTCAACGGTGGCTCTGGTGGCTGCTCTTCTTCTAAACCGGAA			
Original	481	ACTAAAGTTGCTGAAAATAAATCTGCAGCAGATGCTAACAAACAAAGAGAATTAGCTGAA			
Optimized	481	ACCAAAGTAGCTGAAAACAAGTCTGCTGCAGATGCAAATAAACAGCGCGAACTGGCAGAA			
Original	541	AAGAAGGCTCAATTAGCCAAGGCTGTAAAGAATCCAGCTCCAATCAGCAACCAAGCTCAA			
Optimized	541	AAAAAAGCACAGCTGGCCAAAGCTGTTAAAAACCCGGCGCCTATCTCTAACCAGGCCAG			
Original	601	CAAAAGCCAGAAGAACCAAAGAAGTCCGAGCCTGCTCCCAATAATCTCCAGCTGCTGAT			
Optimized	601	CAGAAACCGGAAGAACCAAAAAAAGCGAACCGGCCCGAACCAACCCGCGGCCGAGAT			
Original	661	GCACCAGCAGCCCAAGCTCCTGCTGCCCTGCTGAACCTGCTCCACAGGATAAGCCAGCT			
Optimized	661	GCCCCGGCGGCTCAGGCGCCGGCTGCGCCGGCCGAACCAGCTCCGCAGGATAAACCAGCC			
Original	721	GATGCCCCAGCTGCTGAAGCTCCAGCTGCTGAACCTGCTGCTCAACAAGACAAGCCAGCT			
Optimized	721	GATGCTCCGGCGGCAGAAGCGCCGGCCGCCGAACCAGGCGCTCAGCAGGACAAACCGCA			
Original	781	GATGCCCCGcatcatcatcatcatcatTAA 810			
Optimized	781	GACGCGCCGCATCATCATCATCATATTAA 810			

Figure 5: Sequence alignment of the original Cp15 and Cp23 GenBank sequences with the recombinant sequence codon optimized for *Salmonella*. Optimizing the sequence increased the GC content from 42.2% to 54.4%.

Figure 6: PCR amplification of Cp15, Cp23, and Cp15-23 sequences

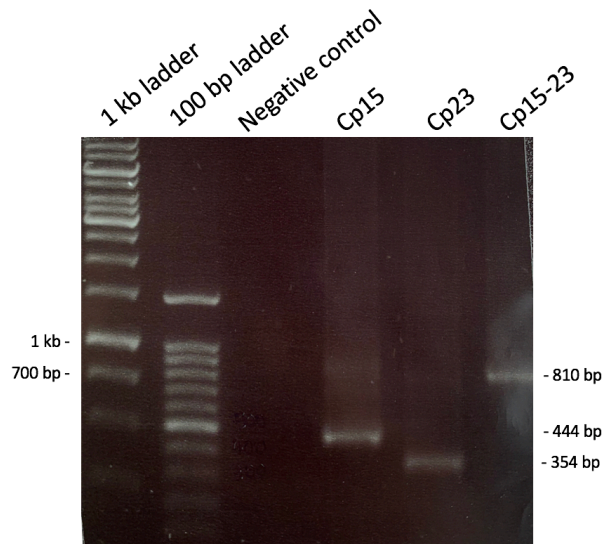


Figure 6: PCR amplification of Cp15, Cp23, and Cp15-23 sequences. Q5 high-fidelity DNA polymerase was used in the PCR amplification of Cp15, Cp23, and Cp15-23 *C. parvum* antigenic sequences. Bands of 444 bp, 354 bp, and 810 bp were observed upon running the samples on gel electrophoresis, indicating the successful amplification of Cp15, Cp23, and Cp15-23, respectively. Negative control lacking *C. parvum* genomic material contains no detectable bands, indicating no contamination in the reagents used.

Figure 7: Immunoblotting of recombinant Cp15 and Cp23 proteins

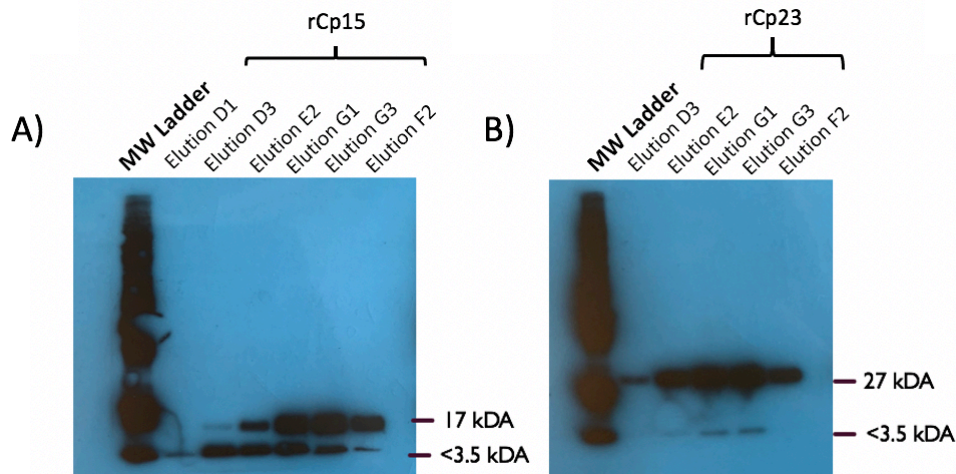


Figure 7: Immunoblotting of recombinant Cp15 and Cp23 proteins in BLR DE3 bacterial lysates. The plasmids pET28_Cp15 and pET28_Cp23 were transformed into BLR DE3 *E. coli* and induced with IPTG. Bacterial cell lysates were purified using Ni-NTA affinity chromatography and eluted based on decreasing pH levels. Three aliquots (i.e., 1, 2, 3) of four elution buffers were collected (elutions D to G of pH= 5.4, 5.0, 4.7, to 4.3, respectively). A mouse anti-polyhistidine primary antibody and goat anti-mouse secondary antibody conjugated to horseradish peroxidase were used for detection of his-tagged A) rCp15 or B) rCp23 of sizes 17 kDA and 27 kDA, respectively.

Figure 8: Immunoblotting of recombinant Cp15-23 proteins

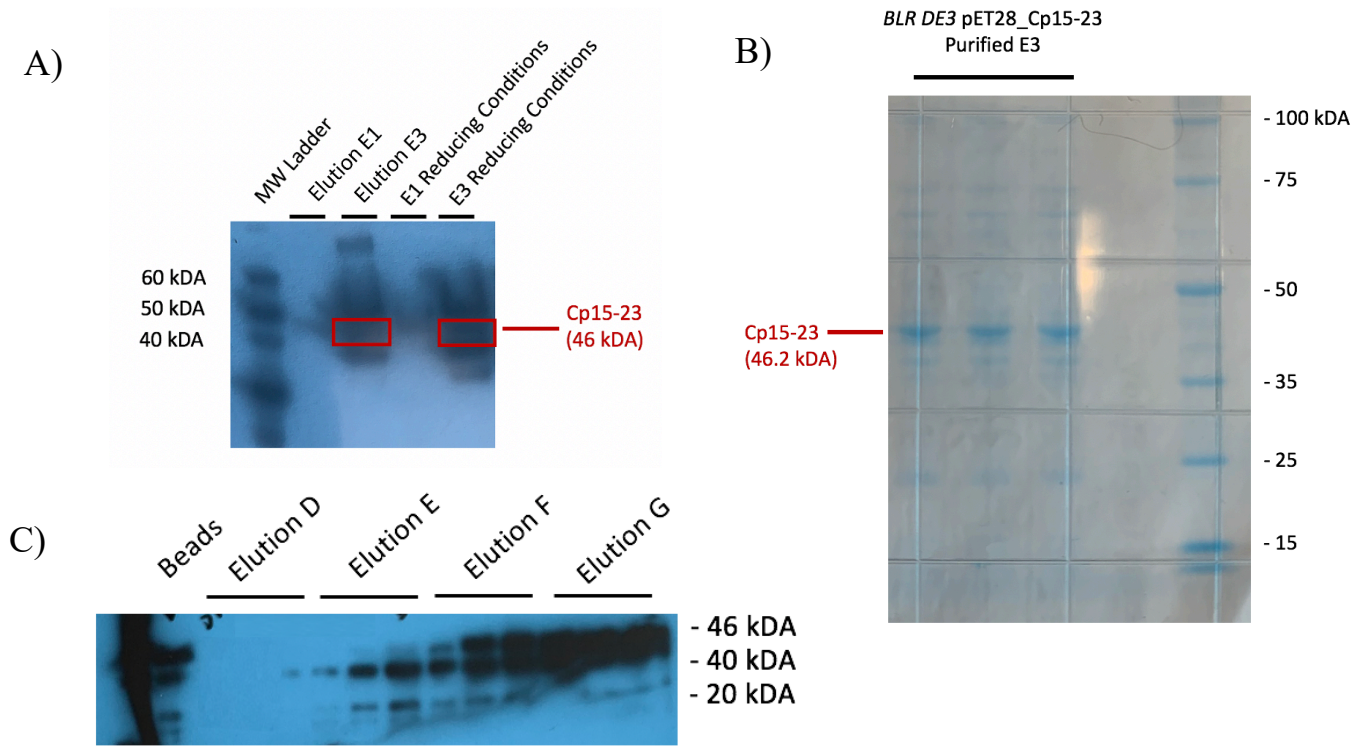


Figure 8: Immunoblotting of recombinant Cp15-23 proteins in BLR DE3 bacterial lysates. The plasmids pET28_Cp15-23 were transformed into BLR DE3 *E. coli* and induced with IPTG. Bacterial cell lysates were purified using Ni-NTA affinity chromatography and eluted based on decreasing pH levels. Three aliquots (i.e., 1, 2, 3) of four elution buffers were collected (elutions D to G of pH= 5.4, 5.0, 4.7, to 4.3, respectively). Samples were either run in a western using a mouse anti-polyhistidine primary antibody and goat anti-mouse secondary antibody conjugated to horseradish peroxidase or stained with Coomassie blue. A) A protein band of size 46 kDA, indicative of rCp15-23, can be observed in all elutions. Multiple other his-tagged bands can be detected in elution E3 and E3 reducing condition lanes, indicating the presence of protein impurities. B) Densitometry analysis of the Coomassie blue stain revealed the rCp15-23 protein to be exactly 46.2 kDA in size, and 40% of all detected protein sample. C) A second protein purification showed a protein band of 46 kDA in elutions F and G. Similarly, additional his-tagged bands of sizes 15, 20, and 40 kDA can also be observed all three aliquots of elutions E, F, and G.

Figure 9: Weight change in C57BL/6 mice after Cp15-23 immunization

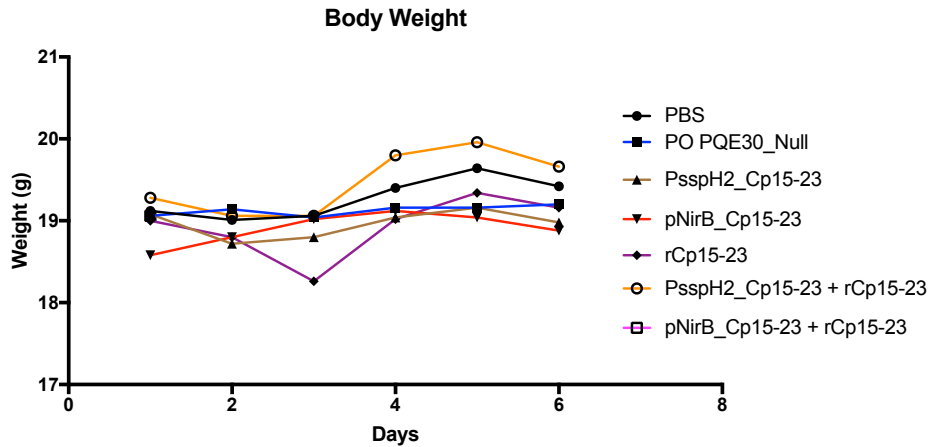


Figure 9: Weight change in C57BL/6 mice after Cp15-23 immunization. The graph depicts the progression of an average of body weights over a period of 1 week following vaccination. Body weight was measured days 1 through 6.

Figure 10: Cp15-23-specific humoral immune responses

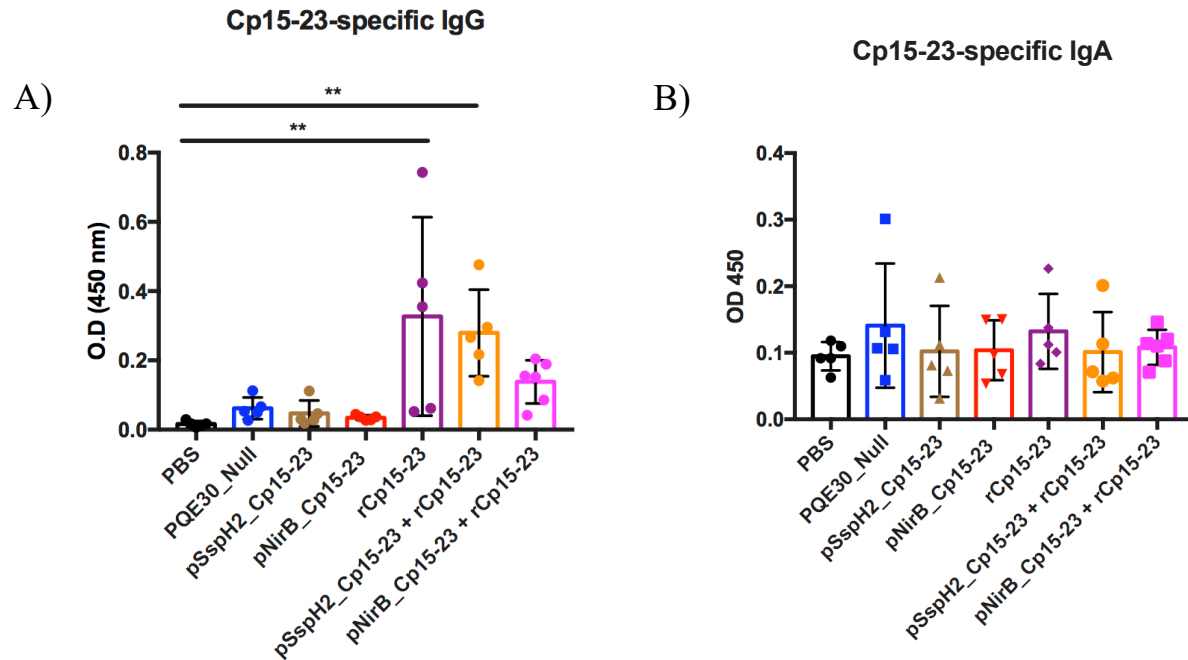


Figure 10: Vaccination groups rCp15-23 and pSspH2_Cp15-23 generate Cp15-23-specific antibody titers five weeks after initial vaccination. Mice were vaccinated via a multi-modal schedule with PO immunization on days 1, 3, and 5 with 10^9 CFU/mouse of the respective YSS1646 strain, and/or IM immunization with $10 \mu\text{g}$ of rCp15-23. Following initial multi-modal vaccination, serum IgG (A) and intestinal IgA titers (B) were quantified using ELISA and measured as a value of the mean optical density (O.D) at $450 \text{ nm} \pm$ standard deviation. All P values are by comparison to the PBS control group (** = $P < 0.01$).

Figure 11: Weight change in C57BL/6 mice after Cp15 and Cp23 immunization

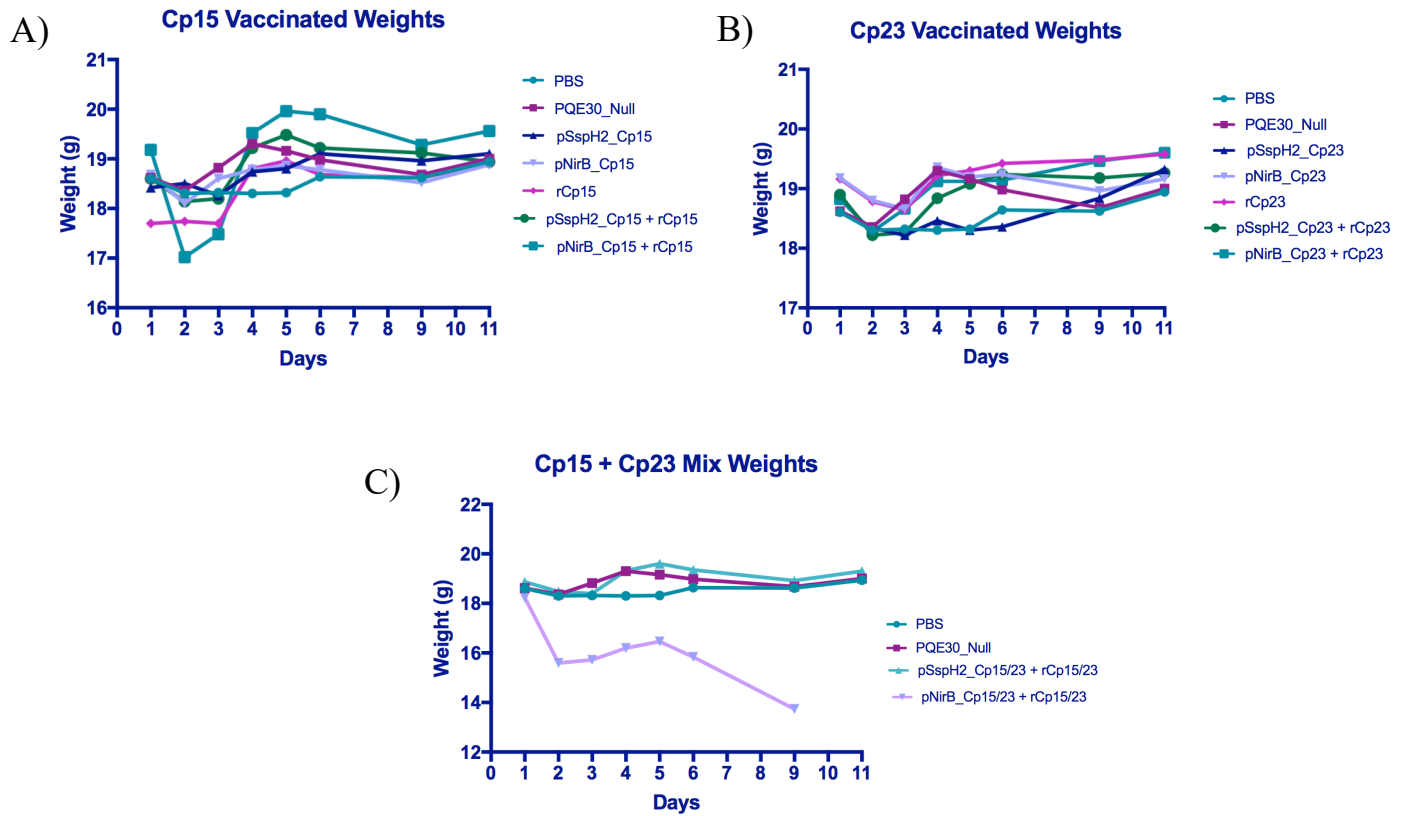


Figure 11: Weight change in C57BL/6 mice after A) Cp15, B) Cp23, or C) a combination of Cp15 and Cp23 immunization. The graph depicts the progression of an average of body weights of mice immunized with a A) Cp15, B) Cp23, or C) Cp15 and Cp23 mixed vaccine candidate over a period of 1 week following vaccination. Body weight was measured days 1 through 11. Control groups PBS and pQE30_Null were graphed on all weight charts.

Figure 12: Cp15- and Cp23-specific serum IgG humoral immune responses

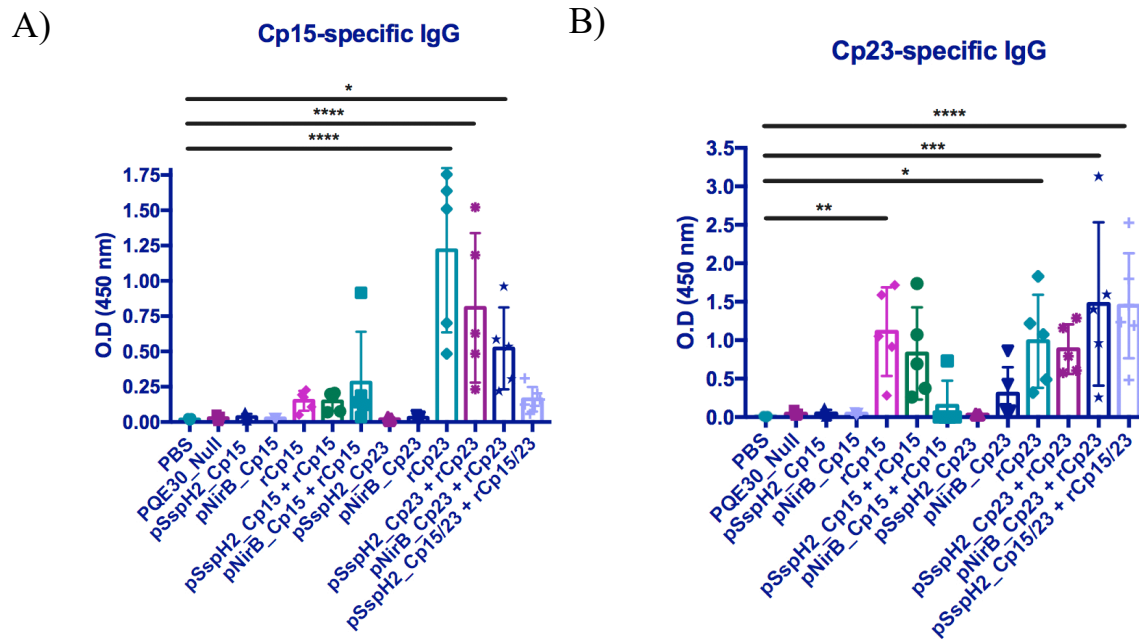


Figure 12: Cross-reactivity of Cp15- and Cp23-specific IgG antibodies detected five weeks after initial vaccination. Mice were vaccinated via a multi-modal schedule with PO immunization on days 1, 3, and 5 with 10^9 CFU/mouse of the respective YSS1646 strain, and/or IM immunization with $10 \mu\text{g}$ of rCp15, $10 \mu\text{g}$ of rCp23, or $5 \mu\text{g}$ of rCp15 with $5 \mu\text{g}$ of rCp23. Following initial multi-modal vaccination, A) Cp15-specific and B) Cp23-specific serum IgG titers were diluted at 1:50 and quantified using ELISA and measured as a value of the mean optical density (O.D) at $450 \text{ nm} \pm$ standard deviation. All P values are by comparison to the PBS control group (* = $P < 0.05$, ** = $P < 0.01$, *** = $P = 0.0002$, **** = $P = 0.0001$).

Figure 13: Cp23-specific intestinal IgA humoral immune responses

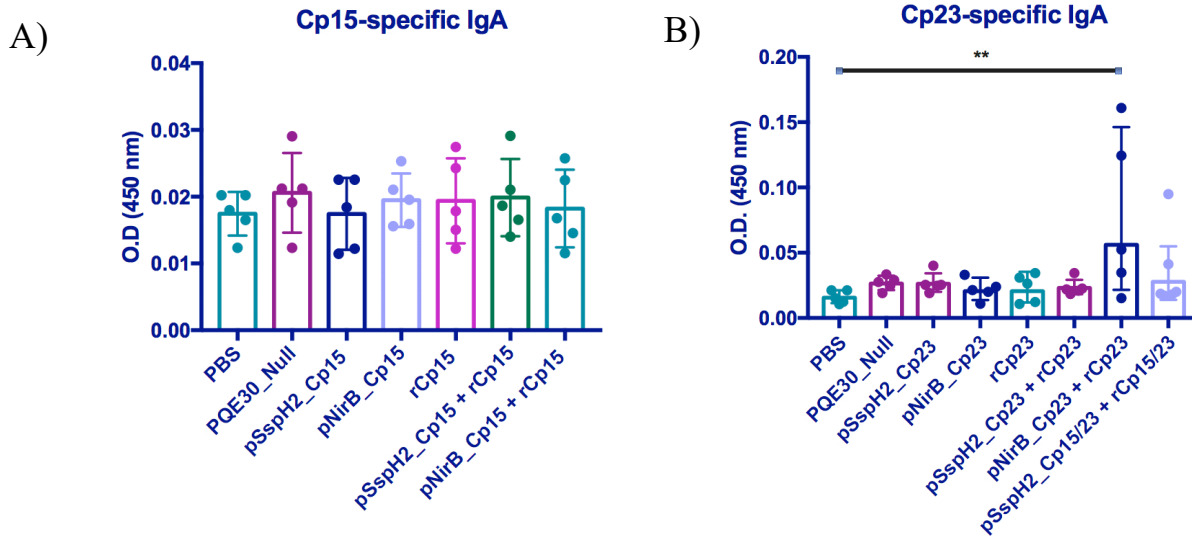


Figure 13: The pNirB_Cp23 + rCp23 multi-modal vaccination group elicits a significant increase in IgA antibody titers five weeks after initial vaccination. Mice were vaccinated via a multi-modal schedule with PO immunization on days 1, 3, and 5 with 10^9 CFU/mouse of the respective YSS1646 strain, and/or IM immunization with $10 \mu\text{g}$ of rCp15, $10 \mu\text{g}$ of rCp23, or $5 \mu\text{g}$ of rCp15 with $5 \mu\text{g}$ of rCp23. Following initial multi-modal vaccination, A) Cp15-specific and B) Cp23-specific intestinal IgA titers were quantified using ELISA and measured as a value of the mean optical density (O.D) at $450 \text{ nm} \pm$ standard deviation. All P values are by comparison to the PBS control group (** = $P < 0.01$).

Figure 14: Splenocyte Counts

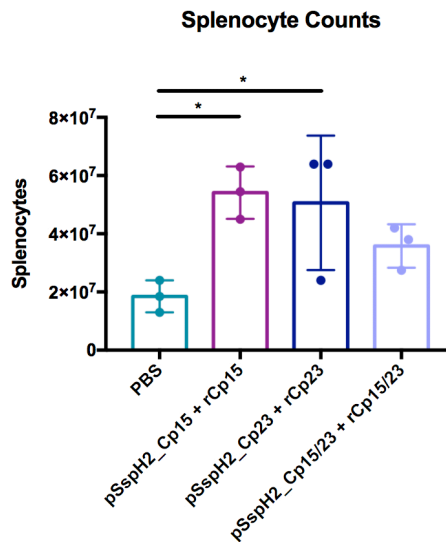


Figure 14: Increased splenocyte counts following vaccination. Splens of four groups, PBS, pSspH2_Cp15 + rCp15, pSspH2_Cp23 + rCp23, and pSspH2_Cp15/23 + rCp15/23, were processed through a 0.22-micron syringe and washed with HBSS. Cells were counted using a compound microscope. All P values are by comparison to the PBS control group (* = $P < 0.05$).

Figure 15: CD4+ and CD8+ T Cell Gating Strategy

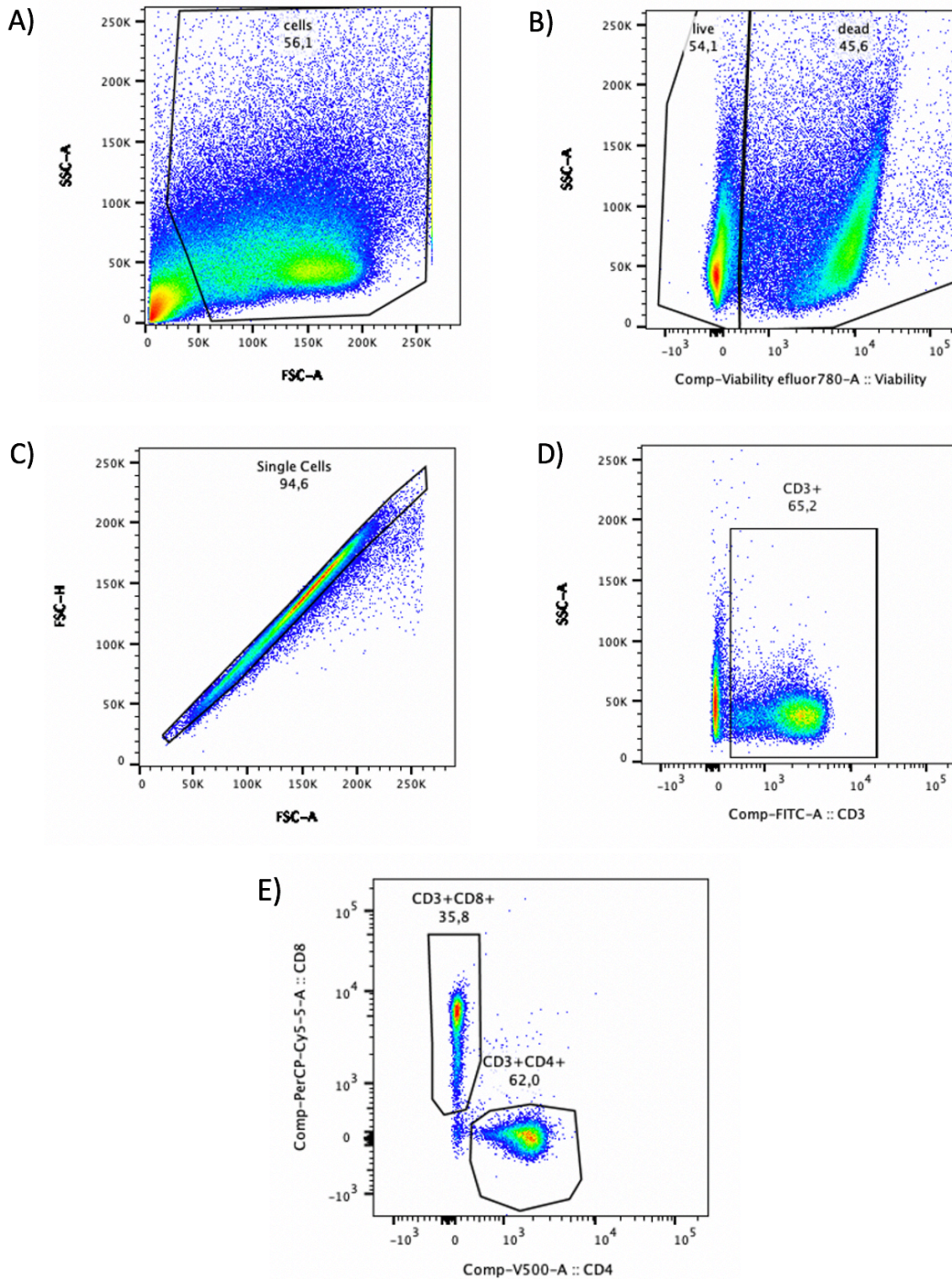


Figure 15: Gating strategy to identify CD4+ and CD8+ T cells from isolated splenocytes. Cells were stained with viability efluor 780, anti-CD3 FITC, anti-CD4+ V500, anti-CD8+ PerCP-Cy5.5, and anti-CD44 BUV737 antibodies used to visualize distinct cell populations. Events were acquired on a BD LSRFortessa cell analyzer. Gating strategies were developed using FlowJo. A) Cells were differentiated from debris. B) Live and dead cells were identified. C) Single cells were isolated. D) CD3+ T cells were identified. E) CD3+CD8+ and CD3+CD4+ T cell populations were separated.

Figure 16: CD4+ and CD8+ T Cell Populations

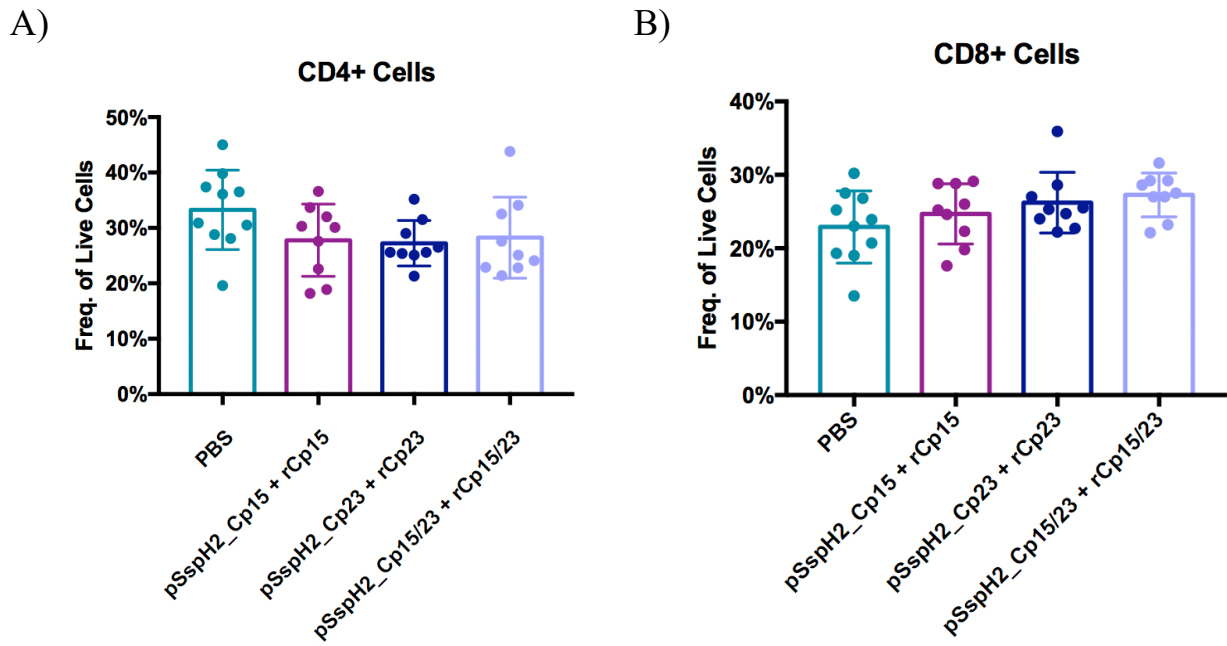


Figure 16: No observed difference in CD4+ and CD8+ T cell populations between vaccinated and PBS groups. A) CD4+ and B) CD8+ T cells in each experimental group were measured as a frequency (%) of the total live cells \pm standard deviation.

Figure 17: CD44+ T Cell Gating and Populations

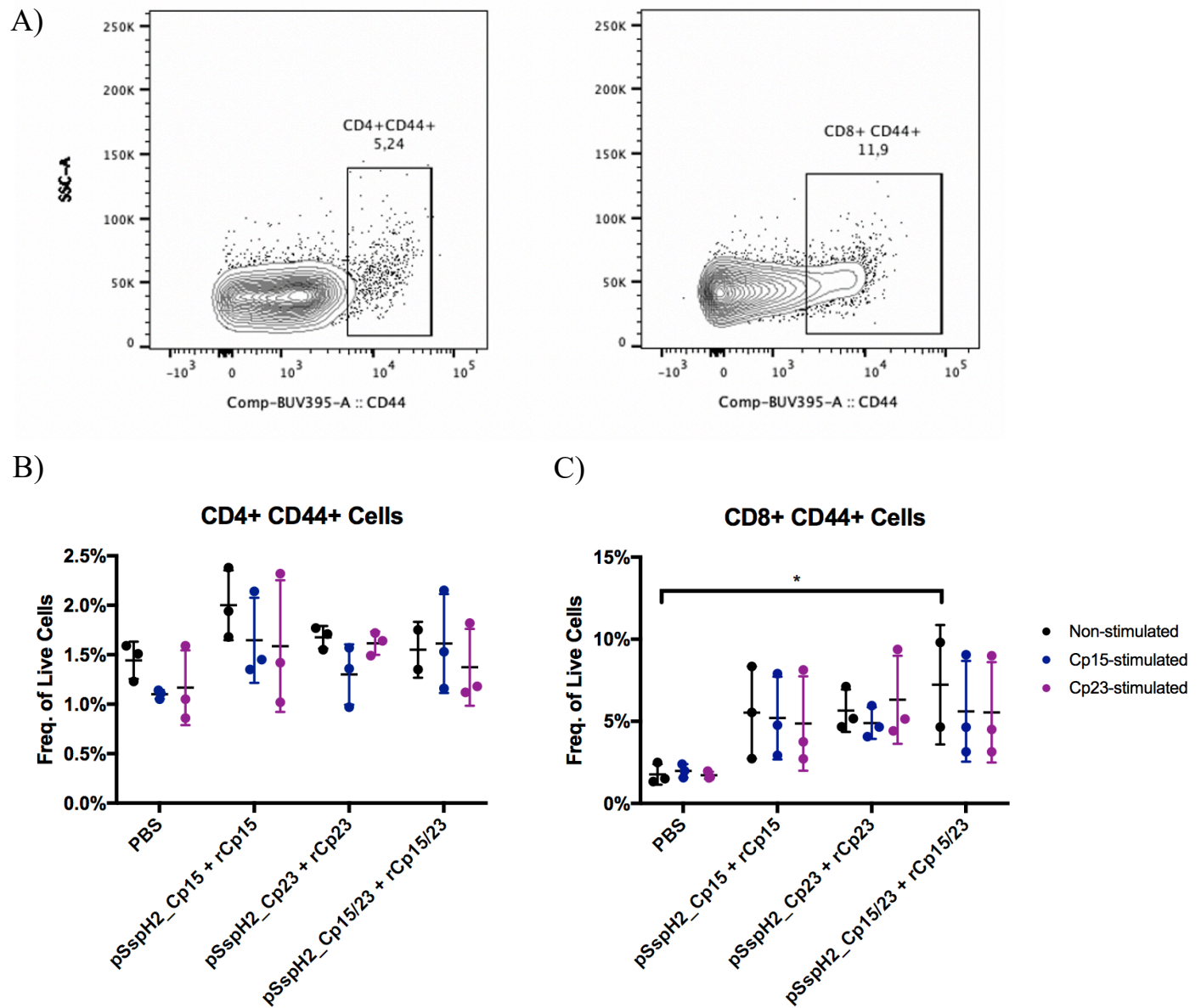


Figure 17: Increase in CD8+ CD44+ T cells populations in the Cp23-stimulated pSspH2_Cp15/23 + rCp15/23 vaccinated group. A) CD4+ (left) and CD8+ (right) T cells were gated for being CD44 positive. B) CD4+ CD44+ and C) CD8+ CD44+ T cells populations in each experimental group were measured as a frequency (%) of the total live cells \pm standard deviation. All P values are by comparison to their respective stimulation condition of the PBS control group (* = $P < 0.05$).

Figure 18: IFN- γ and TNF- α Producing T Cell Populations

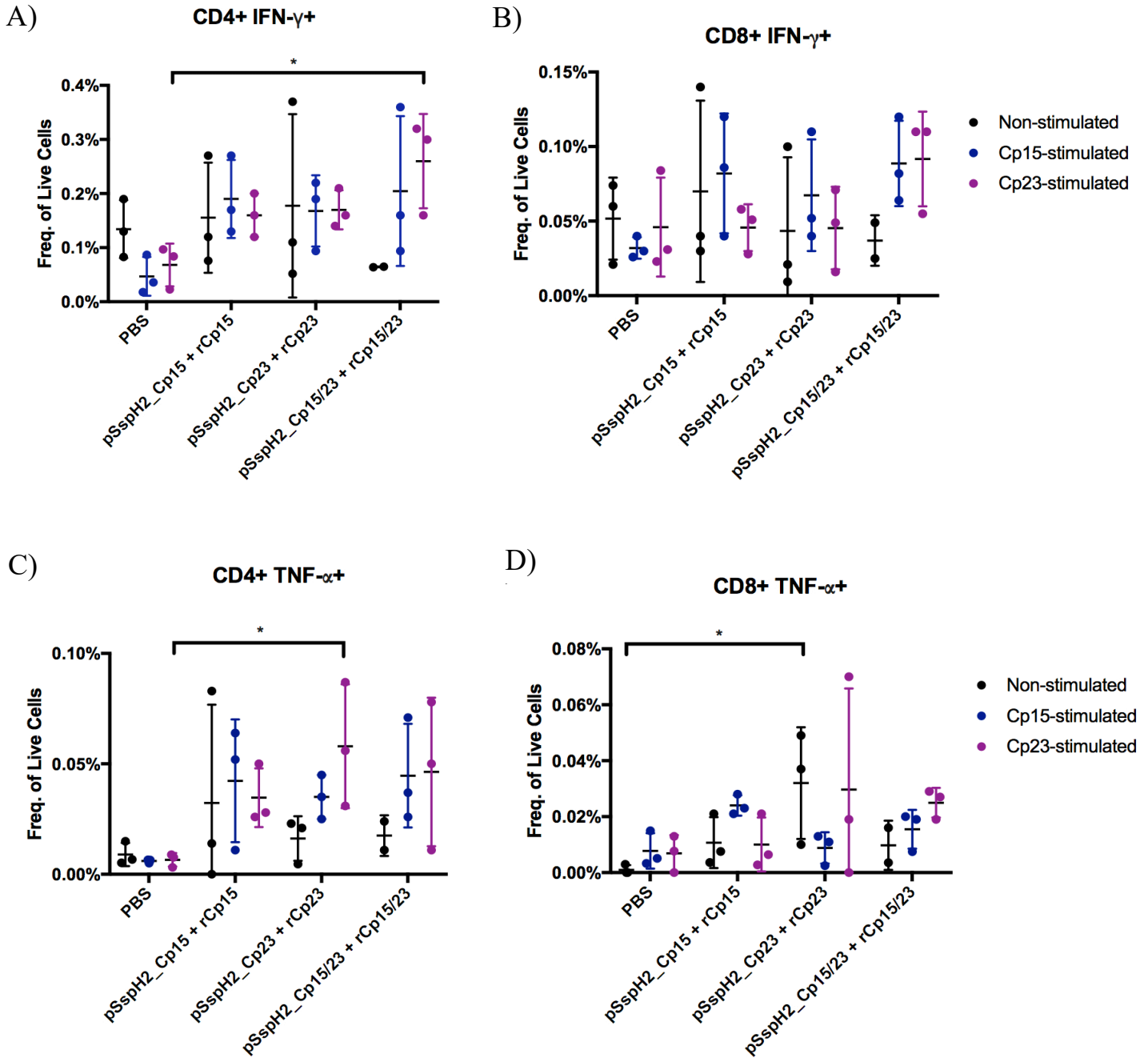


Figure 18: Increase in CD4+ IFN- γ +, CD4+ TNF- α +, CD8+ TNF- α + T cells populations in multi-modal Cp23 and Cp15/23 vaccinated groups. Cells were stained with anti-IFN- γ PE and anti-TNF- α eFluor450 antibodies used to visualize distinct cell populations. Events were acquired on a BD LSRFortessa cell analyzer. A) CD4+IFN- γ +, B) CD8+ IFN- γ +, C) CD4+TNF- α +, and D) CD8+TNF- α + T cell populations in each experimental group were measured as a frequency (%) of the total live cells \pm standard deviation. All P values are by comparison to their respective stimulation condition of the PBS control group (* = P<0.05).

Figure 19: Oocyst Gating Strategy and Burden

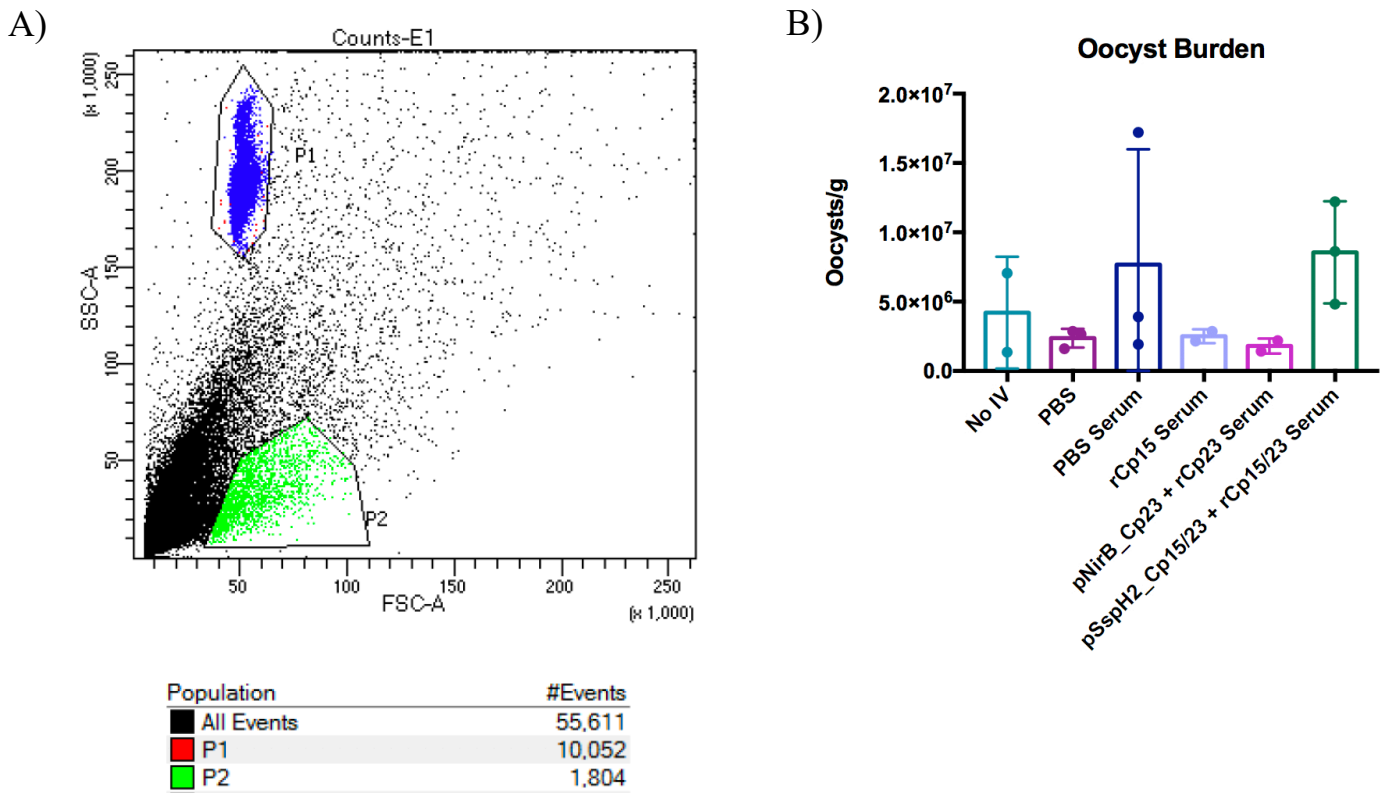


Figure 19: No significant difference in oocyst burden between IFN- γ R KO mice administered IgG serum antibodies from previously vaccinated C57BL/6 mice via adoptive transfer and control mice administered no IV injection, PBS, or serum from PBS mice. On day one, 200 μ L of either PBS or serum was injected intravenously in the lateral tail vein of mice. Serum used in this experiment was obtained from C57BL/6 mice vaccinated in the previous Cp15 and Cp23 immunogenicity experiment (Table 3). Mice were challenged with 3000 oocysts for nine days. Oocyst burden in the small and large intestine was determined using CountBright Absolute Counting beads in a BD LSRFortessa cell analyzer. A) Gating strategy of the counting beads (i.e., P1) and *C. parvum* oocysts (i.e., P2) on a non-infected sample to serve as a blank for experimental samples. B) Oocyst counts standardized to organ weight (g) \pm standard deviation.

5. Discussion

Cryptosporidium was first observed and characterized in 1907 by Edward Tyzzer as a parasitic disease targeting the mammalian intestinal tract¹⁶⁹. Despite over a century of intensive efforts, including the testing of hundreds of chemotherapeutic agents, there is still no highly effective therapy adequate for the clearance of *C. parvum* from an infected host. The development of a protective vaccine that could either prevent disease or reduce the severity of infection would be a considerable advance, especially for the protection of children and individuals with HIV who are the most susceptible to cryptosporidiosis. The findings of the current project have confirmed the immunogenicity of three *C. parvum* antigens delivered both orally in a *S. Typhimurium* vector and intramuscularly as recombinant protein, using a prime-pull vaccination approach, but did not provide evidence that the humoral response was protective in a severe murine challenge model.

5.1 Managing Codon Usage for Recombinant Protein Expression in Bacteria

Codon optimization of the Cp15-23 sequence for translation by *Salmonella Typhimurium* was performed to account for the strong codon bias known to occur in many fast-growing bacterial species, including *Salmonella enterica*¹⁷⁰. As the Cp15 and Cp23 sequences were subsequently amplified from the full Cp15-23 sequence by PCR, this ensured that all three antigenic sequences were codon optimized for *Salmonella*. The genetic code in mRNA is redundant by nature: each amino acid can be encoded by up to six different codons. Many bacterial species have a pronounced codon bias, i.e., a bias in the frequency with which a specific codon is used for synonymous amino acids. Although not yet fully understood, this bias is thought to confer evolutionary advantage by enhancing translational efficiency¹⁷¹. While consideration of codon bias is integral to ensuring efficient translation of a sequence in the target organism, such bias can result in experimental complications such as significantly increasing the GC content through CpG sites. The selection of optimal codons in a bacterium is often consistent with mutational bias present in that particular species. For example, in GC rich organisms, there is an increased likelihood of selecting G- or C- ending codons¹⁷². The *Salmonella enterica* genome itself has a relatively high GC content of approximately 52.1%¹⁷³ compared to *C. parvum* which has a GC content of approximately 30%¹⁷⁴. Optimizing both the native Cp15 and Cp23 sequences for efficient expression in the YS1646 vector raised the total GC content from 42.2% to 54.4% (Fig 5). In doing so, our codon optimization effort may have inadvertently hindered the expression of the Cp15-23

rather than enhanced it. In bacterial species, increased GC content in mRNA often results in the formation of secondary structures that can impede mRNA-ribosome interactions, thus halting translation¹⁷⁵. While expression of the recombinant Cp15-23 fusion protein by YS1646 was not directly measured *in vitro*, this construct nonetheless elicited a significant humoral immune response in two of the five vaccination groups (i.e., rCp15-23, pSspH2_Cp15-23) (Fig 10a). Difficulties in expression and purification of the recombinant fusion protein by *E. coli* could potentially be attributed to the increased GC content hindering *in vitro* translational efforts. Thus, there may be benefits to further optimize the Cp15-23 sequence for effective expression in *Salmonella*. While optimizer algorithms are programmed to predict highly expressed genes, codon optimization remains largely random and synonymous codon changes have been found to alter protein conformation, stability, and function, as well as change sites of post-translational modifications¹⁷⁶. Last, while an avoidable limitation, consideration must be given to the fact that the YS1646 delivery system is a prokaryote model responsible for translating and secreting a eukaryote protein molecule. Thus, even with “optimal” codon optimization, the final Cp15-23 protein product is unlikely to be 100% representative of the surface proteins found naturally on *C. parvum*.

5.2 Troubleshooting Recombinant Cp15-23 Protein Expression *in vitro* by *E. coli*

Cp15-23 was originally selected as the third vaccine candidate as it was previously shown to reduce *C. parvum* parasite burden when administered as recombinant protein vaccine¹¹⁵. Selection of an unnatural divalent protein, however, may have resulted in several unintended consequences including degradation of the recombinant Cp15-23 protein, and/or potential aggregation of the resulting fragments (Fig 8). Both the western blots (Fig 8a, 8c) and the Coomassie stain (Fig 8b) revealed a number of other his-tagged protein bands other than the expected 46 kDA band of interest. The conjecture of protein degradation and aggregation is further supported by the disappearance of a larger protein band following addition of DTT to the E3 protein sample (Fig 8a). DTT is used to break disulfide bonds, thus reducing unwanted protein aggregation¹⁷⁷. Another possibility to explain the low protein yields is poor stability. Low protein stability can give rise to protein degradation, precipitation, and folding instability¹⁷⁸, all of which might contribute to the presence of additional bands in the Western blots. A multitude of factors can result in poor protein stability, both during protein expression and purification: the primary

protein structure, the construct design of the expression plasmid, the temperature and expression medium used, and the toxicity of the protein¹⁷⁹. The potential factors affecting protein stability in this case may include the non-optimized codon usage and the temperature during expression. As the Cp15-23 sequence was optimized for expression by *Salmonella* spp., it is possible that the codon usage was not optimal for expression of the recombinant Cp15-23 in competent *E. coli*. Lowering the temperature at which protein expression was carried out (37°C) could improve the stability of the protein. Bacterial protein synthesis decreases as the environmental temperature deviates from the optimum growth range, which in the case of *E. coli* ranges from 20-45°C, and subsequently, also reduces the expression of endogenous proteases^{179, 180}. In the future, it would be useful to examine our recombinant proteins using nuclear magnetic resonance (NMR) spectroscopy. NMR spectroscopy would determine the stability of the Cp15-23 and individual proteins in solution, as well as assess effects of environmental conditions (i.e., pH, temperature)¹⁸¹.

In response to the observation of excess bands detected from the initial rCp15-32 purification, repeat attempts were made to elute solely the target rCp15-23. From the results obtained in Figure 8a, a first hypothesis was that higher pH elution conditions (i.e., E1) would improve elution of only rCp15-23, albeit less of the protein as exhibited by the faintness of the band. Initially, it was thought that further pH adjustment of the purification protocol would be required to establish an optimal elution condition. However, the second protein purification for rCp15-23 in Figure 8c contradicts the previous finding, observing rCp15-23 to be more concentrated in lower pH elutions (i.e., elution groups F and G with pH = 4.7 and pH = 4.3 respectively), and observing no elution condition to only have a single band indicative of rCp15-23. Furthermore, it appears that a significant portion of rCp15-23 is still attached to the beads of the Ni-NTA affinity chromatography column (Fig 8c), suggesting the affinity between the nickel ligand on the columns and the histidine tags of the protein is very strong. This finding suggests that perhaps elution via pH-changing urea may not be the most efficient method in collecting the purified rCp15-23 protein. Urea was selected to use in the elution buffer for its chaotropic effects, eliminating unwanted secondary protein structures through disrupting hydrogen bonds and hydrophobic interactions and solubilizing proteins^{166, 167}. In the future, elution with varying concentrations of competitor substrates, in this case imidazole or free histidine, may prove to be more efficient in eluting greater quantities of all his-tagged proteins at the very least, if not rCp15-23 specifically. Addition of lysozyme (Millipore-Sigma; Burlington, USA) and B-PER

(ThermoFisher Scientific; Waltham USA), both of which act as cell-lysis reagents, to the protein purification protocol can also help release additional recombinant protein trapped in *E. coli*.

It is important to note that while several excess bands are detected in both rCp15-23 protein purifications, all detected proteins carried a poly-histidine tag, indicating they were translated from the inserted Cp15-23 sequence; no other genes in BLR DE3 *E. coli* give rise to the same amino acid motif. While this finding may be problematic as it may introduce the recombinant vaccine antigen in novel conformations, rCp15-23 already exists as an unnatural fusion protein. Thus, further degradation and subsequent aggregation merely increases the different combination of antigen epitopes to which immune cells are exposed to. This result may also indicate that while densitometry analysis of the percentage of the intact Cp15-23 from the initial protein purification was only 40% of the total protein present (Fig 8b), consideration of degraded Cp15-23 protein components may increase this value. However, further protein analysis (i.e., proteomics) must be carried out to verify the identities of the additional bands.

5.3 Reliability of *Salmonella* YS1646 *in vitro* Protein Expression to Predict *in vivo* Expression

Recombinant protein expression by *S. Typhimurium* YS1646 strains was not evaluated in this project. The success of this novel vaccine is dependent on the ability of YS1646 to deliver the Cp15, Cp23, or the Cp15-23 protein to the intestinal epithelium, mimicking where *C. parvum* would invade and replicate during a natural infection and priming the surrounding mucosal immunity. However, as noted in the results, the immunogenicity studies described above demonstrated both a detectable humoral response as well as several select cell-mediated responses to Cp15, Cp23, and Cp15-23 *in vivo*, despite not verifying protein expression by YS1646 strains *in vitro*.

The expression of recombinant Cp15-23 by YS1646 *in vitro* was not verified for two reasons. First, it is extremely difficult to successfully mimic the protein-inducing conditions of *Salmonella* in an *in vitro* model, even using a murine Raw 264.7 macrophage infection model. An abundance of research demonstrates that differing *in vitro* growth conditions can greatly affect expression levels of effector proteins. Oxygen concentration, pH, osmolarity, culture nutrients, and bacterial growth state are all factors that have been shown to influence the secretion of T3SS effectors in *S. Typhimurium*^{182, 183, 184, 185}. While alterations may be made to culture media and oxygen levels during incubation, both monomicrobial cultures and Raw 264.7 macrophage cells

are inadequate in modelling the conditions of the gastrointestinal tract that will be experienced by YS1646 strains upon *in vivo* vaccination. Second, antigen expression, or the lack thereof, *in vitro* does not directly translate to an antigen-specific immune response *in vivo*. Previously, in the Ward-Ndao lab, the *Salmonella* YS1646 vector has been used successfully as an antigen delivery system to deliver the receptor binding domain of Toxin A and Toxin B of *Clostridium difficile*¹⁴⁵, and the digestive enzyme Cathepsin B of *Schistosoma mansoni*¹⁴⁶. During the development of both vaccines, detection of antigen expression by the YS1646 vector during Raw 264.7 infection was absent or limited in most of the generated strains. Despite the lack of observable recombinant protein expression during *in vitro*, however, most YS1646 delivered vaccines provided substantial protection against challenge from the respective pathogen following a similar multi-modality vaccination.

5.4 Proof-of-Concept: Immunogenicity of the Candidate Vaccines

Since vaccines are typically used in otherwise healthy individuals, pre-clinical evaluations typically focus on safety/toxicity followed by two levels of “proof-of-concept” (POC): first POC immunogenicity followed by POC efficacy. C57BL/6 mice were chosen for the POC immunogenicity studies since the laboratory had considerable experience with a highly susceptible IFN- γ -R KO murine model on a C56BL/6 background.

5.4.1 Immunogenicity of the Cp15-23 Candidate Vaccines

With our first immunogenicity study using the fusion protein Cp15-23, we observed no significant weight loss within the first six days following PO or IM vaccine administration. This indicated that there were no immediately detectable pathological consequences oral vaccination. Two vaccination groups, rCp15-23 and pSspH2_Cp15-23 + rCp15-23, were both found to have significantly increased Cp15-23-specific serum IgG titers compared to the PBS control group (Fig 10a). No groups demonstrated a significant increase in intestinal IgA titers at week five (Fig 10b). While these results indicate that the candidate Cp15-23 vaccines were capable of eliciting an IgG-type humoral immune response, the ELISAs used had to be coated with 4 times the regular amount of protein (i.e., 4 μ g/mL vs. 1 μ g/mL) to obtain these results. Furthermore, it is important to recall that during a *C. parvum* infection, antibodies only play a supportive role in protection against *C. parvum* and are insufficient by themselves to prevent infection or parasite clearance^{82, 83}. Thus,

while both rCp15-23 and pSspH2_Cp15-23 + rCp15-23 vaccination groups appear promising in their ability to elicit an anti-*C. parvum* humoral immune response, the protective efficacy of this response remains undetermined.

5.4.2 *Weight Fluctuations and Humoral Immunogenicity of the Cp15 and Cp23 Candidate Vaccines*

The second immunogenicity study focused on the individual surface proteins Cp15 and Cp23. In two of the vaccination groups, pNirB_Cp15 + rCp15 and pNirB_Cp15/23 + rCp15/23, there were marked decreases in their average weights of the mice following administration of the first PO and IM immunization (Fig 11a, 11c). While the pNirB_Cp15 + rCp15 vaccination group recovered the weight loss by day four, the pNirB_Cp15/23 + rCp15/23 vaccinated group did not. By day nine, the pNirB_Cp15/23 + rCp15/23 vaccinated group reached critical weight loss of 20% of their original weight or more¹⁸⁶ and had to be euthanized. As the weights of every mouse decreased in this vaccination group, we can rule out the issue of improper vaccine administration as a cause of the weight loss. Upon first examination, it appears that the weight loss may be attributable to the potential toxicity of the pNirB_Cp15 YS1646 strain or of the recombinant Cp15 protein; both groups in which the weight loss occurred had received both components. However, as neither the pNirB_Cp15 only nor the rCp15 only vaccination groups experienced a similar decrease in average weights during the initial vaccination period, the reason for this unexpected weight loss remains undetermined.

Interestingly, the ELISA data from Figure 12 indicates substantial cross-reactivity between the Cp15 and Cp23 proteins. Figure 12a indicates that it was the rCp23 only, pSspH2_Cp23 + rCp23, and the pNirB_Cp23 + rCp23 vaccinated groups that had significantly increased Cp15-specific serum IgG titers. Similarly, Figure 12b illustrates the rCp15 only vaccinated group also had significantly increased Cp23-specific IgG titers, despite not having been exposed to the Cp23 protein. A partial explanation of such cross-reactivity may be a serological response to the 6x-histidine tag present at the ends of both the Cp15 and Cp23 recombinant proteins used for vaccination and in the ELISAs. The histidine tags can be observed in the western blots of both purified recombinant Cp15 (Fig 7a) and Cp23 (Fig 7b). In particular, the purified rCp15 had a prominent <3.5 kDa band, suggesting a large quantity of 6x-histidine tags had been cleaved from the Cp15 protein. Combined with the possibility that the Cp23 is generally more

immunogenic than Cp15, this could possibly contribute to the apparent presence of Cp15-specific IgG antibodies in Cp23 vaccinated mice. The apparent presence of significant Cp23-specific IgG titers in the rCp15 vaccinated group, on the other hand, cannot be explained so easily. One theory to explain the prominent cross-reactivity observed could be that our sub-optimal protein purification protocol led to the presence of non-histidine tagged *E. coli* proteins native to the protein-expressing *E. coli* host may have also been collected in both rCp15 and rCp23 protein samples. The presence of these “contaminants” in could have generated antibodies that would be detected in the ELISAs, as the antigens used to coat the plates also contained the “contaminants”. All groups that demonstrated apparent cross-reactivity were immunized IM with at least one of the two recombinant antigens.

In addition to the observation of increased serum IgG titers in several vaccine groups, the pNirB_Cp23 + rCp23 group also elicited a significant mucosal IgA immune response compared to the PBS control group. Even if humoral immune responses serve only a supportive role in a *C. parvum* infection, a significant mucosal response at the site of infection would likely be beneficial.

5.4.3 Cell-mediated Immunogenicity of the Cp15 and Cp23 Candidate Vaccines

Initial increased splenocyte counts for all three investigated vaccinated groups, pSspH2_Cp15 + rCp15, pSspH2_Cp23 + rCp23, and pSspH2_Cp15/23 + rCp15/23, suggest a vaccine-induced influx or expansion of leukocyte migration in the spleen (Fig 14). As the spleen plays an important role in the maturation of T and B cells, and subsequently in the clearance of microorganisms and antigens, it is not surprising that vaccinated animals that received both a recombinant foreign antigen as well as a bacterial delivery vector would elicit greater splenic responses¹⁸⁷.

Interestingly, although no differences were detected in the frequency of CD4+ and CD8+ T cell counts between the PBS and vaccinated groups, the observed increase in the frequency of CD8+ CD44+ T cells in some groups suggest that vaccination can shift the distribution of CD8+ T cells in favour of mature, activated T cells (Fig 17c). While the role of cytotoxic CD8+ T cells in the context of a *C. parvum* infection has yet to be established, upon a second exposure to either the Cp15 or Cp23 by infection, for example, animals that had been vaccinated with pSspH2_Cp15 + rCp15, pSspH2_Cp23 + rCp23, or pSspH2_Cp15/23 + rCp15/23 would be expected to have a

greater population of effector or memory CD8+ T cells ready to proliferate, enact cytotoxic functions, and secrete effector cytokines¹⁸⁸.

Similarly, despite the absence of changes in total CD4+ and CD8+ T cell counts, vaccinated groups had more IFN- γ - and TNF- α -producing CD4+ and CD8+ T cells in response to the targeted *C. parvum* antigens (Fig 18). A trend for increased CD4+ IFN- γ + T cells was observed in all vaccinated groups for both Cp15 and Cp23 stimulated conditions compared to the PBS group (Fig 18a). While only the Cp23-stimulated pSspH2_Cp15/23 + rCp15/23 vaccinated group produced a significant increase in CD4+ IFN- γ + T cells, this trend suggests that these animals would have, in theory, greater production of IFN- γ by their CD4+ T cells upon challenge. As established previously, IFN- γ -production by CD4+ contributes greatly to the elimination of intracellular pathogens such as *C. parvum* by promoting a T_h1 environment, subsequently favouring increased phagocytosis, neutrophil degranulation, release of reactive oxygen species, and differentiation of cytotoxic T cells from CD8+ precursors^{74,75,76,77}. As previously noted, CD4+ T cells are the predominant cell type necessary to fight against *C. parvum* with severe cryptosporidiosis persisting in individuals with CD4+ T cell counts of 50 cells/mm or less³.

Further research in SCID mice demonstrated that CD4+ T cells were the predominant cell type necessary to fight against *C. parvum*. Mice specifically deficient in major histocompatibility complex (MHC) class II, important for antigen presentation to CD4+ T cells, were significantly more susceptible to *C. parvum* infection compared to mice deficient in MHC class I which is important for antigen presentation to CD8+ T cells⁶⁹. Furthermore, administration of anti-CD4 monoclonal antibodies (mAb) reduced or completely eliminated the ability of SCID mice to resolve *C. parvum* infection, following adoptive transfer of splenocytes from immunocompetent donors⁷⁰. The same effect was not observed following treatment with either anti-CD8 mAbs or anti-asialo-GMI (to deplete NK cells) antibodies. Similarly, human studies have consistently shown that fulminant cryptosporidiosis predominantly occurs in immunocompromised individuals with CD4+ T cell counts of less than 50 cells/mm³. Individuals with CD4+ T cell counts greater than 180-200 cells/mm³ typically only experience a transient and self-limited form of the disease⁷¹.

Likewise, while only the Cp23-stimulated pSspH2_Cp23 + rCp23 vaccinated group had a significant increase in the frequency of CD4+ TNF- α + T cells, a trend for increased CD4+ TNF- α + T cells was observed for all vaccinated groups, in both Cp15 and Cp23 stimulated

conditions, compared to the PBS group (Fig 18c). TNF- α is a key inflammatory cytokine that is normally upregulated in the intestine of humans upon *C. parvum* infection¹⁸⁹. While TNF- α may not be necessary for the control of a *C. parvum* infection, TNF- α has been shown to inhibit parasite invasion *in vitro* in a murine enterocyte cell line by up to 79%¹⁹⁰.

A limitation of this part of the project was the variability of the flow cytometric analyses for some of the vaccination groups. Groups were generally small and the standard deviation for all cell counts obtained were very large for a small sample size. These experiments should be repeated for the most promising vaccination schedules with more animals per vaccination group.

5.5 Proof-of-Concept: Efficacy of the Candidate Vaccines

IFN- γ -R KO C57BL/6 mice were previously used in the laboratory to evaluate the efficacy of *C. parvum* candidate vaccines and were chosen for this POC efficacy study for their high susceptibility to *C. parvum* infection.

5.5.1 Initial *C. parvum* Challenge Study featuring Direct Vaccination of IFN- γ R KO mice

An initial *C. parvum* challenge study was organized and started using the same prime-pull vaccination in IFN- γ R KO mice. Three weeks after the last immunization, mice were challenged with 3000 oocysts/mouse and monitored for ten days. Our intent was to assess parasite burden at day nine to evaluate the protective efficacy of the vaccine candidates. However, only 11 days following the third PO immunization dose, the vaccinated mice succumbed to sickness, or had reached a critical state (i.e., severe weight loss, lethargic and non-responsive, hunched posture¹⁹¹) and were euthanized. As IFN- γ plays an essential role in resistance to early *S. Typhimurium* infection in mice¹⁹², it is hypothesized that the absence of the IFN- γ receptor in this particular mouse model rendered the mice susceptible to systemic infection by the YS1646 strains. Bao et al. found that in IFN- γ knockout mice, inoculation with 5×10^8 CFUs of attenuated *S. Typhimurium* resulted in disseminated septicemia two weeks later. Splenomegaly, tissue necrosis, and moderate foci of leukocyte infiltration in the liver were all detected by the end of the second week¹⁹³; all of these pathologies were observed during necropsy of our euthanized mice (data not shown).

5.5.2 Second *C. parvum* Challenge Study featuring Adoptive Transfer of Serum from Vaccinated C57BL/6 mice into IFN- γ R KO mice

A secondary pilot *C. parvum* challenge study was designed to evaluate the protective efficacy of adoptively transferred serum antibodies into susceptible IFN- γ R KO mice. Despite this project emphasizing the importance of the cell-mediated immune response in *C. parvum* infection, the unexpected outcome of the initial challenge study at the end of MSc. Work did not permit us to investigate cell-mediated immunity. As serum was available from prior immunogenicity experiments, a modified *C. parvum* challenge study involving adoptive transfer of serum antibodies was planned. Donor groups were chosen based on serum availabilities and antigen-specific antibody titers. Antibody titers were standardized between donor groups to a specific O.D range (Table 3).

Nine days following intravenous administration of serum antibodies and subsequent *C. parvum* challenge, mice were euthanized, and oocyst burdens were quantified using flow cytometry analysis (Fig 19). No significant decrease in oocyst burden could be observed for any of three adoptive transfer groups (receiving rCp15-, pNirB_Cp23 + rCp23-, or pSspH2_Cp15/23 + rCp15/23-induced serum antibodies) (Fig 19b). Among the many possible explanations for this result, small group size and the intrinsic variability of oocyst shedding in this model are undoubtedly major contributors¹⁹⁴. The presence of feces at the time of intestine collection can also significantly influence oocyst counts since the oocysts shed in the feces would only be accounted for in some mice but not others. While these factors may possibly explain the lack impact, another explanation, as explored in the literature review, is that while antibodies play a supportive role in protection, they are insufficient by themselves to prevent infection^{82, 83} and non-essential for parasite clearance⁸⁴. Furthermore, while certain mucosal antibodies have been previously shown to partially reduce oocyst shedding and parasite burden^{89,90,91}, the antibodies administered in our experiment were serum IgG. Thus, in the future, it will be important to repeat this adoptive transfer experiment using splenocytes from vaccinated wild type mice.

5.6 Conclusion

In conclusion, this project was successful in the development of two *S. Typhimurium* YS1646 expression vectors for the delivery of three *C. parvum* recombinant antigens: Cp15, Cp23, and Cp15-23. Significant increases in antigen-specific serum IgG were detected, compared to the

PBS control group, following immunization of C57BL/6 mice with several candidates and schedules. A significant increase in intestinal antigen-specific IgA was detected only in the pNirB_Cp23 + rCp23 group which was one of the most promising candidates overall. Splenocyte CD4+ and CD8+ responses were also detected in several groups, suggesting that these candidates have the potential to elicit both humoral and cellular responses. Although no difference in oocyst burden was observed following adoptive transfer of vaccine-induced serum antibodies, this observation was not unexpected given the known importance of cellular responses in protecting against *C. parvum*. While this project remains inconclusive about whether or not our vaccine candidates are protective against *C. parvum* challenge, our data demonstrate that several of our vaccine candidates are capable of eliciting both a humoral and cellular immune response to *C. parvum* antigens.

6. Future Directions

To complete the development of a successful vaccine candidate for *C. parvum*, several additional experiments must first be conducted.

Ideally, optimization of the protein purification protocol should be completed so that upon elution, only proteins of the desired size are obtained. As previously described, strategies to optimize protein expression could include better codon usage for all three antigenic sequences for ease of expression in *E. coli*, as well as lowering the temperature at which protein expression is carried out. However, as the quality of protein purification can be influenced by many factors, it may be beneficial to focus first on characterizing additional bands using proteomics.

Given the known importance of T cell responses in cryptosporidiosis, a second adoptive transfer experiment should be carried out, this time transferring T cells from newly vaccinated C57BL/6 mice to *C. parvum* challenged-IFN- γ R KO mice. Since the knock out animals proved to be exquisitely sensitive to the YS1646 vector, this is the only way to evaluate the importance of a cell-mediated immunity and verify the protective efficacy of the vaccine candidates. To conduct this experiment, WT C57BL/6 mice would be vaccinated according to the pre-established multi-modal vaccination schedule. Mice would be euthanized at 35 days (5 weeks) and the splenocytes would be isolated and adoptively transferred into IFN- γ R KO mice by intravenous infusion. The IFN- γ R KO mice would then be challenged with *C. parvum*. At the end of nine days, mice would be euthanized, and parasite burden would be used to assess the protective efficacy of the transferred immune cells elicited from each different vaccination condition.

Following the optimization of this proof-of-concept study, further development of this *C. parvum* vaccine candidate would include chromosomal integration of the most promising antigenic sequences into the YS1646 *Salmonella*. Chromosomal integration would mitigate the possibility of spontaneous loss of the plasmid within the *Salmonella* delivery vector; an event that has been previously observed to occur in other bacteria (i.e., *E. coli*) in rat and pig models^{195, 196}. Furthermore, this process would involve the removal of antibiotic resistance genes present in the recombinant plasmid, to prevent bacteria present in the host gut from acquiring these genes.

This project serves as the first of many steps in the development of a novel vaccine for *C. parvum*. Cryptosporidiosis is a significant diarrheal disease that affects both developing and developed countries. Currently, no therapeutic nor prophylactic treatment exists for immunocompromised individuals who are most at risk for the disease. The results of this project suggest that the pNirB_Cp23 + rCp23 combination has the potential to be an effective vaccine. While it remains inconclusive whether or not our vaccine candidates can elicit a protective, cell-mediated immune response against *C. parvum* infection, several candidates proved to be immunogenic and this research brings us one step closer to better understanding the requirements of an effective vaccine against cryptosporidiosis.

References

1. Tyzzer, E.E. A sporozoan found in the peptic glands of the common mouse. *Proceedings of the Society for Experimental Biology and Medicine*, **5**, 12-13 (1907).
2. Slavin, D. *Cryptosporidium meleagridis* (sp. nov.). *J Comp Pathol* **65**, 262-266 (1955).
3. Panciera, R.J., Thomassen, R.W. & Garner, F.M. Cryptosporidial Infection in a Calf. *Vet Pathol* **8**, 479-484 (1971).
4. Meisel, J.L., Perera, D.R., Meligro, C. & Rubin, C.E. Overwhelming watery diarrhea associated with a cryptosporidium in an immunosuppressed patient. *Gastroenterology* **70**, 1156-1160 (1976).
5. Nime, F.A., Burek, J.D., Page, D.L., Holscher, M.A. & Yardley, J.H. Acute enterocolitis in a human being infected with the protozoan *Cryptosporidium*. *Gastroenterology* **70**, 592-598 (1976).
6. Leitch, G.J. & He, Q. Cryptosporidiosis-an overview. *J Biomed Res* **25**, 1-16 (2012).
7. Bouzid, M., Hunter, P.R., Chalmers, R.M. & Tyler, K.M. *Cryptosporidium* pathogenicity and virulence. *Clin Microbiol Rev* **26**, 115-134 (2013).
8. Fayer, R. Taxonomy and species delimitation in *Cryptosporidium*. *Exp Parasitol* **124**, 90-97 (2010).
9. Current, W.L. *et al.* Human cryptosporidiosis in immunocompetent and immunodeficient persons. Studies of an outbreak and experimental transmission. *N Engl J Med* **308**, 1252-1257 (1983).
10. Collaborators, G.B.D.D.D. Estimates of the global, regional, and national morbidity, mortality, and aetiologies of diarrhoea in 195 countries: a systematic analysis for the Global Burden of Disease Study 2016. *Lancet Infect Dis* **18**, 1211-1228 (2018).
11. Bouzid, M., Kintz, E. & Hunter, P.R. Risk factors for *Cryptosporidium* infection in low and middle income countries: A systematic review and meta-analysis. *PLoS Negl Trop Dis* **12**, e0006553 (2018).
12. Kotloff, K.L. *et al.* Burden and aetiology of diarrhoeal disease in infants and young children in developing countries (the Global Enteric Multicenter Study, GEMS): a prospective, case-control study. *Lancet* **382**, 209-222 (2013).

13. Slapeta, J. Cryptosporidiosis and *Cryptosporidium* species in animals and humans: a thirty colour rainbow? *Int J Parasitol* **43**, 957-970 (2013).
14. Gerace, E., Lo Presti, V.D.M. & Biondo, C. *Cryptosporidium* Infection: Epidemiology, Pathogenesis, and Differential Diagnosis. *Eur J Microbiol Immunol (Bp)* **9**, 119-123 (2019).
15. Desai, N.T., Sarkar, R. & Kang, G. Cryptosporidiosis: An under-recognized public health problem. *Trop Parasitol* **2**, 91-98 (2012).
16. Dixon, B., Parrington, L., Cook, A., Pollari, F. & Farber, J. Detection of *Cyclospora*, *Cryptosporidium*, and *Giardia* in ready-to-eat packaged leafy greens in Ontario, Canada. *J Food Prot* **76**, 307-313 (2013).
17. Chalmers, R.M. Waterborne outbreaks of cryptosporidiosis. *Ann Ist Super Sanita* **48**, 429-446 (2012).
18. Hoxie, N.J., Davis, J.P., Vergeront, J.M., Nashold, R.D. & Blair, K.A. Cryptosporidiosis-associated mortality following a massive waterborne outbreak in Milwaukee, Wisconsin. *Am J Public Health* **87**, 2032-2035 (1997).
19. Mac Kenzie, W.R. *et al.* A massive outbreak in Milwaukee of cryptosporidium infection transmitted through the public water supply. *N Engl J Med* **331**, 161-167 (1994).
20. Hunter, P.R. & Thompson, R.C. The zoonotic transmission of *Giardia* and *Cryptosporidium*. *Int J Parasitol* **35**, 1181-1190 (2005).
21. Shrivastava, A.K., Kumar, S., Smith, W.A. & Sahu, P.S. Revisiting the global problem of cryptosporidiosis and recommendations. *Trop Parasitol* **7**, 8-17 (2017).
22. O'Handley, R.M. *et al.* Duration of naturally acquired giardiasis and cryptosporidiosis in dairy calves and their association with diarrhea. *J Am Vet Med Assoc* **214**, 391-396 (1999).
23. Anderson, B.C. Patterns of shedding of cryptosporidial oocysts in Idaho calves. *J Am Vet Med Assoc* **178**, 982-984 (1981).
24. Xiao, L. & Herd, R.P. Infection pattern of *Cryptosporidium* and *Giardia* in calves. *Vet Parasitol* **55**, 257-262 (1994).
25. Tzipori, S. Cryptosporidiosis in animals and humans. *Microbiol Rev* **47**, 84-96 (1983).
26. Fayer, R. *et al.* *Cryptosporidium parvum* infection in bovine neonates: dynamic clinical, parasitic and immunologic patterns. *Int J Parasitol* **28**, 49-56 (1998).

27. DuPont, H.L. *et al.* The infectivity of *Cryptosporidium parvum* in healthy volunteers. *N Engl J Med* **332**, 855-859 (1995).
28. Barrington, G.M., Gay, J.M. & Evermann, J.F. Biosecurity for neonatal gastrointestinal diseases. *Vet Clin North Am Food Anim Pract* **18**, 7-34 (2002).
29. Yoder, J.S., Beach, M.J., Centers for Disease, C. & Prevention. Cryptosporidiosis surveillance--United States, 2003-2005. *MMWR Surveill Summ* **56**, 1-10 (2007).
30. O'Donoghue, P.J. *Cryptosporidium* and cryptosporidiosis in man and animals. *Int J Parasitol* **25**, 139-195 (1995).
31. Hunter, P.R. *et al.* Sporadic cryptosporidiosis case-control study with genotyping. *Emerg Infect Dis* **10**, 1241-1249 (2004).
32. Chen, X.M., Keithly, J.S., Paya, C.V. & LaRusso, N.F. Cryptosporidiosis. *N Engl J Med* **346**, 1723-1731 (2002).
33. Hunter, P.R. & Nichols, G. Epidemiology and clinical features of *Cryptosporidium* infection in immunocompromised patients. *Clin Microbiol Rev* **15**, 145-154 (2002).
34. Borad, A. & Ward, H. Human immune responses in cryptosporidiosis. *Future Microbiol* **5**, 507-519 (2010).
35. Petry, F., Jakobi, V. & Tessema, T.S. Host immune response to *Cryptosporidium parvum* infection. *Exp Parasitol* **126**, 304-309 (2010).
36. Laurent, F. & Lacroix-Lamande, S. Innate immune responses play a key role in controlling infection of the intestinal epithelium by *Cryptosporidium*. *Int J Parasitol* **47**, 711-721 (2017).
37. Chen, X.M., Splinter, P.L., O'Hara, S.P. & LaRusso, N.F. A cellular micro-RNA, let-7i, regulates Toll-like receptor 4 expression and contributes to cholangiocyte immune responses against *Cryptosporidium parvum* infection. *J Biol Chem* **282**, 28929-28938 (2007).
38. Chen, X.M. *et al.* Multiple TLRs are expressed in human cholangiocytes and mediate host epithelial defense responses to *Cryptosporidium parvum* via activation of NF-kappaB. *J Immunol* **175**, 7447-7456 (2005).
39. de Sablet, T. *et al.* *Cryptosporidium parvum* increases intestinal permeability through interaction with epithelial cells and IL-1beta and TNFalpha released by inflammatory monocytes. *Cell Microbiol* **18**, 1871-1880 (2016).

40. Auray, G., Lacroix-Lamande, S., Mancassola, R., Dimier-Poisson, I. & Laurent, F. Involvement of intestinal epithelial cells in dendritic cell recruitment during *C. parvum* infection. *Microbes Infect* **9**, 574-582 (2007).
41. Tessema, T.S. *et al.* Dynamics of gut mucosal and systemic Th1/Th2 cytokine responses in interferon-gamma and interleukin-12p40 knock out mice during primary and challenge *Cryptosporidium parvum* infection. *Immunobiology* **214**, 454-466 (2009).
42. McDonald, V. *et al.* A potential role for interleukin-18 in inhibition of the development of *Cryptosporidium parvum*. *Clin Exp Immunol* **145**, 555-562 (2006).
43. Bedi, B., McNair, N.N., Forster, I. & Mead, J.R. IL-18 cytokine levels modulate innate immune responses and cryptosporidiosis in mice. *J Eukaryot Microbiol* **62**, 44-50 (2015).
44. Dann, S.M. *et al.* Interleukin-15 activates human natural killer cells to clear the intestinal protozoan *cryptosporidium*. *J Infect Dis* **192**, 1294-1302 (2005).
45. Robinson, P. *et al.* Expression of IL-15 and IL-4 in IFN-gamma-independent control of experimental human *Cryptosporidium parvum* infection. *Cytokine* **15**, 39-46 (2001).
46. Ungar, B.L., Kao, T.C., Burris, J.A. & Finkelman, F.D. *Cryptosporidium* infection in an adult mouse model. Independent roles for IFN-gamma and CD4+ T lymphocytes in protective immunity. *J Immunol* **147**, 1014-1022 (1991).
47. Chen, W., Harp, J.A., Harmsen, A.G. & Havell, E.A. Gamma interferon functions in resistance to *Cryptosporidium parvum* infection in severe combined immunodeficient mice. *Infect Immun* **61**, 3548-3551 (1993).
48. McDonald, V. & Bancroft, G.J. Mechanisms of innate and acquired resistance to *Cryptosporidium parvum* infection in SCID mice. *Parasite Immunol* **16**, 315-320 (1994).
49. Pollok, R.C., Farthing, M.J., Bajaj-Elliott, M., Sanderson, I.R. & McDonald, V. Interferon gamma induces enterocyte resistance against infection by the intracellular pathogen *Cryptosporidium parvum*. *Gastroenterology* **120**, 99-107 (2001).
50. Ludington, J.G. & Ward, H.D. Systemic and Mucosal Immune Responses to *Cryptosporidium*-Vaccine Development. *Curr Trop Med Rep* **2**, 171-180 (2015).
51. McDonald, V., Korbil, D.S., Barakat, F.M., Choudhry, N. & Petry, F. Innate immune responses against *Cryptosporidium parvum* infection. *Parasite Immunol* **35**, 55-64 (2013).

52. Gookin, J.L. *et al.* NF-kappaB-mediated expression of iNOS promotes epithelial defense against infection by *Cryptosporidium parvum* in neonatal piglets. *Am J Physiol Gastrointest Liver Physiol* **290**, G164-174 (2006).
53. Leitch, G.J. & He, Q. Reactive nitrogen and oxygen species ameliorate experimental cryptosporidiosis in the neonatal BALB/c mouse model. *Infect Immun* **67**, 5885-5891 (1999).
54. Leitch, G.J. & He, Q. Arginine-derived nitric oxide reduces fecal oocyst shedding in nude mice infected with *Cryptosporidium parvum*. *Infect Immun* **62**, 5173-5176 (1994).
55. Barakat, F.M., McDonald, V., Di Santo, J.P. & Korb, D.S. Roles for NK cells and an NK cell-independent source of intestinal gamma interferon for innate immunity to *Cryptosporidium parvum* infection. *Infect Immun* **77**, 5044-5049 (2009).
56. Bedi, B. & Mead, J.R. *Cryptosporidium parvum* antigens induce mouse and human dendritic cells to generate Th1-enhancing cytokines. *Parasite Immunol* **34**, 473-485 (2012).
57. Barakat, F.M., McDonald, V., Foster, G.R., Tovey, M.G. & Korb, D.S. *Cryptosporidium parvum* infection rapidly induces a protective innate immune response involving type I interferon. *J Infect Dis* **200**, 1548-1555 (2009).
58. Perez-Cordon, G. *et al.* Interaction of *Cryptosporidium parvum* with mouse dendritic cells leads to their activation and parasite transportation to mesenteric lymph nodes. *Pathog Dis* **70**, 17-27 (2014).
59. Bedi, B., McNair, N.N. & Mead, J.R. Dendritic cells play a role in host susceptibility to *Cryptosporidium parvum* infection. *Immunol Lett* **158**, 42-51 (2014).
60. von Oettingen, J. *et al.* High-yield amplification of *Cryptosporidium parvum* in interferon gamma receptor knockout mice. *Parasitology* **135**, 1151-1156 (2008).
61. Ndao, M. *et al.* A cysteine protease inhibitor rescues mice from a lethal *Cryptosporidium parvum* infection. *Antimicrob Agents Chemother* **57**, 6063-6073 (2013).
62. Bonafonte, M.T., Smith, L.M. & Mead, J.R. A 23-kDa recombinant antigen of *Cryptosporidium parvum* induces a cellular immune response on in vitro stimulated spleen and mesenteric lymph node cells from infected mice. *Exp Parasitol* **96**, 32-41 (2000).
63. Mead, J.R. & You, X. Susceptibility differences to *Cryptosporidium parvum* infection in two strains of gamma interferon knockout mice. *J Parasitol* **84**, 1045-1048 (1998).

64. Ehigiator, H.N., McNair, N. & Mead, J.R. Cryptosporidium parvum: the contribution of Th1-inducing pathways to the resolution of infection in mice. *Exp Parasitol* **115**, 107-113 (2007).
65. Wang, C. *et al.* Multivalent DNA vaccine induces protective immune responses and enhanced resistance against Cryptosporidium parvum infection. *Vaccine* **29**, 323-328 (2010).
66. Ehigiator, H.N., Romagnoli, P., Priest, J.W., Secor, W.E. & Mead, J.R. Induction of murine immune responses by DNA encoding a 23-kDa antigen of Cryptosporidium parvum. *Parasitol Res* **101**, 943-950 (2007).
67. Heine, J., Moon, H.W. & Woodmansee, D.B. Persistent Cryptosporidium infection in congenitally athymic (nude) mice. *Infect Immun* **43**, 856-859 (1984).
68. Mead, J.R., Arrowood, M.J., Healey, M.C. & Sidwell, R.W. Cryptosporidial infections in SCID mice reconstituted with human or murine lymphocytes. *J Protozool* **38**, 59S-61S (1991).
69. Aguirre, S.A., Mason, P.H. & Perryman, L.E. Susceptibility of major histocompatibility complex (MHC) class I- and MHC class II-deficient mice to Cryptosporidium parvum infection. *Infect Immun* **62**, 697-699 (1994).
70. Chen, W., Harp, J.A. & Harmsen, A.G. Requirements for CD4+ cells and gamma interferon in resolution of established Cryptosporidium parvum infection in mice. *Infect Immun* **61**, 3928-3932 (1993).
71. Huang, D.B. & White, A.C. An updated review on Cryptosporidium and Giardia. *Gastroenterol Clin North Am* **35**, 291-314, viii (2006).
72. Zhao, G.H. *et al.* Dynamics of Th17 associating cytokines in Cryptosporidium parvum-infected mice. *Parasitol Res* **115**, 879-887 (2016).
73. Enriquez, F.J. & Sterling, C.R. Role of CD4+ TH1- and TH2-cell-secreted cytokines in cryptosporidiosis. *Folia Parasitol (Praha)* **40**, 307-311 (1993).
74. Lemieux, M.W., Sonzogni-Desautels, K. & Ndao, M. Lessons Learned from Protective Immune Responses to Optimize Vaccines against Cryptosporidiosis. *Pathogens* **7** (2017).
75. Kindt, T.J., Goldsby, R.A., Osborne, B.A. & Kuby, J. *Kuby immunology*, 6th edn. W.H. Freeman: New York, 2007.
76. Lean, I.S., McDonald, V. & Pollok, R.C. The role of cytokines in the pathogenesis of Cryptosporidium infection. *Curr Opin Infect Dis* **15**, 229-234 (2002).

77. Marchi, L.F., Sesti-Costa, R., Ignacchiti, M.D., Chedraoui-Silva, S. & Mantovani, B. In vitro activation of mouse neutrophils by recombinant human interferon-gamma: increased phagocytosis and release of reactive oxygen species and pro-inflammatory cytokines. *Int Immunopharmacol* **18**, 228-235 (2014).
78. McDonald, V. Host cell-mediated responses to infection with *Cryptosporidium*. *Parasite Immunol* **22**, 597-604 (2000).
79. Aguirre, S.A., Perryman, L.E., Davis, W.C. & McGuire, T.C. IL-4 protects adult C57BL/6 mice from prolonged *Cryptosporidium parvum* infection: analysis of CD4+alpha beta+IFN-gamma+ and CD4+alpha beta+IL-4+ lymphocytes in gut-associated lymphoid tissue during resolution of infection. *J Immunol* **161**, 1891-1900 (1998).
80. Abrahamsen, M.S., Lancto, C.A., Walcheck, B., Layton, W. & Jutila, M.A. Localization of alpha/beta and gamma/delta T lymphocytes in *Cryptosporidium parvum*-infected tissues in naive and immune calves. *Infect Immun* **65**, 2428-2433 (1997).
81. Pantenburg, B. *et al.* Human CD8(+) T cells clear *Cryptosporidium parvum* from infected intestinal epithelial cells. *Am J Trop Med Hyg* **82**, 600-607 (2010).
82. Kassa, M., Comby, E., Lemeteil, D., Brasseur, P. & Ballet, J.J. Characterization of anti-*Cryptosporidium* IgA antibodies in sera from immunocompetent individuals and HIV-infected patients. *J Protozool* **38**, 179S-180S (1991).
83. McDonald, V., Deer, R., Uni, S., Iseki, M. & Bancroft, G.J. Immune responses to *Cryptosporidium muris* and *Cryptosporidium parvum* in adult immunocompetent or immunocompromised (nude and SCID) mice. *Infect Immun* **60**, 3325-3331 (1992).
84. Mead, J.R. Prospects for immunotherapy and vaccines against *Cryptosporidium*. *Hum Vaccin Immunother* **10**, 1505-1513 (2014).
85. Riggs, M.W. Recent advances in cryptosporidiosis: the immune response. *Microbes Infect* **4**, 1067-1080 (2002).
86. Borad, A.J. *et al.* Systemic antibody responses to the immunodominant p23 antigen and p23 polymorphisms in children with cryptosporidiosis in Bangladesh. *Am J Trop Med Hyg* **86**, 214-222 (2012).
87. Wanyiri, J.W. *et al.* Cryptosporidiosis in HIV/AIDS patients in Kenya: clinical features, epidemiology, molecular characterization and antibody responses. *Am J Trop Med Hyg* **91**, 319-328 (2014).

88. Allison, G.M. *et al.* Antibody responses to the immunodominant *Cryptosporidium* gp15 antigen and gp15 polymorphisms in a case-control study of cryptosporidiosis in children in Bangladesh. *Am J Trop Med Hyg* **85**, 97-104 (2011).
89. Perryman, L.E., Kegerris, K.A. & Mason, P.H. Effect of orally administered monoclonal antibody on persistent *Cryptosporidium parvum* infection in scid mice. *Infect Immun* **61**, 4906-4908 (1993).
90. Riggs, M.W., Schaefer, D.A., Kapil, S.J., Barley-Maloney, L. & Perryman, L.E. Efficacy of monoclonal antibodies against defined antigens for passive immunotherapy of chronic gastrointestinal cryptosporidiosis. *Antimicrob Agents Chemother* **46**, 275-282 (2002).
91. Enriquez, F.J. & Riggs, M.W. Role of immunoglobulin A monoclonal antibodies against P23 in controlling murine *Cryptosporidium parvum* infection. *Infect Immun* **66**, 4469-4473 (1998).
92. Crabb, J.H. Antibody-based immunotherapy of cryptosporidiosis. *Adv Parasitol* **40**, 121-149 (1998).
93. Tzipori, S., Robertson, D. & Chapman, C. Remission of diarrhoea due to cryptosporidiosis in an immunodeficient child treated with hyperimmune bovine colostrum. *Br Med J (Clin Res Ed)* **293**, 1276-1277 (1986).
94. Ungar, B.L., Ward, D.J., Fayer, R. & Quinn, C.A. Cessation of *Cryptosporidium*-associated diarrhea in an acquired immunodeficiency syndrome patient after treatment with hyperimmune bovine colostrum. *Gastroenterology* **98**, 486-489 (1990).
95. Nord, J., Ma, P., DiJohn, D., Tzipori, S. & Tacket, C.O. Treatment with bovine hyperimmune colostrum of cryptosporidial diarrhea in AIDS patients. *AIDS* **4**, 581-584 (1990).
96. Plettenberg, A., Stoehr, A., Stellbrink, H.J., Albrecht, H. & Meigel, W. A preparation from bovine colostrum in the treatment of HIV-positive patients with chronic diarrhea. *Clin Investig* **71**, 42-45 (1993).
97. Rump, J.A. *et al.* Treatment of diarrhoea in human immunodeficiency virus-infected patients with immunoglobulins from bovine colostrum. *Clin Investig* **70**, 588-594 (1992).
98. Fayer, R. & Ungar, B.L. *Cryptosporidium* spp. and cryptosporidiosis. *Microbiol Rev* **50**, 458-483 (1986).
99. Webster, K.A., Smith, H.V., Giles, M., Dawson, L. & Robertson, L.J. Detection of *Cryptosporidium parvum* oocysts in faeces: comparison of conventional coproscopical methods and the polymerase chain reaction. *Vet Parasitol* **61**, 5-13 (1996).

100. Stibbs, H.H. & Ongerth, J.E. Immunofluorescence detection of *Cryptosporidium* oocysts in fecal smears. *J Clin Microbiol* **24**, 517-521 (1986).
101. Khurana, S. & Chaudhary, P. Laboratory diagnosis of cryptosporidiosis. *Trop Parasitol* **8**, 2-7 (2018).
102. Garcia, L.S. *Diagnostic medical parasitology*, 4th edn. ASM Press: Washington, D.C., 2001.
103. Anusz, K.Z., Mason, P.H., Riggs, M.W. & Perryman, L.E. Detection of *Cryptosporidium parvum* oocysts in bovine feces by monoclonal antibody capture enzyme-linked immunosorbent assay. *J Clin Microbiol* **28**, 2770-2774 (1990).
104. Kaushik, K., Khurana, S., Wanchu, A. & Malla, N. Evaluation of staining techniques, antigen detection and nested PCR for the diagnosis of cryptosporidiosis in HIV seropositive and seronegative patients. *Acta Trop* **107**, 1-7 (2008).
105. Hadfield, S.J., Robinson, G., Elwin, K. & Chalmers, R.M. Detection and differentiation of *Cryptosporidium* spp. in human clinical samples by use of real-time PCR. *J Clin Microbiol* **49**, 918-924 (2011).
106. Ghaffari, S. & Kalantari, N. Molecular analysis of 18S rRNA gene of *Cryptosporidium* parasites from patients living in Iran, Malawi, Nigeria and Vietnam. *Int J Mol Cell Med* **1**, 153-161 (2012).
107. Kato, S., Lindergard, G. & Mohammed, H.O. Utility of the *Cryptosporidium* oocyst wall protein (COWP) gene in a nested PCR approach for detection infection in cattle. *Vet Parasitol* **111**, 153-159 (2003).
108. Straub, T.M. *et al.* Genotyping *Cryptosporidium parvum* with an hsp70 single-nucleotide polymorphism microarray. *Appl Environ Microbiol* **68**, 1817-1826 (2002).
109. Pulendran, B. & Ahmed, R. Immunological mechanisms of vaccination. *Nat Immunol* **12**, 509-517 (2011).
110. Jenkins, M., Higgins, J., Kniel, K., Trout, J. & Fayer, R. Protection of calves against cryptosporiosis by oral inoculation with gamma-irradiated *Cryptosporidium parvum* oocysts. *J Parasitol* **90**, 1178-1180 (2004).
111. Wanyiri, J.W. *et al.* Proteolytic processing of the *Cryptosporidium* glycoprotein gp40/15 by human furin and by a parasite-derived furin-like protease activity. *Infect Immun* **75**, 184-192 (2007).

112. Priest, J.W., Xie, L.T., Arrowood, M.J. & Lammie, P.J. The immunodominant 17-kDa antigen from *Cryptosporidium parvum* is glycosylphosphatidylinositol-anchored. *Mol Biochem Parasitol* **113**, 117-126 (2001).
113. Reperant, J.M., Naciri, M., lochmann, S., Tilley, M. & Bout, D.T. Major antigens of *Cryptosporidium parvum* recognised by serum antibodies from different infected animal species and man. *Vet Parasitol* **55**, 1-13 (1994).
114. Liu, K. *et al.* Divalent Cp15-23 vaccine enhances immune responses and protection against *Cryptosporidium parvum* infection. *Parasite Immunol* **32**, 335-344 (2010).
115. Hong-Xuan, H. *et al.* Expression of the recombinant fusion protein CP15-23 of *Cryptosporidium parvum* and its protective test. *J Nanosci Nanotechnol* **5**, 1292-1296 (2005).
116. Perryman, L.E., Kapil, S.J., Jones, M.L. & Hunt, E.L. Protection of calves against cryptosporidiosis with immune bovine colostrum induced by a *Cryptosporidium parvum* recombinant protein. *Vaccine* **17**, 2142-2149 (1999).
117. Nascimento, I.P. & Leite, L.C. Recombinant vaccines and the development of new vaccine strategies. *Braz J Med Biol Res* **45**, 1102-1111 (2012).
118. Flingai, S. *et al.* Synthetic DNA vaccines: improved vaccine potency by electroporation and co-delivered genetic adjuvants. *Front Immunol* **4**, 354 (2013).
119. Sagodira, S., lochmann, S., Mevelec, M.N., Dimier-Poisson, I. & Bout, D. Nasal immunization of mice with *Cryptosporidium parvum* DNA induces systemic and intestinal immune responses. *Parasite Immunol* **21**, 507-516 (1999).
120. Yu, Q. *et al.* Induction of immune responses in mice by a DNA vaccine encoding *Cryptosporidium parvum* Cp12 and Cp21 and its effect against homologous oocyst challenge. *Vet Parasitol* **172**, 1-7 (2010).
121. Shahabi, V., Maciag, P.C., Rivera, S. & Wallecha, A. Live, attenuated strains of *Listeria* and *Salmonella* as vaccine vectors in cancer treatment. *Bioeng Bugs* **1**, 235-243 (2010).
122. Hume, P.J., Singh, V., Davidson, A.C. & Koronakis, V. Swiss Army Pathogen: The *Salmonella* Entry Toolkit. *Front Cell Infect Microbiol* **7**, 348 (2017).
123. Benitez, A.J., McNair, N. & Mead, J.R. Oral immunization with attenuated *Salmonella enterica* serovar Typhimurium encoding *Cryptosporidium parvum* Cp23 and Cp40 antigens induces a specific immune response in mice. *Clin Vaccine Immunol* **16**, 1272-1278 (2009).

124. Manque, P.A. *et al.* Identification and immunological characterization of three potential vaccinogens against *Cryptosporidium* species. *Clin Vaccine Immunol* **18**, 1796-1802 (2011).
125. Roche, J.K. *et al.* Intranasal vaccination in mice with an attenuated *Salmonella enterica* Serovar 908hr A expressing Cp15 of *Cryptosporidium*: impact of malnutrition with preservation of cytokine secretion. *Vaccine* **31**, 912-918 (2013).
126. Kim, K. & Weiss, L.M. *Toxoplasma gondii*: the model apicomplexan. *Int J Parasitol* **34**, 423-432 (2004).
127. O'Connor, R.M., Wanyiri, J.W., Wojczyk, B.S., Kim, K. & Ward, H. Stable expression of *Cryptosporidium parvum* glycoprotein gp40/15 in *Toxoplasma gondii*. *Mol Biochem Parasitol* **152**, 149-158 (2007).
128. Shirafuji, H. *et al.* Expression of P23 of *Cryptosporidium parvum* in *Toxoplasma gondii* and evaluation of its protective effects. *J Parasitol* **91**, 476-479 (2005).
129. Jongert, E., Roberts, C.W., Gargano, N., Forster-Waldl, E. & Petersen, E. Vaccines against *Toxoplasma gondii*: challenges and opportunities. *Mem Inst Oswaldo Cruz* **104**, 252-266 (2009).
130. Bernstein, D.I. *et al.* Successful application of prime and pull strategy for a therapeutic HSV vaccine. *NPJ Vaccines* **4**, 33 (2019).
131. Reed, S.G., Orr, M.T. & Fox, C.B. Key roles of adjuvants in modern vaccines. *Nat Med* **19**, 1597-1608 (2013).
132. Stills, H.F., Jr. Adjuvants and antibody production: dispelling the myths associated with Freund's complete and other adjuvants. *ILAR J* **46**, 280-293 (2005).
133. Andino, A. & Hanning, I. *Salmonella enterica*: survival, colonization, and virulence differences among serovars. *ScientificWorldJournal* **2015**, 520179 (2015).
134. Batz, M.B., Hoffmann, S. & Morris, J.G., Jr. Ranking the disease burden of 14 pathogens in food sources in the United States using attribution data from outbreak investigations and expert elicitation. *J Food Prot* **75**, 1278-1291 (2012).
135. Coburn, B., Sekirov, I. & Finlay, B.B. Type III secretion systems and disease. *Clin Microbiol Rev* **20**, 535-549 (2007).
136. Schlumberger, M.C. & Hardt, W.D. *Salmonella* type III secretion effectors: pulling the host cell's strings. *Curr Opin Microbiol* **9**, 46-54 (2006).

137. Winter, S.E. & Baumler, A.J. Salmonella exploits suicidal behavior of epithelial cells. *Front Microbiol* **2**, 48 (2011).
138. Zhao, X. *et al.* Recombinant attenuated Salmonella Typhimurium with heterologous expression of the Salmonella Choleraesuis O-polysaccharide: high immunogenicity and protection. *Sci Rep* **7**, 7127 (2017).
139. Ku, Y.W., McDonough, S.P., Palaniappan, R.U., Chang, C.F. & Chang, Y.F. Novel attenuated Salmonella enterica serovar Choleraesuis strains as live vaccine candidates generated by signature-tagged mutagenesis. *Infect Immun* **73**, 8194-8203 (2005).
140. Pesciaroli, M. *et al.* An attenuated Salmonella enterica serovar Typhimurium strain lacking the ZnuABC transporter induces protection in a mouse intestinal model of Salmonella infection. *Vaccine* **29**, 1783-1790 (2011).
141. Roland, K.L. & Brenneman, K.E. Salmonella as a vaccine delivery vehicle. *Expert Rev Vaccines* **12**, 1033-1045 (2013).
142. Cheng, X., Zhang, X., Zhou, Y., Zhang, C. & Hua, Z.C. A Salmonella Typhimurium mutant strain capable of RNAi delivery: higher tumor-targeting and lower toxicity. *Cancer Biol Ther* **15**, 1068-1076 (2014).
143. Spooner, C.E., Markowitz, N.P. & Saravolatz, L.D. The role of tumor necrosis factor in sepsis. *Clin Immunol Immunopathol* **62**, S11-17 (1992).
144. Toso, J.F. *et al.* Phase I study of the intravenous administration of attenuated Salmonella typhimurium to patients with metastatic melanoma. *J Clin Oncol* **20**, 142-152 (2002).
145. Winter, K., Xing, L., Kassardjian, A. & Ward, B.J. Vaccination against Clostridium difficile by Use of an Attenuated Salmonella enterica Serovar Typhimurium Vector (YS1646) Protects Mice from Lethal Challenge. *Infect Immun* **87** (2019).
146. Hassan, A.S., Zelt, N.H., Perera, D.J., Ndao, M. & Ward, B.J. Vaccination against the digestive enzyme Cathepsin B using a YS1646 Salmonella enterica Typhimurium vector provides almost complete protection against Schistosoma mansoni challenge in a mouse model. *PLoS Negl Trop Dis* **13**, e0007490 (2019).
147. Rossignol, J.F., Kabil, S.M., el-Gohary, Y. & Younis, A.M. Effect of nitazoxanide in diarrhea and enteritis caused by Cryptosporidium species. *Clin Gastroenterol Hepatol* **4**, 320-324 (2006).
148. Amadi, B. *et al.* High dose prolonged treatment with nitazoxanide is not effective for cryptosporidiosis in HIV positive Zambian children: a randomised controlled trial. *BMC Infect Dis* **9**, 195 (2009).

149. Bhadauria, D. *et al.* Cryptosporidium infection after renal transplantation in an endemic area. *Transpl Infect Dis* **17**, 48-55 (2015).
150. Kadappu, K.K., Nagaraja, M.V., Rao, P.V. & Shastri, B.A. Azithromycin as treatment for cryptosporidiosis in human immunodeficiency virus disease. *J Postgrad Med* **48**, 179-181 (2002).
151. Asadpour, M., Namazi, F., Razavi, S.M. & Nazifi, S. Comparative efficacy of curcumin and paromomycin against *Cryptosporidium parvum* infection in a BALB/c model. *Vet Parasitol* **250**, 7-14 (2018).
152. Mancassola, R., Reperant, J.M., Naciri, M. & Chartier, C. Chemoprophylaxis of *Cryptosporidium parvum* infection with paromomycin in kids and immunological study. *Antimicrob Agents Chemother* **39**, 75-78 (1995).
153. Hewitt, R.G. *et al.* Paromomycin: no more effective than placebo for treatment of cryptosporidiosis in patients with advanced human immunodeficiency virus infection. AIDS Clinical Trial Group. *Clin Infect Dis* **31**, 1084-1092 (2000).
154. Hussien, S.M. *et al.* Comparative study between the effect of nitazoxanide and paromomycine in treatment of cryptosporidiosis in hospitalized children. *J Egypt Soc Parasitol* **43**, 463-470 (2013).
155. Giacometti, A., Cirioni, O., Barchiesi, F., Ancarani, F. & Scalise, G. Activity of nitazoxanide alone and in combination with azithromycin and rifabutin against *Cryptosporidium parvum* in cell culture. *J Antimicrob Chemother* **45**, 453-456 (2000).
156. Holmberg, S.D. *et al.* Possible effectiveness of clarithromycin and rifabutin for cryptosporidiosis chemoprophylaxis in HIV disease. HIV Outpatient Study (HOPS) Investigators. *JAMA* **279**, 384-386 (1998).
157. Gathe, J.C., Jr., Mayberry, C., Clemmons, J. & Nemecek, J. Resolution of severe cryptosporidial diarrhea with rifaximin in patients with AIDS. *J Acquir Immune Defic Syndr* **48**, 363-364 (2008).
158. Castellanos-Gonzalez, A. *et al.* A novel calcium-dependent protein kinase inhibitor as a lead compound for treating cryptosporidiosis. *J Infect Dis* **208**, 1342-1348 (2013).
159. Kothavade, R.J. Challenges in understanding the immunopathogenesis of *Cryptosporidium* infections in humans. *Eur J Clin Microbiol Infect Dis* **30**, 1461-1472 (2011).

160. Feng, H., Nie, W., Sheoran, A., Zhang, Q. & Tzipori, S. Bile acids enhance invasiveness of *Cryptosporidium* spp. into cultured cells. *Infect Immun* **74**, 3342-3346 (2006).
161. Sharma, D., Mishra, A., Newaskar, V. & Khasgiwala, A. Bioterrorism: Law Enforcement, Public Health & Role of Oral and Maxillofacial Surgeon in Emergency Preparedness. *J Maxillofac Oral Surg* **15**, 137-143 (2016).
162. Checkley, W. *et al.* A review of the global burden, novel diagnostics, therapeutics, and vaccine targets for cryptosporidium. *Lancet Infect Dis* **15**, 85-94 (2015).
163. Haraga, A. & Miller, S.I. A Salmonella type III secretion effector interacts with the mammalian serine/threonine protein kinase PKN1. *Cell Microbiol* **8**, 837-846 (2006).
164. Hensel, M. Salmonella pathogenicity island 2. *Mol Microbiol* **36**, 1015-1023 (2000).
165. Grote, A. *et al.* JCat: a novel tool to adapt codon usage of a target gene to its potential expression host. *Nucleic Acids Res* **33**, W526-531 (2005).
166. Marston, F.A. & Hartley, D.L. Solubilization of protein aggregates. *Methods Enzymol* **182**, 264-276 (1990).
167. Rabilloud, T. Solubilization of proteins for electrophoretic analyses. *Electrophoresis* **17**, 813-829 (1996).
168. Schumann, J., Stanko, K., Schliesser, U., Appelt, C. & Sawitzki, B. Differences in CD44 Surface Expression Levels and Function Discriminates IL-17 and IFN-gamma Producing Helper T Cells. *PLoS One* **10**, e0132479 (2015).
169. Current, W.L., Upton, S.J. & Haynes, T.B. The life cycle of *Cryptosporidium baileyi* n. sp. (Apicomplexa, Cryptosporidiidae) infecting chickens. *J Protozool* **33**, 289-296 (1986).
170. Sharp, P.M., Bailes, E., Grocock, R.J., Peden, J.F. & Sockett, R.E. Variation in the strength of selected codon usage bias among bacteria. *Nucleic Acids Res* **33**, 1141-1153 (2005).
171. Brandis, G. & Hughes, D. The Selective Advantage of Synonymous Codon Usage Bias in Salmonella. *PLoS Genet* **12**, e1005926 (2016).
172. Puigbo, P., Guzman, E., Romeu, A. & Garcia-Vallve, S. OPTIMIZER: a web server for optimizing the codon usage of DNA sequences. *Nucleic Acids Res* **35**, W126-131 (2007).
173. Lawrence, J.G. & Ochman, H. Amelioration of bacterial genomes: rates of change and exchange. *J Mol Evol* **44**, 383-397 (1997).

174. Widmer, G. & Sullivan, S. Genomics and population biology of *Cryptosporidium* species. *Parasite Immunol* **34**, 61-71 (2012).
175. de Smit, M.H. & van Duin, J. Secondary structure of the ribosome binding site determines translational efficiency: a quantitative analysis. *Proc Natl Acad Sci U S A* **87**, 7668-7672 (1990).
176. Mauro, V.P. & Chappell, S.A. A critical analysis of codon optimization in human therapeutics. *Trends Mol Med* **20**, 604-613 (2014).
177. Ho, J.G., Middelberg, A.P., Ramage, P. & Kocher, H.P. The likelihood of aggregation during protein renaturation can be assessed using the second virial coefficient. *Protein Sci* **12**, 708-716 (2003).
178. Boivin, S., Kozak, S. & Meijers, R. Optimization of protein purification and characterization using Thermofluor screens. *Protein Expr Purif* **91**, 192-206 (2013).
179. Deller, M.C., Kong, L. & Rupp, B. Protein stability: a crystallographer's perspective. *Acta Crystallogr F Struct Biol Commun* **72**, 72-95 (2016).
180. Perrot, F., Hebraud, M., Junter, G.A. & Jouenne, T. Protein synthesis in *Escherichia coli* at 4 degrees C. *Electrophoresis* **21**, 1625-1629 (2000).
181. Bieri, M. *et al.* Macromolecular NMR spectroscopy for the non-spectroscopist: beyond macromolecular solution structure determination. *FEBS J* **278**, 704-715 (2011).
182. Ellermeier, J.R. & Slauch, J.M. Adaptation to the host environment: regulation of the SPI1 type III secretion system in *Salmonella enterica* serovar Typhimurium. *Curr Opin Microbiol* **10**, 24-29 (2007).
183. Lober, S., Jackel, D., Kaiser, N. & Hensel, M. Regulation of *Salmonella* pathogenicity island 2 genes by independent environmental signals. *Int J Med Microbiol* **296**, 435-447 (2006).
184. Nikolaus, T. *et al.* SseBCD proteins are secreted by the type III secretion system of *Salmonella* pathogenicity island 2 and function as a translocon. *J Bacteriol* **183**, 6036-6045 (2001).
185. Ibarra, J.A. *et al.* Induction of *Salmonella* pathogenicity island 1 under different growth conditions can affect *Salmonella*-host cell interactions in vitro. *Microbiology* **156**, 1120-1133 (2010).
186. Talbot, S.R. *et al.* Defining body-weight reduction as a humane endpoint: a critical appraisal. *Lab Anim* **54**, 99-110 (2020).

187. Bronte, V. & Pittet, M.J. The spleen in local and systemic regulation of immunity. *Immunity* **39**, 806-818 (2013).
188. Martin, M.D. & Badovinac, V.P. Defining Memory CD8 T Cell. *Front Immunol* **9**, 2692 (2018).
189. Robinson, P. *et al.* Expression of tumor necrosis factor alpha and interleukin 1 beta in jejunum of volunteers after experimental challenge with *Cryptosporidium parvum* correlates with exposure but not with symptoms. *Infect Immun* **69**, 1172-1174 (2001).
190. Lean, I.S., Lacroix-Lamande, S., Laurent, F. & McDonald, V. Role of tumor necrosis factor alpha in development of immunity against *Cryptosporidium parvum* infection. *Infect Immun* **74**, 4379-4382 (2006).
191. Burkholder, T., Foltz, C., Karlsson, E., Linton, C.G. & Smith, J.M. Health Evaluation of Experimental Laboratory Mice. *Curr Protoc Mouse Biol* **2**, 145-165 (2012).
192. Benbernou, N. & Nauciel, C. Influence of mouse genotype and bacterial virulence in the generation of interferon-gamma-producing cells during the early phase of *Salmonella typhimurium* infection. *Immunology* **83**, 245-249 (1994).
193. Bao, S., Beagley, K.W., France, M.P., Shen, J. & Husband, A.J. Interferon-gamma plays a critical role in intestinal immunity against *Salmonella typhimurium* infection. *Immunology* **99**, 464-472 (2000).
194. Kadam, P. & Bhalerao, S. Sample size calculation. *Int J Ayurveda Res* **1**, 55-57 (2010).
195. Inoue, Y. Spontaneous loss of antibiotic-resistant plasmids transferred to *Escherichia coli* in experimental chronic bladder infection. *Int J Urol* **4**, 285-288 (1997).
196. Mourand, G. *et al.* Rare Spontaneous Loss of Multiresistance Gene Carrying IncI/ST12 Plasmid in *Escherichia coli* in Pig Microbiota. *Antimicrob Agents Chemother* **60**, 6046-6049 (2016).